

Early warning signals for non-smooth bifurcations in population dynamics



Dissertation

zur Erlangung des akademischen Grades
doctor rerum naturalium
(Dr.rer.nat)

vorlegt dem Rat der Fakultät für Mathematik und
Informatik
der Friedrich-Schiller-Universität Jena

von

Flavia Remo

Msc. Mathematical modelling.

geboren am 07.08.1986 in Uganda

Gutachter:

1: Prof. Tobias Oertel-Jäger

Fakultät für Mathematik und Informatik, Friedrich-Schiller-Universität
Jena

2: Dr. Gabriel Fuhrmann

Department of Mathematical Sciences, Durham University

3: Prof. Jan Sieber

College of Engineering, Mathematics and Physical Sciences, University
of Exeter

Tag der öffentlichen Verteidigung: 1.12.2021

Zusammenfassung

Die klassische Sattel-Knoten Verzweigung ist ein paradigmatisches Beispiel eine sogenannten “Kritischen Verzweigung” (critical transition). Sie wurde in einer Vielzahl von verschiedenen zusammenhängen herausgezogen, insbesondere in der Ökologie und der Klimawissenschaft um die Rolle von langsamen Ruckkehraten (Recoveryrates) und erhöhten Autokorrelationen als Frühwarnsignale solcher Übergänge zu motivieren. In dieser Arbeit untersuchen wir den Einfluss von externen störungen auf Sattel-Knoten Verzweigung und die entsprechenden Frühwarnsignale. Unsere Hauptbeispiele sind dabei zwei spezifische Parameterfamilien, die eine Sattelknoten- Bifurkation durchlaufen: die arctan-Familie in diskreter Zeit und populationsdynamische Modelle mit Allee-Effekt in kontinuierlicher Zeit. In beiden Fällen untersuchen wir den Einfluss von quasiperiodischem Antrieb, beschränkten zufälligen Rauschen und einer Kombination aus beiden Antriebsprozessen, die wir als hybriden Antrieb bezeichnen. Wir zeigen, dass die Existenz dieser externen Faktoren zu sogenannten nicht-glatten Verzweigungen führen kann, die durch das Auftreten von seltsamen nicht-chaotischen Attraktoren (SNA) und Repellern charakterisiert sind. Dies hat einen signifikanten Einfluss auf das Verhalten der Lyapunov-Exponenten (und damit der Ruckkehraten). Während die kritische Verlangsamung (critical slowing down) durch verschwindende Lyapunov-Exponenten am Verzweigungspunkt charakterisiert ist, bleiben die Lyapunov-Exponenten des Attraktors und des Repellers bei einer nicht-glatten Sattel-Knoten Verzweigung von Null verschieden und lassen eine sogenannte “Lyapunov Lücke” (Lyapuno gap) zwischen den beiden Exponenten. Diese kann insbesondere dazu führen, dass es vor der Bifurkation und dann eventuell kollaps der population keine kritische Verlangsamung gibt und die entsprechende Frühwarnsignale den entsprechend nicht anschlagen. Genauer gesagt, hängt die Frage, ob langsame Ruckkehraten vor dem Übergang beobachtet werden können, entscheidend von den gewählten Zeitskalen und der Größe des betrachteten Datensatzes ab. Um dies zu präzisieren, untersuchen wir Lyapunov Exponenten in endliche zeit (Finite Time Lyapunov Exponenten, FTLE) als zusätzliches Werkzeug, um eine Sattelknoten-Verzweigungen in getriebenen Systemen zu antizipieren

und zeigen, wie diese sich in Frühwarnsignale für die Vorhersage eines bevorstehenden Übergangs umsetzen lassen. Wir stellen auch einen mathematischen Rahmen für die Beschreibung von Frühwarnsignalen zur Verfügung, die in biologischen und geophysikalischen Systemen beobachtet und numerisch und experimentell untersucht werden.

In der Einführung werden einige grundlegende Begriffe erläutert und Beispiele vorgestellt, darunter bekannte biologische Modelle, um den Zusammenhang zwischen Sattel-Knoten Verzweigung und Frühwarnsignalen zu erläutern. Weiterhin zeigen wir, wie nicht-glatte Bifurkationen und SNA in solchen Modellen auftreten können und stellen Beispiele vor, in denen sich diese Phänomene zeigen. Insbesondere stellen wir ein Populationsmodell mit Allee-Effekt vor, das in den meisten Teilen der Arbeit zur Illustration der Ergebnisse verwendet wird. In Kapitel 2 sammeln wir die erforderlichen Fakten bezüglich der Theorie nicht-autonomer Dynamik und der Produktsysteme mit besonderem Schwerpunkt auf invarianten Graphen und Sattel-Knoten Verzweigungen in der Produktumgebung. Wir stellen auch die verschiedenen Arten von Antriebsprozessen vor, die wir in dieser Umgebung betrachten, und illustrieren numerisch die Bildung von SNAs unter diesen Antriebsprozessen. Wir beginnen mit zeitdiskreten Produktsystemen, die man sich als vereinfachte Modelle für die Zeit -1- Abbildungen des Produktflusses vorstellen kann, welches durch das Allee-Modell induziert werden. Die Anwendung auf letzteres wird dann am Ende des Kapitels 3 diskutiert. Im selben Kapitel liefern wir rigorose Aussagen über nicht-glatte Sattel-Knoten Verzweigungen, beginnend mit quasiperiodischen getriebenen Systemen. Wir fahren dann fort, indem wir Satz 3.3 und Satz 3.7 über das Auftreten von nicht-glatte Sattel-Knoten Verzweigungen in zufällig und hybrid angetriebenen Systemen, zusammen mit ihren Beweisen, angeben. Wir bieten auch eine numerische Veranschaulichung dieses Szenarios in allen drei Fällen und diskutieren wie bereits erwähnt, zum Abschluss des Kapitels die Anwendung auf das getriebene Allee-Modell. In Kapitel 4 fahren wir fort, indem wir langsame Rückkehrzeiten und kritische Verlangsamung als Frühwarnsignal zur Erkennung einer glatten Bifurkation diskutieren. Wir geben eine präzise Aussage, in Form von Satz 4.2 und Satz 4.3, für die Existenz der Lyapunov-Lücke (siehe oben), die eine Abwesenheit von kritischer Verlangsamung für nicht-glatte Sattel-Knoten-Verzweigungen anzeigt. Wir liefern auch ein Ergebnis für die Steigung der Lyapunov-Exponenten am Bifurkationspunkt in Fall

diskreter Zeit. Weiterhin liefern wir numerische B... für die Existenz einer Lyapunov-Lücke sowohl im Zeit-diskreten als auch im Zeit-kontinuierlichen Fall (Allee-Effekt-Modell), um das Fehlen einer kritischen Verlangsamung zu veranschaulichen. In Kapitel 5 führen wir Finite time Lyapunov Exponenten (FTLE) als Frühwarnsignal zur Erkennung von nicht-glaten Sattel-Knoten-Verzweigung ein, motiviert durch die vorherige Beobachtung, dass langsame Recoveryrates nur das glatte Bifurkationsszenario detektieren können. Wir zeigen dann, dass FTLE nahe Null oder sogar im positiven Bereich vor einer nicht-glaten Sattel-Knoten-Verzweigung auftreten. Dies geschieht zuerst im quasiperiodischen Fall in Satz 5.1, gefolgt vom zufälligen Fall in Satz 5.3 und schließlich im hybriden Fall in Satz 5.5. Die Ergebnisse deuten darauf hin, dass zumindest im Prinzip positive oder kleine negative FTLE als Frühwarnsignale für solche Übergänge verwendet werden können. Um die Wahrscheinlichkeit der Beobachtung positiver/kleiner negativer FTLE besser zu verstehen und damit eine Vorstellung von der Größe der Datensätze zu erhalten, die für eine zuverlässige Vorhersage erforderlich sind, präsentieren wir numerische Ergebnisse für die Verteilung der FTLE sowie für die Wahrscheinlichkeit der Beobachtung positiver Lyapunov-Exponenten auf dem Attraktor. Wir möchten darauf hinweisen, dass wir zwar in den meisten Teilen dieser Arbeit das Allee-Effekt-Modell verwenden, um die Hauptergebnisse zu nicht-glaten Faltenbifurkationen zu formulieren, dass aber die Ergebnisse bezüglich der Frühwarnsignale in Kapitel 5 hauptsächlich in der zeitdiskreten Einstellung formuliert und bewiesen werden. Schließlich schließen wir in Kapitel 6 die Arbeit mit einer rigorosen Diskussion einiger relevanter Aspekte ab, die bei der Herleitung der Hauptergebnisse in Kapitel 5 beobachtet wurden, insbesondere hinsichtlich der Wahrscheinlichkeit, positive oder FTLEs nahe Null zu beobachten. Aufgrund der technischen Schwierigkeiten, die beim Umgang mit den in den vorangegangenen Kapiteln betrachteten Systemen auftreten können, führen wir die sogenannten “pinched skew product systems” ein. Diese erlauben uns, das beobachtete Phänomen zu beweisen. Wir zeigen also, dass die Wahrscheinlichkeit verschwindende Null oder positive FTLE zu beobachten, exponentiell gegen Null abfällt. Die genaue Aussage ist in Satz 6.3 formuliert. Dies stellt im Allgemeinen eine Herausforderung bei der Erkennung einer nicht-glaten Sattel-Knoten-Verzweigung in realen Situationen dar, da möglicherweise große Datensätze erforderlich sind, um positive oder verschwindende Lyapunov-Exponenten zu beobach-

ten.

Abstract

The classical fold bifurcation is a paradigmatic example of a critical transition. It has been used in a variety of contexts, including in particular ecology and climate science, to motivate the role of slow recovery rates and increased autocorrelations as early-warning signals of such transitions. In this thesis, we study the influence of external forcing on fold bifurcations and the respective early-warning signals. Thereby, our prime examples are two specific parameter families that undergo a saddle-node or a fold bifurcation; the arctan-family in discrete time and the single-species population dynamical models with Allee-effect in continuous time. In both cases, we study the influence of quasiperiodic forcing, bounded random noise and a combination of both forcing processes that we refer to as hybrid forcing. We show that the presence of these external factors may lead to so-called *non-smooth* fold bifurcations, characterized by the occurrence of strange non chaotic attractors (SNA) and repellers, and thereby has a significant impact on the behaviour of the Lyapunov exponents (and hence the recovery rates). While critical slowing down (slow recovery rates) is characterized by zero Lyapunov exponents at the bifurcation, the Lyapunov exponents of the attractor and repeller in a non-smooth fold bifurcation stay away from zero, leaving a gap between the two exponents. We refer to this as a *Lyapunov gap*. In particular, it may lead to the absence of critical slowing down prior to the bifurcation or population collapse. More precisely, unlike in the unforced case, the question whether slow recovery rates can be observed prior to the transition crucially depends on the chosen time-scales and the size of the considered data set. In order to make this precise, we investigate Finite Time Lyapunov Exponents (FTLE) as an additional tool to signal a saddle-node or fold bifurcation in forced systems and show how these translate into early warning signals for the prediction of an on-coming transition. We also provide a mathematical framework for the description of early warning signals that have been observed and studied numerically and experimentally in biological and geophysical systems.

In the introduction, we provide some basic terminology and introduce examples including some well known biological models to show the connection between fold bifurcations and early warning signals in real life situations.

Further, we show how non-smooth bifurcations and SNA can occur in such models and introduce examples that exhibit that phenomena. In particular, we introduce a single species population model with Allee-effect, which will be used in most parts of the thesis to illustrate the results. In Chapter 2, we collect the required preliminary facts concerning the mathematical theory of non-autonomous dynamics and skew product systems with particular emphasis on invariant graphs and fold bifurcations in the skew product setting. We also introduce the different types of forcing processes we consider in this setting and numerically illustrate the formation of SNAs under these forcing processes. We start with discrete-time skew product systems, which may be thought of as simplified models for the time one maps of the skew product flow induced by the forced Allee-model. The application to the latter is then discussed at the end of Chapter 3. In this same Chapter, we provide rigorous statements on non-smooth fold bifurcations, starting with quasiperiodically forced systems. We then proceed by stating Theorem 3.3 and Theorem 3.7 on the occurrence of non-smooth fold bifurcations in randomly forced and hybrid forced systems, together with their proofs. We also provide a numerical illustration of this scenario in all three cases, and as stated earlier we discuss the application to the forced Allee model to conclude the chapter. In Chapter 4, we proceed by discussing slow recovery rates and critical slowing down as an early warning signal for detecting a smooth bifurcation. We give a precise statement, in form of Theorem 4.2 and Theorem 4.3, for the existence of the Lyapunov gap (see above), which indicates an absence of critical slowing for non-smooth fold bifurcations. We also provide a result on the slope of the Lyapunov exponents at the bifurcation point in the discrete time setting. Further, we provide numerical evidence for the Lyapunov gap both in the discrete time case as well as in the continuous case (Allee effect model) to illustrate the absence of critical slowing down. In Chapter 5, we introduce Finite Time Lyapunov Exponents (FTLE) as an early warning signal for detecting non-smooth fold bifurcations, motivated by the previous observation that slow recovery rates can only signal the smooth bifurcation scenario. We then show that FTLE close to zero, or even in the positive region, occur prior to a non-smooth fold bifurcation, first in the quasiperiodic case in Theorem 5.1, followed by the random case in Theorem 5.3 and finally in the hybrid case in Theorem 5.5. This indicates that at least in principle positive or small negative FTLE may be used as early warning

signals for such transitions. In order to better understand the probability of observing positive/small negative FTLE, and thus to obtain an idea of the size of data-sets required for a reliable prediction, we present numerical results for the distribution of FTLE, as well as for the probability of observing positive Lyapunov exponents on the attractor. We would like to point out that while we use the Allee-effect model to formulate the main results on non-smooth fold bifurcations in most parts of this thesis, the results regarding the early warning signals in Chapter 5 are mainly formulated and proven in the discrete time setting. And finally in Chapter 6, we conclude the thesis by providing a rigorous discussion on some relevant aspects observed during the derivation of the main results in Chapter 5, in particular regarding the probability of observing positive or FTLEs close to zero. Due to the technicalities that may arise in dealing with the systems we consider in the preceding chapters, we introduce the pinched skew product systems which allow us to prove the phenomenon observed. We thus, prove that the probability of observing zero or positive FTLE decays exponentially to zero. The precise statement is formulated in Theorem 6.3. This in general presents a challenge in detecting a non-smooth fold bifurcation in real life situations as large data sets maybe be required in order to observe positive or zero Lyapunov exponents.

Acknowledgements

I would like to commence by thanking the Almighty God for enabling me go through the entire process of my PhD without any health complications. In a very special way, I would like to extend my sincere gratitude to my main Supervisor Prof. Dr. Tobias Oertel-Jäger for his innumerable support. He introduced me to this very interesting topic that I initially had no knowledge of and now has become my research interest in the field of dynamical systems and mathematics in general. Regardless of how abstract it seemed at the onset, having moved from applied mathematics to pure mathematics, he guided me through various discussions from the basics to the more complex concepts of this topic, that I eventually became acquainted with it. Despite the disparity in the approach of problems between applied and pure mathematics, I have been able to appreciate the relation between these two seemingly close fields which will enable me to address and approach real life situations in the dynamic world. What a great milestone achieved throughout my program! Not only did he support me academically, he also believed in my capability which boosted my confidence, a great attribute any PhD student would need to face all challenges that come along during the process. I would say he also had to bear with the many naive and 'stupid' questions I always asked, nevertheless, he exercised patience and answered them in the best way I could understand. From this I learnt to endure and be patient even during times when I felt like giving up. For that I am really very grateful.

Secondly, I greatly appreciate the efforts of my co-supervisor Dr. Fuhrmann Gabriel. And just like Tobias, he offered me a lot of support through numerous discussions. He also taught me a lot of basic concepts in Mathematical theory that have made me appreciate mathematics better. He also provided a very friendly environment that made it easy to approach him whenever I needed to discuss any problems. More so he helped a lot with understanding some numerical concepts which helped improve my numerical skills, a tool that was necessary in understanding how to approach mathematical problems from both numerical and analytical perspectives. Besides the academic support, he also offered emotional support, that the group eventually became more of a family far away from my own homeland. I couldn't have

been any happier to have done my PhD in this group in Jena.

Not forgetting my colleague Dr.Oertel Christian for the wonderful short discussions and the conducive environment he provided in the office which was very necessary for effective working. I can't forget some friends like Dr. Maik Gröger, Dr. Till Hauser, Dr. Louis Suarez and Dr. Bernardo Carvalho who made my stay pleasant at the University and in Jena as a whole.

In a special way, I would also like to thank Prof. Dr. Livingstone .S. Luboobi for guiding and encouraging me to pursue a career in mathematics after my MSc which led to this PhD. He has always been a great inspiration throughout my graduate studies.

Last but not least, I would like to appreciate my immediate family beginning with my Late mother Rose Anitte Remo who sacrificed her all to see me through school, my dear sisters Winniefred Likiso Remo and Janet Byaruhanga, my niece Maxine Mary Mar and my dear nephew Nathanael Denaya for the emotional support.

Dedication

I would like dedicate this thesis to my Late dear Mother Rose Anitte Remo who has been a pillar not only in my life but also in my academic career. Without her sacrifices, I wouldn't have been able to get this far. Likewise, I would like to dedicate it to my dear sisters Winniefred Likiso Remo and Byaruhanga Janet, not forgetting my dear niece Mar Maxine and Nephew Denaya Nathan for their emotional support.

Contents

1	Introduction	1
2	Preliminaries	17
2.1	Basic definitions and Notations	17
2.2	Skew product systems	20
2.3	Fold bifurcations	26
2.3.1	Deterministically forced systems	27
2.3.2	Randomly forced systems	36
2.3.3	Hybrid-forced systems	40
3	Non-smooth bifurcations	44
3.1	Quasiperiodic forcing	44
3.2	Random forcing	45
3.3	Hybrid forcing	54
3.4	Applications	59
4	Lyapunov gap	63
4.1	Slow recovery rates	63
4.2	Slow recovery rates	70
4.3	Slope at the bifurcation point	74
5	Finite time Lyapunov exponents	79
5.1	FTLE	79
5.2	FTLE in hybrid systems	83
5.3	Distributions	87
6	Pinched skew product systems	95

List of Figures

1.1	The classical fold bifurcation	3
1.2	Recovery rates upon small perturbations	3
1.3	Recovery rates in a living system	5
1.4	Some examples of strange non-chaotic attractors	6
1.5	Bifurcations and Lyapunov exponents in the Allee model . . .	8
1.6	Lyapunov exponents during fold bifurcations in the qpf Allee model	9
1.7	Distributions of the finite-time Lyapunov exponents in the qpf Allee model	15
1.8	Relative frequency of positive exponents in the qpf Allee model	16
2.1	Saddle-node bifurcations in qpf systems in discrete time . . .	34
3.1	47
3.1	Saddle-node bifurcations in qpf Allee model	48
3.2	Saddle-node bifurcations in randomly forced systems in dis- crete time	54
3.3	Saddle-node bifurcations in randomly forced systems in con- tinuous time	55
3.4	Non-smooth saddle-node bifurcations in hybrid-forced systems	61
4.1	65
4.1	Lyapunov exponents in qpf and randomly forced discrete time systems	66
4.2	Lyapunov exponents in the forced Allee model	67
4.3	Lyapunov exponents with simultaneous variation of parameters	68
4.4	Lyapunov exponents in discrete time hybrid-forced systems .	73

5.1	Minimal and maximal finite-time Lyapunov exponents in discrete time	84
5.2	Finite time Lyapunov exponents in the Allee model	85
5.3	Minimal and maximal finite-time Lyapunov exponents in hybrid-forced systems in discrete time	87
5.4	Distributions of the finite-time Lyapunov exponents in the qpf discrete time model	89
5.5	Distributions of the finite-time Lyapunov exponents in the randomly forced model in discrete time	90
5.6	Distributions of the finite-time Lyapunov exponents in the hybrid-forced model in discrete time	91
5.7	Distributions of the finite-time Lyapunov exponents in the randomly forced Allee model	92
5.8	Relative frequency of positive Lyapunov exponents in discrete time qpf model	93
5.9	Relative frequency of Lyapunov exponents close to zero in discrete time randomly forced model	93
5.10	Relative frequency of positive Lyapunov exponents in hybrid forced discrete time model	93
5.11	Relative frequency of Lyapunov exponents close to zero in randomly forced Allee model	94
6.1	Strange non-chaotic attractor in pinched systems	97
6.2	Iterates of upper bounding graphs in pinched systems	100
6.3	Heuristic description	101

Chapter 1

Introduction

Change is an aspect of life that is inevitable, but its precise understanding, description and prediction presents a very substantial challenge in many branches of science. The mathematical theory captures change in many physical systems through the bifurcation theory of dynamical systems. The latter describes the sudden topological changes in a systems behavior due to a slight variation of the systems parameters. These captured changes can be drastic/sudden, which leads us to the notion of critical transitions in some fields of study, while other changes may be slow/gradual, depending on how fast the system's parameters affect the dynamics of the system. The notion of critical transitions has received a wide spread of attention throughout a broad scope of sciences in the recent years. The term usually refers to abrupt and drastic changes in a system's behavior upon a small and slow variation of the system parameters [vNS12, MS09, SCL+12, K11]. Such transitions are often described as tipping points or catastrophic shifts or regime shifts in nature. The thresholds that result in regime shifts or critical transition behaviour are often referred to as tipping points. In the theory of dynamical systems, these points are known as bifurcation points. Although critical transitions have been observed to occur in many real life situations, an eminent problem that arises is the prediction of such behaviour to avoid catastrophes. In this context, an important issue of immediate practical interest is that of early warning signals, that is, indicators which allow to anticipate an oncoming transition in a systems qualitative behaviour before it actually occurs. In line with that, a concept that has led to widely recognised advances in this direction are *slow recovery rates (critical slowing down)*, which often come along with an *increase in autocorrelation*

[vNS12, SBB+09, MS09, SCL+12, VFDvN+12]. Both have been described as possible early warning signals in a variety of contexts, in theoretical as well as in experimental settings [DSvN+08, CCP+11, GJT13, vLWC+14, KGB+14, RDB+16].

A paradigmatic example, which has emerged in this context and offers an explanation for critical slowing down, is the classical fold bifurcation.

Fold and saddle-node bifurcations. The fold bifurcation in continuous-time systems, and the saddle-node fold bifurcation as its discrete-time counterpart, is a type of bifurcation that involves the collision and disappearance of two equilibria, one being a saddle (unstable) and the other a node (stable). To be precise, a stable and an unstable equilibrium point of a parameter-dependent map or scalar ODE approach each other and eventually merge to form a single neutral equilibrium point, which then vanishes as the forcing strength is increased. This is illustrated in Figure 1.1(b), where two different saddle-node/fold bifurcations occur at the equilibrium points F_1 and F_2 . Note that the saddle node bifurcation occurs between the stable branch, denoted by the bold lines, and the unstable branch, denoted by dotted lines in 1.1(b). The case represented here is one of bi-stability, where the system exhibits two stable and one unstable equilibrium. As the neutral equilibrium point vanishes after the bifurcation parameter is passed, this leads to the disappearance of all equilibria in a certain region. It is clear from the context that the saddle-node bifurcation presents an abrupt change in the system's qualitative behavior that is typical for a critical transition. In the theory of dynamical systems, with the simplest autonomous case, it has been observed that the Lyapunov exponent, which characterizes the rates of change around the equilibrium, becomes zero close to the bifurcation points F_1 and F_2 in Figure 1.1(b) [SBB+09]. This can be related to slow recovery rates close to the bifurcation point. Considering the fold bifurcation scenario presented in Figure 1.1, recovery rates can also be understood by visualizing the basin of attraction between the stable and the unstable equilibrium shown in the Figure 1.2 below. As the system gets closer to the bifurcation point, the basin of attraction becomes smaller and the slope close to the stable point becomes less steep, implying that the rates of change around the equilibrium become small. Therefore, if a system is perturbed around the equilibrium, it takes a longer time to return to its equilibrium point, leading to slow recovery rates as a bifurcation is approached. In the interest of this work, we

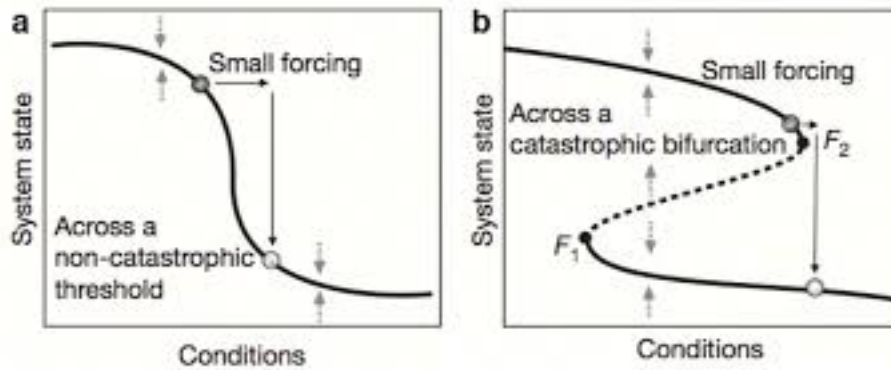


Figure 1.1: (a) Only one equilibrium exists in the system and change is gradual which makes the transition very smooth. However, the system is very insensitive to environmental conditions over certain ranges of external conditions while responding relatively strongly around some threshold conditions. (b) The system has three equilibria represented by bold and dotted curves. The bold curves represent two stable equilibria and the dotted curve represents an unstable equilibrium. Bifurcation points occur at points F_1 and F_2 [MS09].

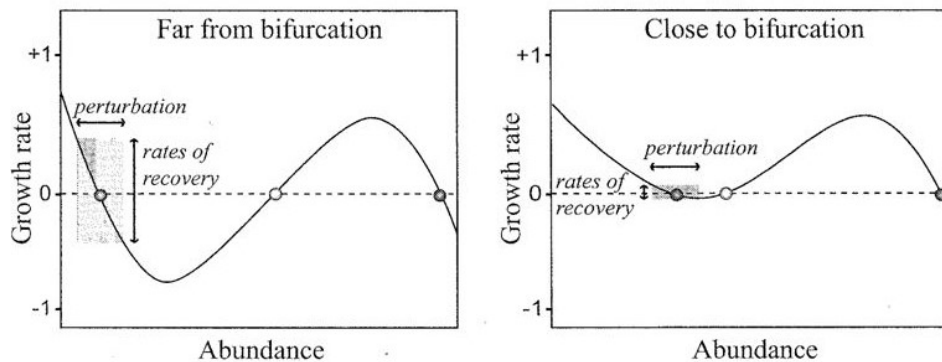


Figure 1.2: The figures above represent the growth rate populations and recovery rates upon small perturbations far and close to the bifurcation. The solid dots represent the stable equilibria and the light dot the unstable equilibrium [MS09].

will put our emphasis on this classical fold bifurcation, which comprises key features of critical transitions and has emerged as a paradigmatic example in this context [MS09].

A real-life example. An experimental framework from theoretical biology of a real life system gives an intuition into how critical slowing down can be observed in natural systems. The experiment was carried out to show how photo-inhibition drives a cyanobacterial population to a classi-

cal tipping point (*fold-bifurcation*) when a critical light level is exceeded [VFDvN+12]. The mechanism of its population growth is such that light is needed to enhance its population. However, an increasing light stress kills off a proportion of the bacterial population. On the other hand, if the biomass is relatively high, there is a positive feedback due to the shading of cyanobacteria, which maintains their population at relatively high levels. Such a positive feedback between organisms and their environment is in most cases the mechanism behind alternative stable states in a range of ecosystems. In this particular situation, it presents a case of bi-stability and thus exhibits two stable states (one at zero/extinction) with tipping points/bifurcation points. In the experiment, cyanobacteria in a chemostat microcosm are exposed to increasing light stress daily until the population collapsed. However, before the point of collapse, the system was perturbed from its equilibrium by flashing out a proportion of its biomass at different points in time indicated by p1-p6 as shown in Figure 1.3. The time intervals range between 4-5 days. This perturbation is equivalent to 3 – 5% reduction of its biomass. The two graphs represent results from two independently controlled chemostat microcosms under the same environmental conditions to measure accuracy. Results from the experiment showed that both systems maintained a relatively high biomass throughout the entire experiment until the population collapsed when the tipping point was reached. The recovery rates from perturbations p1-p6 decreased gradually towards the tipping point, starting far away from the bifurcation and tended to decline more rapidly close to the tipping point [VFDvN+12]. In particular, at position p6, it can be observed that the system took a longer time to recover to its equilibrium. This means that the closer the recovery rates get to zero, the closer the system gets to its critical point, thus indicating critical slowing down.

Forced systems and non-autonomous dynamics. As already stated earlier, our main focus is to understand the effect that external forcing has on these phenomena, and to provide a mathematical framework to describe critical slowing down and slow recovery rates as an early warning signal of non-autonomous fold bifurcations. As discussed earlier, forced systems arise as a result of interactions between systems. More precisely, it results from one way interactions where the dynamics of one system is perturbed by a forcing system whereas the dynamics of this forcing system evolves inde-

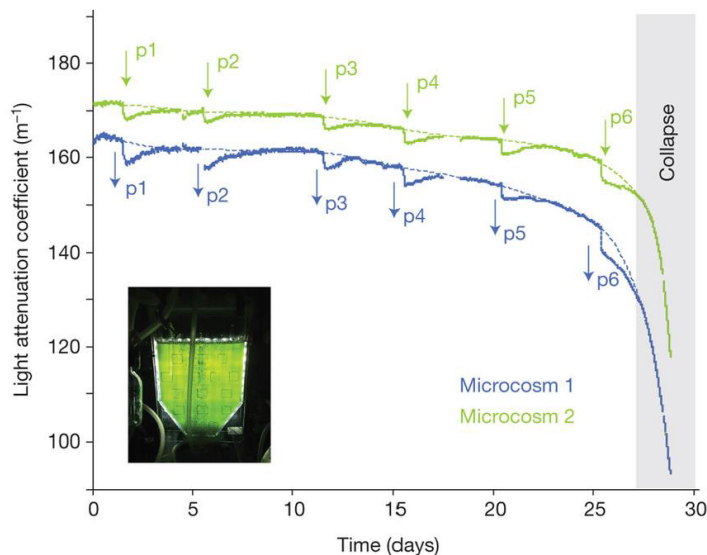


Figure 1.3: The response of two populations of cyanobacteria (*Aphanizomenon flos-aquae*) to dilution events under a regime of gradually increasing light levels [MS09].

pendently of the other. To be precise, we refer to systems of this nature as skew product systems. The perturbation is usually referred to as the external forcing or the forcing process in the context of skew product dynamics. This brings us into the theory of non-autonomous dynamics. In fact, one of the main motivations of studying non-autonomous dynamical systems is to analyse the influence of external forcing processes on the bifurcation pattern observed in autonomous dynamical systems. This has led to the development of non-autonomous bifurcation theory [NO07, Ras06, AJ12, Arn98]. Some of the common forcing processes considered in literature are deterministic, which includes periodic and quasiperiodic motion [Sta03, Gle02, FKP95, Jäg03, CGS95, PF95, DGO89a, RBE+87, RO87, GOPY84], or random forcing processes [Arn98, NDJS10, SMH20]. In most cases, the effect of these forcing processes are known to alter the global dynamics of the systems behavior. For instance, most biological population models are known to exhibit oscillatory behavior in the advent of periodic forcing, yielding a periodic solution as the equilibrium of the system in the long run. However, in some cases when

INTRODUCTION

the forcing is quasiperiodic or random, the geometry of the equilibrium may exhibit some 'strange' behavior which may not necessarily be chaotic, leading to so-called strange non-chaotic attractors (SNAs) [PMR98, GOPY84, RO87, RBE+87, DGO89a, DGO89b, WFP97, FKP06]. Such SNAs have been

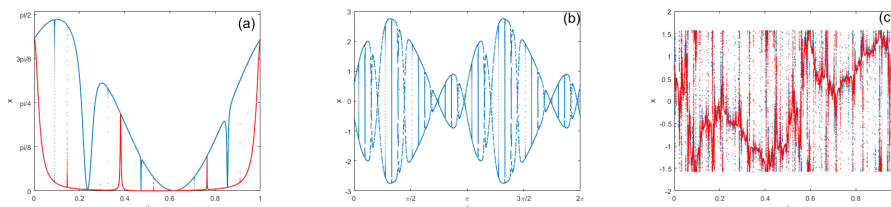


Figure 1.4: Three types of strange non-chaotic attractors. (a) An SNA in a skew product system of the form $(\theta, x) \mapsto (\theta + \omega, \arctan(\alpha x) - \beta(1 + \cos(2\pi\theta)))$, $\beta = 0.7805981$, $\alpha = 100$ and $\omega = (\sqrt{5} - 1)/2$ [Fuh16a]. The topological closure of the attractor is bounded above and below by semi-continuous invariant graphs [AJ12]. (b) An SNA that occurs in a certain class of skew product systems also known as pinched skew product systems of the form $(\theta, x) \mapsto ((\theta + 2\pi\omega) \bmod 2\pi, 2\sigma \tanh(x) \cos(\theta))$, $\sigma = 1.5$ and $\omega = (\sqrt{5} - 1)/2$ [GOPY84]. (c) An SNA that occurs in the critical Harper map of the form $(\theta, x) \mapsto \left(\theta + \omega, \arctan\left(\frac{1}{\tan(-x) - \epsilon + \lambda \cos(2\pi\theta)}\right)\right)$ with $\lambda = 2$ and $\epsilon = 0$.

observed to occur frequently in a broad class of systems under quasiperiodic forcing. They were discovered in quasiperiodically forced systems in the early 1980's by [Her83, GOPY84] and have since received considerable attention by numerous scholars. Their existence has further been proved in some population dynamics models, for instance in the logistic model in discrete time [NPR, PMR98], with extensions being made to a modified version in continuous time [Fuh16b]. More recently, SNAs have been proved to exist in some epidemic models such as the Susceptible-Infectives-Removed (SIR) and the Susceptible-Exposed-Infectives-Remove (SEIR) models [BSPM], which indicates the widespread occurrence of SNAs in a class of models that describe real life situations. There are many different routes to formation of SNAs in various systems, which among others include torus collision, fractalization, intermittency, blowout bifurcation, homoclinic collision, non-smooth saddle-node bifurcations etc, [PF95, HH94, WFP97, Jäg09]. However, in this thesis, we focus mainly on the type of SNAs of a 'strip-like' nature presented in Figure 1.4, which occur due to non-smooth saddle-node bifurcations of equilibria [Jäg09] under various forcing processes. To avoid technicalities at this point, we restrain from giving a precise definition of what we mean by the term 'non-smooth', which will be given in Chapter 2. We will mainly

consider three types of forcing processes, mainly *quasiperiodic forcing*, *random forcing* and finally a combination of the two forcing processes which we refer to as *hybrid forcing*.

In order to fix ideas, we illustrate the phenomena described above with a specific example from mathematical biology, namely a single-species population model with Allee effect.

The single species population model with Allee effect. The single species population model with Allee effect is given by the scalar ODE

$$\begin{aligned} x' &= rx \cdot \left(1 - \frac{x}{K}\right) \cdot \left(\frac{x}{K} - \frac{S}{K}\right) - \beta x, \\ &= \frac{r}{K^2} \cdot x \cdot (K - x) \cdot (x - S) - \beta x =: v_\beta(x). \end{aligned} \tag{1.1}$$

Here $r > 0$ denotes the intrinsic growth factor of the population, $K > 0$ is the maximal carrying capacity and $S \in (0, 1)$ is the threshold value below which the population dies out due to an Allee effect. The term βx represents an external stress factor that puts additional pressure on the population. The model is characterized by alternative stable states (one at zero/extinction) and one unstable equilibrium. An increase of the parameter β leads to a fold bifurcation and the subsequent collapse of the population at some critical value $\beta_c > 0$. Therefore the behaviour of the system state mimics the one in Figure 1.1(b). One obvious possible mathematical interpretation of *recovery rates* is to identify them with the Lyapunov exponents of the stable or neutral equilibria, so that *slow recovery rates* and *critical slowing down* correspond exactly to the Lyapunov exponents of the equilibrium as the system approaches the bifurcation point¹. The bifurcation pattern is drawn in Figure 1.5(a), whereas Figure 1.5(b) shows the behaviour of the Lyapunov exponents of the attracting and repelling equilibria during the bifurcation. Having given a precise mathematical interpretation of recovery rates and critical slowing down in the autonomous case, our main goal is to investigate the same bifurcation pattern in the forced versions of the model 1.1 given in the following section.

The forced Allee model. The forced Allee model is given by the non-autonomous ODE of the form

$$x'(t) = \frac{r}{K^2} \cdot x(t) \cdot (K - x(t)) \cdot (x(t) - S) - (\beta + \kappa \cdot F(t)) \cdot x =: V_{\kappa,\beta}(t, x)$$

(1.2)

¹In fact, a simple calculation yields $\beta_c = \frac{(K-S)^2 \cdot r}{4K^2}$.

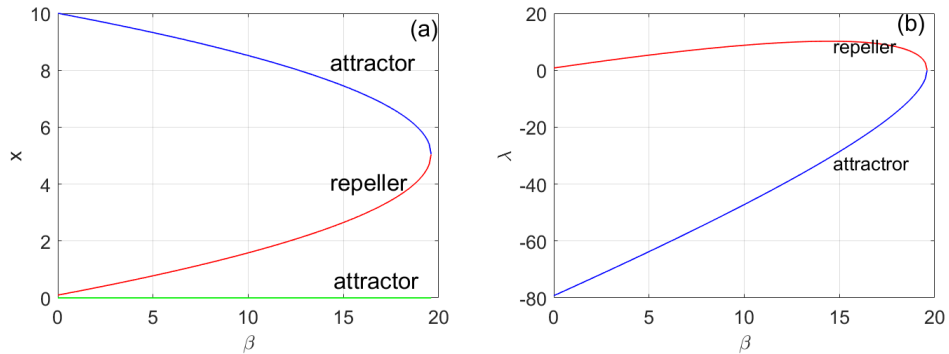


Figure 1.5: (a) Bifurcation diagram of a fold bifurcation in the Allee model (1.1) with parameters $r = 80$, $K = 10$, $S = 0.1$ and a bifurcation at a critical parameter $\beta_c \simeq 19.978$. The stable equilibrium at $x = 0$ is shown in green. (b) Behaviour of the Lyapunov exponents of the upper stable and the unstable equilibrium during the fold bifurcation.

Hence, time-dependence (or external forcing) of the system (1.2) is introduced via a *forcing term* $\kappa \cdot F(t)$, with *coupling constant* $\kappa > 0$ and a forcing function $F : \mathbb{R} \rightarrow [0, 1]$. Thereby, we consider three different types of forcing processes already mentioned above. The precise formula for these forcing processes will be given in Chapter 3. In some cases, we will need to replace the Allee model by discrete time systems with qualitatively similar behaviour in order to obtain rigorous results. These systems should then be considered as simplified models for the time-one-maps of the flow induced by (1.2). However, we refer to the respective later chapters for details, in order to avoid too many technicalities at this point.

Smooth and non-smooth fold bifurcations. In contrast to the unforced case, there are two different ways in which a fold bifurcation can happen in non-autonomous systems due to the fact the fixed equilibrium points are now replaced by moving or random equilibria. As the value of the non-autonomous equilibria depend on the forcing variable, there are two possibilities in which a collision can occur. The first possibility, which results in a bifurcation similar to the unforced case that we refer to as a smooth fold bifurcation in that the two random equilibria approach each other uniformly and merge to form a single neutral random equilibrium at the bifurcation point. This is shown in Chapter 2 in Figure 2.1(a)–(c) in discrete time. The pattern in continuous time is shown in Chapter 3 in Figure 3.1(a)–(d). On the other hand, the two curves or surfaces can also collide only for some values of forcing variable, without merging together uniformly.

This pattern is shown in Figure 2.1(d)–(f) in Chapter 2, as well as in Figure 3.1(e)–(h) in Chapter 3. In this case, one speaks of a *non-smooth fold bifurcation*, in which the neutral equilibrium at the bifurcation point is replaced by an attractor-repeller pair. Moreover, in the case of quasiperiodic forcing the stable and unstable non-autonomous equilibria are called *strange non-chaotic attractors (SNA)* and *strange non-chaotic repellers (SNR)*, due to their unusual combination of a fractal geometry and non-chaotic dynamics [GOPY84, FKP06, Jäg09, Fuh16a, FGJ18].

Lyapunov gap in the forced Allee model. In order to discuss what happens with the corresponding early-warning signals in the forced Allee model (1.2), we will first concentrate on the behaviour of the Lyapunov exponents.

Figure 1.6 shows the Lyapunov exponents of the attractor and the repeller of (1.2) throughout the bifurcation, with two different choices of the parameters κ and q in the case of quasiperiodic forcing in (a) and (b). The case of random and hybrid forcing will be shown in Chapter 3. While the behaviour

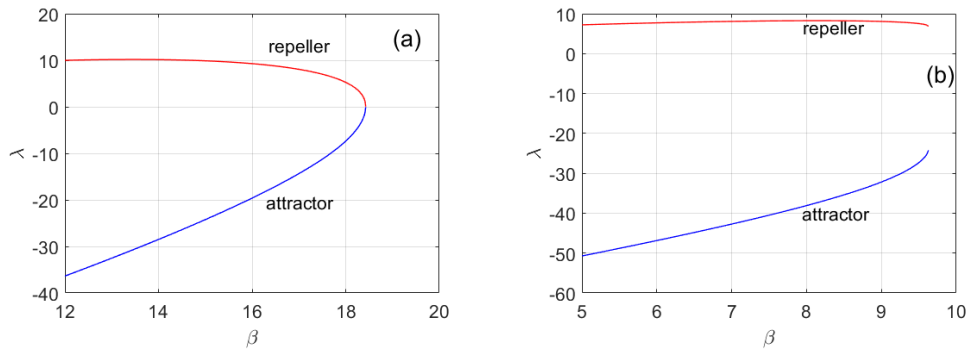


Figure 1.6: **(a) and (b):** Lyapunov exponents during fold bifurcations in the qpf Allee model; (a) smooth bifurcation with $r = 80$, $K = 10$, $S = 0.1$, $q = 1$, $\nu = (2\omega, 2\pi)$ (where ω is the irrational part of the golden mean) and $\kappa = 4$ (bifurcation at $\beta_c \simeq 18.4269$); (b) non-smooth bifurcation with $r = 80$, $K = 10$, $S = 0.1$, $q = 5$, $\nu = (2\omega, 2\pi)$ and $\kappa = 51.2$. The bifurcation occurs at $\beta_c \simeq 9.628$.

in (a) is in perfect analogy with the unforced case in Figure 1.5(b), the situation in (b) is clearly different. Although the Lyapunov exponents of the attractor and the repeller do approach each other, there remains a clear gap at the bifurcation point, and in particular the Lyapunov exponents of the attractor (which are the ‘visible’ or ‘physically relevant’ ones) stay strictly away from zero, a phenomenon we refer to as the *Lyapunov gap*.

Given the significance of zero exponents for the observation of critical slowing down and slow recovery rates, this is certainly noteworthy and deserves a closer examination. It is the dichotomy between smooth and non-smooth fold bifurcations which explains the different behaviours of the Lyapunov exponents observed in Figure 1.6. In order to make this precise, we denote by x_β^s the non-zero stable equilibrium of (1.2) at parameter β ,² and by $\lambda(x_\beta^s)$ its associated Lyapunov exponent. We refer to Chapter 2 for the precise definitions. Moreover, in order to obtain rigorous results we will need to apply a general framework for non-autonomous fold and saddle-node bifurcations that has been established in [AJ12]. An important condition that is required there is the concavity of the fibre maps in the considered region, which is a consequence of the concavity of the right side of the respective non-autonomous ODE. In order to ensure this concavity in (1.2), we need to restrict to suitable parameter ranges, as specified in the following.

Remark 1.1. We let

$$b(r, K, S) = \frac{r}{K^2} \cdot \left(\frac{K - S}{2}\right)^2 \quad \text{and} \quad \gamma(K, S) = \frac{1}{9} \cdot \left(\frac{K + S}{K - S}\right)^2 \quad (1.3)$$

and assume that

$$\kappa < b(r, K, S) \cdot (1 - \gamma(K, S)) . \quad (1.4)$$

Then, as we explain in detail in Chapter 3, the family (1.2) with a quasiperiodic or random or hybrid forcing term undergoes a fold bifurcation in the parameter interval

$$J(r, K, S) = [b(r, K, S) \cdot (1 - \gamma(K, S)), b(r, K, S) + 1] . \quad (1.5)$$

It should be mentioned, however, that this restriction in the parameter ranges is merely a technical condition and could easily be improved, in particular by using numerical methods, in order to include a broader range of parameters. The crucial condition is that the time-one-maps of skew product flow induced by (1.2) are concave for some $t > 0$. We thus, provide a preview of the main result in Chapter 4 on the Lyapunov gap in the statement below.

²Note here that there is always an equilibrium at zero, which is a natural requirement for any population dynamical model and ensured by the multiplicative form of the forcing in (1.2). Due to the Allee effect, the zero equilibrium is stable as well and presents the unique global attractor of the system after the bifurcation.

Theorem 1. *Suppose that (1.4) holds. If the Allee model (1.2) with forcing terms mentioned above undergoes a non-smooth fold bifurcation at critical parameter $\beta_c \in J(r, K, S)$, then we have that*

$$\lim_{\beta \nearrow \beta_c} \lambda(x_\beta^s) = \lambda(x_{\beta_c}^s) < 0. \quad (1.6)$$

If the fold bifurcation is smooth, then we have $\lim_{\beta \nearrow \beta_c} \lambda(x_\beta^s) = 0$. The analogous results hold for the unstable equilibrium x_β^u .

Occurrence of non-smooth fold bifurcations. An immediate question that can be asked in the context of the above observations is whether non-smooth fold bifurcations present a very relevant phenomenon, or if they are rather ‘pathological’ and may not play an important role for the description of real-world processes. However, in the case of quasiperiodic forcing, the wide-spread occurrence of non-smooth bifurcations and the related existence of SNA has been observed in a large number of numerical and experimental studies and in a variety of different contexts, ranging from classical and electronic oscillators to quantum mechanics, conceptual climate models and astrophysics (e.g. [RBE+87, DRC+89, WFP97, VLPR00, HP06, MCA15, RRM15, Zha13, LKK+15]). In addition, the simulations in Figures 1.6(b) and Figure 3.1(e)–(h) provide similar numerical evidence for the existence of non-smooth bifurcations in the qpf Allee model (1.2) with a quasiperiodic forcing. These findings are backed up by rigorous results in [Fuh16a, Fuh16b], showing that non-smooth fold bifurcations occur for open sets of parameter families of quasiperiodically forced scalar ODE’s. They can therefore be robust and persistent under small perturbations of the system. In the light of these results, one may say that fold bifurcations in quasiperiodically forced models may be either smooth or non-smooth, depending on the precise form of the model and the shape and strength of the forcing, and both of the cases are sufficiently widespread and persistent to be relevant in practical considerations and applications. In the case of bounded random forcing, the situation is different in that this balance even swings completely towards the side of non-smooth bifurcations. Roughly speaking, any forcing by a sufficiently random external process inevitably leads to the non-smoothness of the bifurcation. This observation extends to the hybrid forced systems due to the random component as will be shown in Chapter 3. For the case of our model system, this is established by the following result.

Theorem 2. *Suppose that (1.4) holds. Then any fold bifurcation that occurs in the forced Allee model (1.2) with random forcing term at a critical parameter $\beta_c \in J(r, K, S)$ is non-smooth.*

Altogether, the possible non-smoothness of bifurcations is an issue that should arguably be dealt with if one aims at a comprehensive understanding of critical transitions.

Finite time Lyapunov exponents. The interpretation of the Lyapunov gap in a non-smooth fold bifurcation depends on the precise meaning given to the notion of recovery rates. If these are identified with the Lyapunov exponents, then it follows that, unlike in classical fold bifurcations, there are no slow recovery rates in a non-smooth fold bifurcation. However, it seems reasonable to say that the intuitive meaning of recovery rates, as used in experimental studies like [SBB+09], is better captured by the mathematical notion of *finite time Lyapunov exponents*. Instead of measuring the asymptotic stability of an orbit, these only take into account the expansion or contraction around an orbit at some finite time. Given $T > 0$, we denote the Lyapunov exponent at time T of the flow generated by (1.2) and starting at an initial condition in the phase space by λ_T . In a smooth fold bifurcation, it is known that all finite time Lyapunov exponents in the basin of attraction of the stable equilibrium x_β^s will be very close to $\lambda(x_\beta^s)$, provided the time T is sufficiently large [SS00]. In contrast to this, the non-smooth case shows a characteristic spreading of these quantities, which can be observed in Figure 5.2. In order to translate this observation into a rigorous statement, we denote the largest time- T -Lyapunov exponent, that is ‘observable’ on the attractor x_β^s by $\lambda_T^{\max}(x_\beta^s)$, the minimal one by $\lambda_T^{\min}(x_\beta^s)$. (We refer to Chapter 5 for the precise definition.) The behaviour differs according to whether the forcing is quasiperiodic or random or hybrid.

Theorem 3. *Suppose that (1.4) holds. If the forced Allee model (1.2) with a quasiperiodic forcing term undergoes a non-smooth fold bifurcation at some critical parameter $\beta \in J(r, K, S)$, then we have that*

$$\lim_{\beta \nearrow \beta_c} \lambda_T^{\max}(x_\beta^s) \geq \lambda(x_{\beta_c}^u) > 0, \quad (1.7)$$

$$\lim_{\beta \nearrow \beta_c} \lambda_T^{\min}(x_\beta^s) \leq \lambda(x_{\beta_c}^s) < 0. \quad (1.8)$$

In the case of random forcing (3.3), we have that

$$\lim_{\beta \nearrow \beta_c} \lambda_T^{\max}(x_\beta^s) \geq 0. \quad (1.9)$$

And finally in the case of hybrid-forcing

$$\lim_{\beta \nearrow \beta_c} \lambda_T^{\max}(x_{h,\beta}^s) \geq \lambda(x_{\beta_c}^u) > 0 . \quad (1.10)$$

where x_h^s is the stable equilibrium of the hybrid-forced Allee model.

Both the statement and the numerical results imply that at least in theory non-smooth fold bifurcations can be anticipated and detected beforehand via a spread in the distribution of finite-time Lyapunov exponents, which reaches into the positive region. However, at the same time this highlights a variety of practical problems that may arise when trying to establish early-warning signals for forced systems. Unlike for Lyapunov exponents, which are asymptotic quantities and usually show a very uniform behaviour, the use of finite-time Lyapunov exponents requires to make a number of choices. First of all, there is the question of the time-scale (the choice of T) for which these quantities should be measured. When T is too small, it is likely that positive finite-time exponent will be observed already far from any bifurcation (depending on the geometry of the system). Conversely, if T is chosen too large, positive finite-time exponents may exist, but may only be observed with very small probabilities (thus requiring many measurements for a reliable signal). In any case, even with the right choice of time-scale and sufficient data, examples as the one shown in Figure 5.2(c) will remain difficult to treat.

Distribution of Finite time Lyapunov exponents. Finally, we take a brief look at the distribution of finite-time Lyapunov exponents on different timescales, which are shown in Figure 1.7 below. The probability of observing exponents above or close to zero is plotted in Figure 1.8 and decreases quickly. In fact, our simulations show that the rate of decay is exponential which is unanimous with the analytical results obtained in Chapter 6.3. All these illustrations refer to the qpf case although the rigorous results were obtained with the pinched skew product systems. Our reason for introducing the pinched skew product systems in dealing with this problem is discussed in detail in Chapter 6.3. However, the numerical results on the hybrid and random case provided in Chapter 5 show similar results to the qpf case.

Concluding remarks. In the above context, it should also be pointed out that, although finite-time Lyapunov exponents are by definition observable in finite time and may therefore in principle be accessible to experimental

INTRODUCTION

measurements, it is a difficult task to achieve and implement this for any real-life system. At the same time, the alternative use of autocorrelation does not make sense in a forced system with moving random equilibria. Hence, the practical implementation of early-warning signals for critical transitions in forced systems remains a wide open problem, even in the simplest case of fold bifurcations. On the theoretical side, an imminent problem that we tried to highlight by the above discussion is to give a precise mathematical meaning to terms like recovery rates, critical slowing down early warning signals and other notions that come up in the context of critical transitions. If theory and applications are supposed to go hand in hand, this will be an indispensable basis for further progress. The results and findings presented here should be understood as a contribution to that discussion.

We would like to point out that the main material of this thesis comprises a series of three articles. The effect of qpf and random forcing on the fold bifurcation and early warning signals which is already submitted and already in the arXives. The effect of hybrid forcing and the corresponding early warning signals is still in progress and will soon be submitted. And finally, the exponential decay of positive FTLE in pinched skew product systems which is also co-currently under preparation. Most of the ideas of the Thesis were birthed through various discussions with my supervisors.

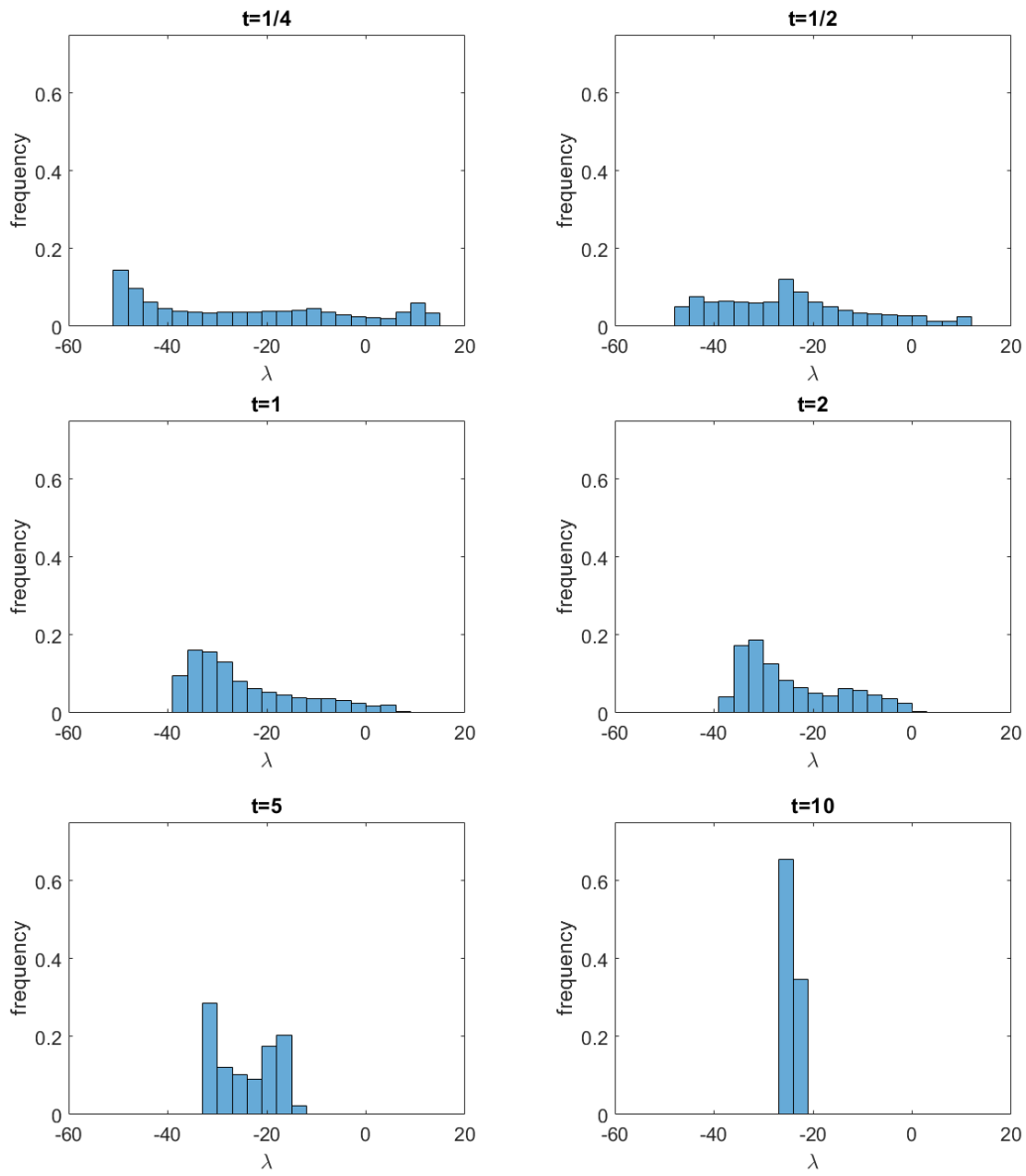


Figure 1.7: Distributions of the finite-time Lyapunov exponents in the qpf Allee model (1.2) with parameters $r = 80$, $K = 10$, $S = 0.1$, $\kappa = 51.2$ and $\beta = 9.629$ on different timescales, computed with sliding windows over a trajectory of length $t = 20000$.

INTRODUCTION

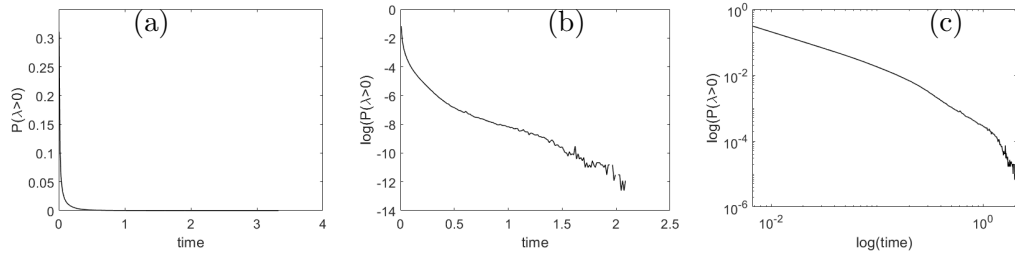


Figure 1.8: A plot of the relative frequency of positive exponents in the qpf Allee model on a (a) standard, (b) logarithmic and (c) log-log-scale.

Chapter 2

Preliminaries

2.1 Basic definitions and Notations

In this chapter, we provide the basic terminology required for the description of the desired results of this work. We will study the dynamics and the corresponding objects necessary for the description of non-smooth saddle-node or fold bifurcations in forced systems from the topological and measure-theoretical points of view. We give the description first in the deterministic case, followed by the random case, and lastly make an extension to the hybrid case. We denote by \mathbb{N} the set of all positive integers, \mathbb{N}_0 the non-negative integers, \mathbb{R} the real numbers and \mathbb{Z} the set of integers. We denote by \mathcal{C}^k the set of continuous functions $f : \mathbb{R} \rightarrow \mathbb{R}$, that are k -times differentiable and such that the k^{th} -derivative is continuous. In order to treat discrete-time dynamics alongside continuous-time dynamics, we refer by \mathbb{T} to the set of times, which either equals \mathbb{Z} (discrete-time) or \mathbb{R} (continuous-time). In both cases, a dynamical system is a pair (Y, Ξ) of a set Y and a flow Ξ on Y , that is, a mapping

$$\Xi : \mathbb{T} \times Y \rightarrow Y \quad , \quad (t, y) \mapsto \Xi^t(y) \quad (2.1)$$

which satisfies the flow properties

$$\Xi^0(y) = y \quad \text{and} \quad \Xi^{t+s}(y) = \Xi^t(\Xi^s(y)). \quad (2.2)$$

In the discrete-time case, this implies that $\Xi^t(y) = f^t(y)$, where $f : Y \rightarrow Y$ is the bijective map given by $f(y) = \Xi^1(y)$. We define the iterates of the map f by $f^n = f \circ \dots \circ f$, where f^0 is the identity map (*i.e.* $f^0(y) = y$) for

all $y \in Y$ and $n \in \mathbb{Z}$. Since we always assume the case of invertibility, we likewise define $f^{-n} = f^{-1} \circ \dots \circ f^{-1}$.

Measure preserving dynamical systems. Now, suppose we assume that Y is equipped with a σ -algebra \mathcal{B} . A probability measure μ on Y is called Ξ -invariant if $\mu \circ \Xi^t = \mu$ for all $t \in \mathbb{T}$. The set of all μ -invariant probability measures on (Y, \mathcal{B}) is denoted by $\mathcal{M}(\Xi)$. Given $\mu \in \mathcal{M}(\Xi)$, we call the quadruple $(Y, \mathcal{B}, \mu, \Xi)$ a *measure-preserving dynamical system (mpds)*. We refer to [Arn98] and references therein for details and background. A mpds $(Y, \mathcal{B}, \mu, \Xi)$ is called ergodic if every invariant set (that is, $\Xi^t(A) = A \forall t \in \mathbb{T}$) $A \in \mathcal{B}$ has measure 0 or 1. In this case we say the flow Ξ is ergodic with respect to μ . We say that the flow Ξ is uniquely ergodic if there exists a unique Borel probability measure μ on Y which is ergodic for Ξ . Furthermore, we say that the flow Ξ is mixing if for any measurable sets $A, B \in \mathcal{B}$,

$$\lim_{t \rightarrow \infty} \mu(A \cap \Xi^{-t}(B)) = \mu(A) \cdot \mu(B)$$

and it is called weakly mixing if

$$\lim_{t \rightarrow \infty} \frac{1}{t} \int_0^t |\mu(A \cap \Xi^{-s}(B)) - \mu(A) \cdot \mu(B)| ds = 0.$$

Theorem 2.1 ([BS02, Theorem,4.10.2]). *Let $(Y, \mathcal{B}, \mu, \Xi)$ and $(X, \mathcal{F}, \nu, \Psi)$ be mpds such that Ξ is weakly mixing. Then $\Xi \times \Psi$ is ergodic with respect to $\mu \times \nu$ for each ergodic Ψ .*

For the proof of this theorem, we refer the interested reader to [BS02]. Our main aim of stating this result is to allow for the construction of ergodic measure preserving dynamical systems in product spaces, in particular in the hybrid forcing case, where we consider the dynamics defined over a product space.

Topological dynamical systems. If Y is a metric space and Ξ is continuous on the product space $\mathbb{T} \times Y$, we call the pair (Y, Ξ) a *topological dynamical system (tds)*. If Y is compact, then (Y, Ξ) is a compact topological dynamical system, which we always assume unless stated otherwise. In this case, we assume throughout that the σ -algebra \mathcal{B} on X is given by the Borel σ -algebra on Y . We denote by $B_r(x) = \{y \in Y : d(x, y) < r\}$, the open ball centered at x with radius r where $r \geq 0$. Given a point $y \in Y$, we define the orbit of y under the flow Ξ by $\mathcal{O}_\Xi(y) = \{\Xi^t(y) \mid t \in \mathbb{T}\}$. An

important aspect of dynamical systems is to study orbits and their qualitative behaviour both locally and globally. These include, among others, fixed points. Fixed points are special kinds of orbits that often help us to understand the general behaviour of a dynamical system. A point $y \in Y$ is a fixed point of the flow Ξ if its orbit is a singleton, that is $\mathcal{O}_\Xi(y) = \{y\}$. Equivalently, $\Xi^t(y) = y$ for all $t \in \mathbb{T}$.

Invariant and minimal sets. Fundamental objects closely related to the notion of fixed points are invariant sets, which are more or less a generalization of fixed points. A set $A \subseteq Y$ is said to be forward invariant if $\Xi^t(A) \subseteq A$ and backward invariant if $\Xi^{-t}(A) \subseteq A$ for all $t > 0$. We say that, it is invariant if $\Xi^t(A) = A$. A forward invariant set $A \subseteq Y$ is called a global attractor of Ξ for any $x \in Y$, $d(\Xi^t(x), A) \rightarrow 0$ as $t \rightarrow \infty$, where $d(x, A) = \inf_{y \in A} \text{dist}(x, y)$ and $\text{dist}(x, y)$ is the metric between any two points $x, y \in Y$. In other words, it is both forward and backward invariant. A particular case of invariant sets more closely related to the notion of fixed points are minimal sets. A set $A \subseteq Y$ is said to be minimal with respect to Ξ if it is forward-invariant, compact, non-empty and strictly contains no proper subset with the same properties. If a compact metric space Y is itself minimal, then we say that the dynamical system (Y, Ξ) is minimal and Ξ is a minimal flow. A dynamical system can often be understood by studying the dynamical properties of the minimal sets of the system.

Stability of equilibria. Given a dynamical system (Y, Ξ) , let $A \subseteq Y$ be Ξ -invariant. We say that A is stable (attracting) if there exists an open neighbourhood U of A such that $\Xi^t(\bar{U}) \subset U$ and $A = \bigcap_{t \in \mathbb{R}_{\geq 0}} \Xi^t(\bar{U})$. On the other hand, A is unstable (repelling) if it is attracting for the time-reversed flow. In case of fixed points of an autonomous dynamical system, we say that a point y_0 is Lyapunov stable if for $\varepsilon > 0$, there exists a $\delta > 0$ such that $\|y(t) - y_0\| < \varepsilon$ whenever $\|y(t_0) - y_0\| < \delta$ for all $t \geq t_0$. We say it is asymptotically stable if there exists a $\delta_0 > 0$ such that $y(t) \rightarrow y_0$ whenever $\|y(t_0) - y_0\| < \delta_0$ as $t \rightarrow \infty$. It is unstable (asymptotically unstable) if it is not stable. If an equilibrium point is Lyapunov stable but not asymptotically stable, then it is neutrally stable. And finally, an equilibrium point y_0 is said to be exponentially stable if there exists a neighbourhood U of y_0 and a constants $k, c > 0$, such that $\|y(t) - y_0\| < k \cdot e^{-ct}$ for all $y(0)$ in U and $t \geq 0$. Exponential stability is a strong form of stability as it not only considers convergence of solutions, but also the speed of convergence of solutions. If

an equilibrium point is exponentially stable, then it is asymptotically stable and hence Lyapunov stable.

Stability criteria for fixed points. Stability of equilibrium points can be established in various ways. To begin with, for a system of ordinary differential equations, stability can be achieved by analyzing the eigenvalues of the Jacobian of the evolution matrix, which characterize the behaviour of nearby points. If all eigenvalues have negative real parts, then the point is stable (attracting). If the eigenvalues have positive real part, then it is unstable, otherwise if any of the eigenvalues have positive real part, while others have negative real part, then it is said to be a saddle (which is neither attracting or repelling). And if the complex eigenvalue has zero real part, the stability cannot be determined and solutions may tend to rotate around the equilibrium resulting into a periodic orbit. For one dimensional interval maps of the real line, a fixed point y of f is said to be stable (*attracting*) if $|f'(y)| < 1$ and unstable (*repelling*) if $|f'(y)| > 1$. And if $|f'(y)| = 1$ then the fixed point is neutral. We refer the interested reader to [KH97, BS02, ASY96, HSD12] for further information. Once we are able to understand the dynamics of a system via its minimal sets or fixed points, our next step is to understand the behaviour of these under the influence of some external forcing, and this leads us to the concept of non-autonomous dynamics.

2.2 Skew product dynamics.

In this section, we would like to introduce forced systems, which model non-autonomous dynamics, and give a general definition for equilibria in non-autonomous systems together with some properties regarding the behaviour of these equilibria. We would like to point out that most of the definitions we give in this section concerning skew product dynamics are taken from the previous work of ([AJ12, Fuh16a, Kel96, Sta03, Jäg13]).

Non-autonomous dynamics are often modeled by skew product systems. Given a tds (Θ, γ) or an mpds $(\Theta, \mathcal{B}, \mu, \gamma)$, a *skew product flow with base Θ and phase space X* is a flow on $Y = \Theta \times X$ of the form

$$\Xi : \mathbb{T} \times \Theta \times X \rightarrow \Theta \times X \quad , \quad (t, \theta, x) \mapsto \Xi^t(\theta, x) = (\gamma^t(\theta), \xi^t(\theta, x)) \quad , \quad (2.3)$$

Hence, if $\pi_\Theta : \Theta \times X$ is the canonical projection to Θ , then $\pi_\Theta \circ \Xi^t(\theta, x) = \gamma^t(\theta)$. The maps $X \ni x \mapsto \xi^t(\theta, x) \in X$, with $\theta \in \Theta$ fixed, are called *fibre*

maps. If X is a metric space, we assume the fibres maps to be continuous without further mentioning. If X is a smooth manifold and all the fibre maps $\xi^t(\theta, \cdot)$ are r times differentiable, we call Ξ a γ -forced C^r flow. If $X = \mathbb{R}$ and the fibre maps are all monotonically increasing, we say Ξ is a γ -forced monotone flow. The advantage of the skew product setting lies in the fact that the classical notion of equilibrium points – which does not make sense anymore for time-dependent systems as (1.2) – can be replaced by that of *random* or *non-autonomous equilibria*. These are defined as measurable functions $x : \Theta \rightarrow \mathbb{R}$, $\theta \mapsto x(\theta)$ that satisfy $\Xi^t(\theta, x(\theta)) = x(\gamma_t(\theta))$. Hence, a non-autonomous equilibrium can be thought of as a curve, surface or higher-dimensional submanifold of the product space $\Theta \times \mathbb{R}$ that can be represented as a graph over the base space Θ , is invariant under the skew product flow Ξ and is composed of solutions of (1.2) with varying initial conditions. With this new notion of an equilibrium, fold bifurcations in forced systems can be described, in perfect analogy to the classical case, as the collision and subsequent extinction of a stable and an unstable equilibrium [NO07, AJ12]. The process in the example (1.2) is shown in Chapter 3, Figure 3.1, where two such equilibria collide. The random or non-autonomous equilibrium is referred to as an invariant graph.

Invariant graphs and invariant measures.

Definition 2.2 (Invariant graph). A measurable function $\varphi : \Theta \rightarrow X$ is called an invariant graph of the flow Ξ if it satisfies

$$\Xi_\theta^t(\varphi(\theta)) = \varphi(\gamma^t(\theta)) \quad \forall \theta \in \Theta \text{ and for all } t \in \mathbb{T}. \quad (2.4)$$

In other words, φ is an invariant graph of Ξ , if the point set $\tilde{\Phi} = \{(\theta, \varphi(\theta)) \mid \theta \in \Theta\} \subseteq \Theta \times X$, which is the graph φ , is invariant under Ξ . In the topological setting, invariant graphs are assumed to be defined everywhere. In the measure theoretic setting, if μ is a γ -invariant measure and equation (2.4) holds μ -almost surely, then φ is called a (Ξ, μ) -invariant graph. For more details, see ([AJ12]).

One of the main reasons for concentrating on invariant graphs is the fact that, these are directly related, and in the case of monotone flows are in a one-to-one correspondence, with invariant ergodic measures of forced interval maps. Let $\mathcal{M}_\mu(\Xi)$ denote the set of all Ξ -invariant measures m which project to μ in the first coordinate, that is $\mu = m \circ \pi_\Theta^{-1} = \pi_\Theta^* m$, where $\pi_\Theta^* m$

denotes the push-forward measure. Given a (Ξ, μ) invariant graph φ , where μ is an invariant ergodic measure, we define a Ξ -invariant ergodic measure μ_φ as

$$\mu_\varphi(K) = \mu(\pi_\Theta(K \cap \tilde{\Phi})) = \mu(\{\theta \in \Theta \mid (\theta, \varphi(\theta)) \in K\}).$$

for any measurable subset $K \subseteq \Theta \times X$. Since μ is ergodic, this implies that to each invariant graph φ we can associate an Ξ -invariant ergodic measure μ_φ . The following theorem provides the converse of the above observation for ergodically forced monotone flows.

Theorem 2.3 ([Fur61, Theorem 4.1] & [Arn98, Theorem 1.84]). *Suppose Ξ is a γ -forced monotone flow, $\mu \in \mathcal{M}(\gamma)$ and $m \in \mathcal{M}_\mu(\Xi)$ is ergodic. Then there exists an (Ξ, μ) invariant graph φ such that $m = \mu_\varphi$.*

Forced one dimensional systems

We begin this section by defining global attractors in forced one dimensional systems.

Definition 2.4. ([Jäg03]) Let Ξ be a γ -forced monotone \mathcal{C}^2 flow of the form (2.3). Then the global attractor of Ξ is defined as

$$\mathcal{A}_\Xi = \bigcap_{t \in \mathbb{T}} \Xi^t(\Theta \times X). \quad (2.5)$$

The global attractor \mathcal{A}_Ξ is an invariant set under the monotone flow Ξ and is bounded above and below by measurable functions which are invariant graphs. The invariant graphs in this case can be defined as limits of monotonically increasing and monotonically decreasing functions which we define explicitly in Chapter 3.

Bounding graphs In the descriptions, we assume $X \subseteq \mathbb{R}$ to be a compact metric space. To be precise, we consider X to be an interval of the real line $I = [a, b]$. Let $K \subseteq \Theta \times X$ be a closed invariant set of the flow Ξ , such that $\Xi_\theta^t(K_\theta) = K_{\gamma^t\theta}$ for all $\theta \in \Theta$, $t \in \mathbb{T}$, where $K_\theta = \{x \in X \mid (\theta, x) \in K\}$. We say that K is Θ -covering if

$$\pi_\Theta(K) = \Theta. \quad (2.6)$$

Definition 2.5. Suppose $K \subseteq \Theta \times X$ is a compact invariant set for Ξ . Let $\varphi^-, \varphi^+ : \Theta \rightarrow X$ be measurable functions such that $[\varphi^-, \varphi^+] = \{(\theta, x) \mid x \in [\varphi^-(\theta), \varphi^+(\theta)]\}$ with

$$\varphi_K^-(\theta) = \inf K_\theta \quad \text{and} \quad \varphi_K^+(\theta) = \sup K_\theta. \quad (2.7)$$

Then

$$\inf \bigcup_{\theta \in \Theta} K_\theta \in X \quad \text{and} \quad \sup \bigcup_{\theta \in \Theta} K_\theta \in X. \quad (2.8)$$

According to [Jäg13], $\varphi_K^\pm(\theta)$ are referred to as upper and lower bounding graphs of K . If K is closed, bounded and Θ -covering, where Θ is a topological space, then φ_K^\pm are semi-continuous functions $\varphi_K^\pm : \Theta \rightarrow X$.

Corollary 2.5.1 ([Sta03, Corollary 1]). *Let $K \subset \Theta \times X$ be a compact invariant set of Ξ which is Θ -covering with boundary graphs φ_K^\pm . Then φ_K^+ is usc and φ_K^- is lsc.*

Definition 2.6. ([Sta03])(Upper and lower semi-continuous functions) A function $\varphi : \Theta \rightarrow \mathbb{R}$ is an upper semi-continuous function (usc) at $\theta_0 \in \Theta$ on a topological space Θ if for all $\epsilon > 0$, there exists a neighborhood U of θ_0 such that for all $\theta \in U$, we have

$$\varphi(\theta) \leq \varphi(\theta_0) + \epsilon. \quad (2.9)$$

And we say that φ is lower semi-continuous (lsc) at θ_0 if $-\varphi$ is usc at θ_0 .

Remark 2.7. A function φ is lower semi-continuous if $-\varphi$ is upper semi-continuous and the sum of usc(lsc) functions is usc(lsc).

Lemma 2.8 ([Sta03, Lemma 3]). *A function $\varphi : \Theta \rightarrow X$ is upper semi-continuous if and only if the set*

$$\{\theta \in \Theta \mid \varphi(\theta) \geq a\} = \pi_\Theta(K \cap \Theta \times [a, +\infty))$$

is closed for all $a \in \mathbb{R}$ and similarly lower semi-continuous if and only if the set

$$\{\theta \in \Theta \mid \varphi(\theta) \leq a\} = \pi_\Theta(K \cap \Theta \times (-\infty, a])$$

is closed.

And consequently

$$[\varphi_K^-, \varphi_K^+] := \{(\theta, x) \in \Theta \times X \mid \varphi_K^-(\theta) \leq x \leq \varphi_K^+(\theta)\}$$

is compact and defines a strip which is bounded by graphs of semi-continuous functions if Θ is compact.

Lemma 2.9 ([Sta03, Lemma 4]). *Let $\varphi^-, \varphi^+ : \Theta \rightarrow X$ be upper and lower semi-continuous invariant graphs respectively. If for some $\theta_0 \in \Theta$, $\varphi^-(\theta_0) \leq \varphi^+(\theta_0)$, then there exists some $\varepsilon > 0$ such that for all $\theta \in \Theta$, $\varphi^-(\theta) \leq \varphi^+(\theta) - \varepsilon$.*

The converse of this statement is given in the following corollary.

Corollary 2.9.1 ([Sta03, Corollary 3]). *Let $\varphi^-, \varphi^+ : \Theta \rightarrow X$ be lower and upper semi-continuous invariant graphs respectively. If for some $\theta_0 \in \Theta$, $\varphi^-(\theta_0) \leq \varphi^+(\theta_0)$, then for all $\theta \in \Theta$, $\varphi^-(\theta) \leq \varphi^+(\theta)$.*

The lemma and corollary assert that invariant graphs do not cross each other for all $\theta \in \Theta$. However, in the examples that we consider in this thesis, we will see that there is a possibility that invariant graphs may coincide at some points of θ , i.e $\varphi^-(\theta_0) = \varphi^+(\theta_0)$, while at some other points we still have $\varphi^-(\theta_0) < \varphi^+(\theta_0)$.

Lemma 2.10 ([Sta03, Lemma 5]). *Suppose Ξ is a minimally forced skew product flow. Let $\varphi^-, \varphi^+ : \Theta \rightarrow X$ be upper and lower semi-continuous invariant graphs respectively. If for some $\theta_0 \in \Theta$, $\varphi^-(\theta_0) = \varphi^+(\theta_0)$, then for a residual set of $\theta \in \Theta$, $\varphi^-(\theta) = \varphi^+(\theta)$. Furthermore φ^- and φ^+ are continuous at all $\theta \in \Theta$ such that $\varphi^-(\theta) = \varphi^+(\theta)$.*

Pinching For minimally forced one dimensional maps, we now discuss the notion of pinched invariant graphs, which was introduced earlier in [Sta03, Gle02, JS06, RJRG05].

Definition 2.11. (Pinched invariant graphs) Let $\varphi^-, \varphi^+ : \Theta \rightarrow X$ be upper and lower semi-continuous invariant graphs such that $\varphi^- \leq \varphi^+$. Then we say that φ^- and φ^+ are pinched if there exists a $\theta_0 \in \Theta$ such that $\varphi^-(\theta_0) = \varphi^+(\theta_0)$.

Furthermore, in the context of skew product systems, we say that a compact invariant subset $K \subseteq \mathbb{T} \times \Theta \times X$ with π_Θ is pinched if the pair φ_K^-, φ_K^+ is pinched. If we let $P(K) = \{\theta \in \Theta | \varphi_K^-(\theta) = \varphi_K^+(\theta)\}$, then the set $P(K)$ is residual in Θ in this case (see [Sta03, Lemma 5]).

Theorem 2.12 ([Sta03, Lemma 6] & [AJ12, Theorem 3.2,]). *Let $K \subseteq \mathbb{T} \times \Theta \times X$ be a pinched invariant subset of the minimally forced monotone flow Ξ . Then K contains exactly one minimal set. Conversely, if K is minimal, then it is pinched.*

The theorem shows the close relation between pinched invariant graphs and minimal sets. For non-minimal systems, the following slightly weaker notion of pinching is also relevant.

Definition 2.13 ([AJ12]). (Weakly pinched invariant graphs) Let $\varphi^-, \varphi^+ : \Theta \rightarrow X$ be upper and lower semi-continuous invariant graphs over a compact metric space Θ such that $\varphi^- \leq \varphi^+$. Then we say that φ^- and φ^+ are weakly pinched if $\inf_{\theta \in \Theta} \varphi^+(\theta) - \varphi^-(\theta) = 0$. Otherwise the graphs are called uniformly separated.

The measure theoretic analogue of pinching is defined as follows;

Definition 2.14 ([AJ12]). (Measurably pinched invariant graphs) Let $\varphi^-, \varphi^+ : \Theta \rightarrow X$ be measurable functions over a measure space $(\Theta, \mathcal{B}, \mu)$ such that $\varphi^- \leq \varphi^+$. Then we say that φ^- and φ^+ are measurably pinched if the set $A_\delta = \{\theta \in \Theta \mid \varphi^+(\theta) - \varphi^-(\theta) < \delta\}$ has positive measure for all $\delta > 0$. Otherwise, the graphs are called uniformly separated.

However, in cases where the forcing process is minimal, all three notions of pinching coincide and the result is stated in the following statement.

Lemma 2.15 ([AJ12, Lemma 3.5]). *Suppose Θ is a compact metric space and γ is a minimal homeomorphism. Let Ξ be a γ -forced monotone \mathcal{C}^0 flow such that $\varphi^-, \varphi^+ : \Theta \rightarrow X$ are Ξ -invariant graphs with φ^- l.s.c and φ^+ u.s.c. Then φ^- and φ^+ are pinched if and only if they are weakly pinched if and only if they are measurably pinched with respect to every γ -invariant measure μ .*

Lyapunov exponents and stability of invariant graphs. Since invariant graphs play the role of fixed points in forced systems, we provide a criteria to determine the nature of their stability. This is achieved by computing their Lyapunov exponents. To that end, we assume, that the flow Ξ is at least \mathcal{C}^1 with respect to x .

Definition 2.16. Suppose Ξ is a γ forced \mathcal{C}^1 flow of the form (2.3) and $(\theta, x) \in \Theta \times X$, the (vertical) forward and backward Lyapunov exponent of a point (θ, x) is given by

$$\lambda^+(\theta, x) = \lim_{t \rightarrow \infty} \frac{1}{t} \log |\partial_x \xi(t, \theta, x)| \quad \text{and} \quad \lambda^-(\theta, x) = \lim_{t \rightarrow \infty} -\frac{1}{t} \log |\partial_x \xi(-t, \theta, x)|,$$

if the limit exists.

Given any invariant graph φ , $\lambda^+(\theta, \varphi(\theta)) = -\lambda^-(\theta, \varphi(\theta)) = \lambda(\varphi)$ holds for μ -a.e $\theta \in \Theta$ by the Birkhoff Ergodic Theorem. Similarly, Lyapunov exponents of invariant graphs ψ and φ in discrete and continuous time are given by

$$\lambda(\psi) = \int_{\Theta} \log |\partial_x f_{\theta}(\psi(\theta))| d\mu(\theta) \quad \text{and} \quad \lambda(\varphi) = \frac{1}{t} \int_{\Theta} \log |\partial_x \xi_{\theta}^t(\varphi(\theta))| d\mu(\theta),$$

respectively, where Ξ and ψ, φ are the invariant graphs of f , respectively Ξ . Considering the discrete time case and applying Birkhoff Ergodic Theorem, we have

$$\begin{aligned} \lambda(\psi) &= \lambda^+(\theta, \psi(\theta)) = \lim_{n \rightarrow \infty} \frac{1}{n} \log |\partial_x f_{\theta}^n(\psi(\theta))|, \\ &= \lim_{n \rightarrow \infty} \frac{1}{n} \sum_{k=0}^{n-1} \log |\partial_x f_{\theta+k\gamma}(\psi(\theta+k\gamma))| \end{aligned}$$

for every $\theta \in \Theta$.

Proposition 2.16.1 ([Jäg03, Proposition 3.3]). *Suppose Ξ is of the form (2.3) and φ is an invariant graph such that $\lambda(\varphi) < 0$. Then there exists $\delta_{\theta} > 0$ such that for all $x \in B_{\delta_{\theta}}(\varphi(\theta))$*

$$|\xi^t(\theta, x) - \varphi(\gamma^t(\theta))| \rightarrow 0 \quad \text{as} \quad t \rightarrow \infty \quad \text{for} \quad \mu \text{ a.e } \theta \in \Theta.$$

The result here is stated for one dimensional skew product systems however, it holds true in higher dimensions. The proposition suggests that, an invariant graph φ is attracting if $\lambda(\varphi) < 0$ and repelling if $\lambda(\varphi) > 0$ and it is neutral if $\lambda(\varphi) = 0$. The same condition holds for the repeller as $t \rightarrow -\infty$ and by replacing the forward Lyapunov exponent with the backward Lyapunov exponent. In that case, we assume that, the flow is invertible. Therefore, we will refer to the graphs with the corresponding Lyapunov exponents as attractors and repellers respectively.

2.3 Fold and Saddle-node bifurcations in skew product systems

After giving the technical background, we now want to describe the fold/saddle-node bifurcation pattern of invariant graphs in parameter families of skew

product systems. We study this pattern under deterministic (*quasiperiodic*), random and hybrid forcing processes. To that end, we first concentrate on the case of quasiperiodic forcing that has already been studied [GOPY84, Gle02, Bje05, Jäg03, Jäg09b, FKP95, HP06, NPR]. Recent studies that provide conditions for a saddle-node bifurcation to occur can be found in [NO07, AJ12]. Hence, we would like to point out that the general setting and most of the rigorous results concerning saddle-node bifurcations in deterministically forced systems in this section are adopted from the earlier work of Jäger and Fuhrmann [AJ12, Fuh16a].

Classification for systems with concave fibres. Before we turn to non-autonomous fold bifurcations, we provide the following result, which allows to control the number of invariant graphs in a given region and their Lyapunov exponents. It holds for γ -forced monotone interval maps or flows with a concavity property on the fibres. Analogous results hold for fibre maps with a convexity property as well. However, in the interest of this work, we will only concentrate on the concave case.

Theorem 2.17 ([AJ12, Theorem 1.2]). *Let Ξ be a γ -forced \mathcal{C}^2 -flow of the form (2.3), where $(\Theta, \mathcal{B}, \gamma, \mu)$ is a mpds. Assume that for μ a.e $\theta \in \Theta$ there exists measurable functions $\phi^- < \phi^+ : \Theta \rightarrow X$ such that the fibre maps are monotonically increasing and strictly concave on $\Gamma_\theta = [\phi^-(\theta), \phi^+(\theta)]$, where $\Gamma = \{(\theta, x) \mid \theta \in \Theta, \phi^-(\theta) < x < \phi^+(\theta)\}$. Further assume that $\eta(\theta) = \inf_{x \in \Gamma_\theta} \log \xi'_\theta(x)$ has a μ -integrable minorant. Then there exists at most two (Ξ, μ) -invariant graphs in Γ . Moreover if there exists two distinct (Ξ, μ) -invariant graphs $\varphi^- \leq \varphi^+$ in Γ then $\lambda_\mu(\varphi^-) > 0$ and $\lambda_\mu(\varphi^+) < 0$.*

2.3.1 Fold bifurcations in deterministically forced systems

In order to study fold bifurcations in deterministically forced skew product systems, we assume (Θ, ρ) to be a topological dynamical system and consider parameter families $(\Xi_\beta)_{\beta \in [0,1]}$ of ρ -forced monotone \mathcal{C}^2 flows of the form

$$\Xi_\beta : \mathbb{T} \times \Theta \times X \rightarrow \Theta \times X, \quad (\theta, x) \mapsto \Xi_\beta^t(\theta, x) = (\rho^t(\theta), \xi_\beta^t(\theta, x)). \quad (2.10)$$

If $\mathbb{T} = \mathbb{R}$, we assume that the flow is defined via non-autonomous vector fields given by differentiable functions of the form

$$V_\beta : \Theta \times X \rightarrow \mathbb{R}, \quad (2.11)$$

which induce deterministically forced flows via the corresponding ordinary differential equations given by

$$\partial_t \xi_\beta(t, \theta, x) = V_\beta(\rho^t(\theta), \xi(t, \theta, x)) \quad (2.12)$$

Then $t \mapsto \xi_\beta(t, \theta, x)$ is the maximal solution of (2.10) with initial condition $\xi_\beta(0, \theta, x) = x$ for each (θ, x) contained in $\text{dom}(\xi_\beta) \subseteq \Theta \times X$, where $\text{dom}(\xi_\beta)$ stands for the domain of ξ_β . By the Picard-Lindelöf Theorem [Har64, Theorem 1.1 & 3.1], if V_β is Lipschitz continuous with respect to x , then $\xi_\beta(\cdot, \theta, x)$ is uniquely defined as the solution of (2.10). The flow ξ_β is a dynamical system such that

$$\xi_\beta(t + s, \theta, x) = \xi_\beta(t, \rho^t(\theta), \xi_\beta(s, \theta, x)) \quad (2.13)$$

for any $t \in B_r(0)$. We can also write the solution in backward time as

$$\xi_\beta^- : (t, \theta, x) \mapsto \xi_\beta(-t, \theta, x) \quad (2.14)$$

assuming invertibility of V that is by considering $V^- = -V$ and $\rho_{(\cdot)}^- = \rho_{(\cdot)}$. It is important to note that $\xi_\beta^-(t, \rho^t(\theta), \xi_\beta(t, \theta, x)) = \xi(0, \theta, x) = x$ for all $t \in B_r(0)$.

To describe fold bifurcations in deterministically forced systems, we provide some conditions under which such a bifurcation happens. The setting is formulated in a semi-local way by restricting the dynamics to a subset $\Gamma \subseteq \Theta \times [\phi^-, \phi^+]$ with measurable functions $\phi^- \leq \phi^+ : \Theta \rightarrow X$, and describe bifurcations of invariant graphs in Γ (similar to Theorem 2.17). The theorem in general stipulates the properties of the autonomous family that one needs to check before applying the forcing. For instance, one property that one needs to check is if the system has a stable and an unstable equilibrium at the onset of the bifurcation. Such properties are inherited by the forced system in the skew product setting. This not only regards the deterministically forced systems, but works similarly for all types of forcing processes. Among other properties, we also check for the monotonicity of the fibres with respect to x , which allows using upper and lower bounding graphs to define the invariant graphs of the system. We also require strict concavity of the fibres, which allows for the existence of at most two distinct invariant graphs due to Theorem 2.17, the upper one being the attractor and the lower one the repeller. And finally, the continuous and monotonically decreasing dependence on the parameter $\beta \in [0, 1]$ guarantees the existence of a unique critical parameter β_c , at which the bifurcation takes place. This

also ensures that the invariant graphs approach each other monotonically as the parameter is increased. As mentioned earlier, all these extend naturally from the properties of the autonomous system and therefore it is imperative that these be checked for the autonomous system first before they are checked for the non-autonomous system. The precise statement is the following:

Theorem 2.18 ([AJ12, Theorem 6.1]). *Let ρ be a flow on a compact metric space Θ and suppose $(\Xi_\beta)_{\beta \in [0,1]}$ is a parameter family of ρ -forced monotone \mathcal{C}^2 flows. Further assume that there exist continuous functions $\phi^-, \phi^+ : \Theta \rightarrow X$ with $\phi^- < \phi^+$ such that the following conditions hold for all $\beta \in [0, 1]$, $\theta \in \Theta$ and all positive $t \in \mathbb{T}$, where applicable.*

- (i) *There exist two distinct continuous Ξ_0 -invariant graphs and no Ξ_1 -invariant graph in $\Gamma = \{(\theta, x) \mid \phi^-(\theta) < x < \phi^+(\theta)\}$;*
- (ii) $\xi_\beta^t(\theta, \phi^\pm(\theta)) \leq \phi^\pm(\rho^t(\theta))$;
- (iii) *the maps $(\beta, \theta, x) \mapsto \partial_x^i \xi_\beta^t(\theta, x)$ with $i = 0, 1, 2$ and $(\beta, \theta, x) \mapsto \partial_\beta \xi_\beta^t(\theta, x)$ are continuous;*
- (iv) $\partial_x \xi_\beta^t(\theta, x) > 0 \forall x \in \Gamma_\theta$
- (v) $\partial_\beta \xi_\beta^t(\theta, x) < 0 \forall x \in \Gamma_\theta$
- (vi) $\partial_x^2 \xi_\beta^t(\theta, x) < 0 \forall x \in \Gamma_\theta$.

Then there exists a unique critical parameter $\beta_c \in [0, 1]$ such that

- *If $\beta < \beta_c$, then there exist two continuous Ξ_β -invariant graphs $\varphi_\beta^- < \varphi_\beta^+$ in Γ . For any ρ -invariant measure ν we have $\lambda_\nu(\varphi_\beta^-) > 0$ and $\lambda_\nu(\varphi_\beta^+) < 0$.*
- *If $\beta = \beta_c$, then either there exists exactly one continuous Ξ_β -invariant graph φ_β in Γ or there exists a pair of weakly pinched Ξ_β -invariant graphs $\varphi_\beta^- \leq \varphi_\beta^+$ in Γ with φ_β^- lower and φ_β^+ upper semi-continuous. If ν is an ρ -invariant measure, then in the first case $\lambda_\nu(\varphi_\beta) = 0$. In the second case $\varphi_\beta^-(\theta) = \varphi_\beta^+(\theta)$ ν -almost surely implies $\lambda_\nu(\varphi_\beta^\pm) = 0$, whereas $\varphi_\beta^-(\theta) < \varphi_\beta^+(\theta)$ ν -almost surely implies $\lambda_\nu(\varphi_\beta^-) > 0$ and $\lambda_\nu(\varphi_\beta^+) < 0$.*
- *If $\beta > \beta_c$, then no Ξ_β -invariant graphs exist in Γ .*

Remark 2.19.

We note that the result in [AJ12] is stated for convex fibre maps but the above version for concave fibre maps is equivalent and discussed in [AJ12, Remark 6.2 (c)].

Likewise, the statement in [AJ12] is given for the closed region $\bar{\Gamma}$ instead of the open set Γ that we use here (for convenience later on), but the proof in [AJ12] can be adjusted with minor modifications.

In the situation where $\beta = \beta_c$, the above results hence allow for two scenarios.

- **Smooth bifurcation:** Ξ_{β_c} has a unique invariant graph in Γ such that $\lambda(\varphi_{\beta_c}) = 0$. Similar to the autonomous case, we can say that the invariant graph is neutral.
- **Non-smooth bifurcation:** Ξ_{β_c} has exactly two semi-continuous invariant graphs with non-zero Lyapunov exponents leading to a gap in the exponents of the attractor and the repeller which we refer to as a Lyapunov gap.

Non-continuous invariant graphs with negative Lyapunov exponents, as they appear in non-smooth fold bifurcation of quasiperiodically forced systems, are called *strange non-chaotic attractors* (SNA). If the Lyapunov exponent is positive, they are called non-chaotic repellers (SNR) [GOPY84, Kel96, Sta03, FKP06, NO07, AJ12].

Moving on from the general description and setting, the widespread occurrence of non-smooth bifurcations have been observed in various examples of deterministically forced systems.

Quasiperiodic forcing (qpf). The rigorous analysis of non-autonomous ODE's, such as the one given by (1.2) and a quasiperiodic forcing $F(t)$, hinges on the fact that the family of equations (1.2), with all possible initial conditions $\theta = (\theta_1 \cdots \theta_d) \in \mathbb{T}^d$, defines a skew product flow

$$\Xi : \mathbb{R} \times \Theta \times \mathbb{R} \rightarrow \Theta \times \mathbb{R} \quad , \quad (t, \theta, x) \mapsto \Xi^t(\theta, x) = (\rho_t(\theta), \xi^t(\theta, x)) . \quad (2.15)$$

Here the *driving space* Θ is the d -torus, $\Theta = \mathbb{T}^d = \mathbb{R}^d / \mathbb{Z}^d$ (corresponding to the set of possible initial conditions) and the *driving flow* $\rho : \mathbb{R} \times \Theta \rightarrow \Theta$ is given by the irrational Kronecker flow $\rho_t(\theta) = \theta + t \cdot v$ with translation

vector $v = (\nu_1 \cdots \nu_d)$,¹ and models the quasiperiodic dynamics of the external driving factor. The flow Ξ is uniquely determined by the fact that the mapping $t \mapsto \xi^t(\theta, x)$ is the solution to (1.2) with forcing function $F(t)$. A similar flow representation can be given in the case of random forcing, however, with $F(t)$ modeled by a random process that is uniformly bounded. In the hybrid case, $F(t)$ is modeled by a combination of both quasiperiodic and random forcing terms. The precise formulae for $F(t)$ in all cases will be given later in Chapter 3. We will also describe this passage from non-autonomous equations to skew product flows in more detail in the subsequent sections, but also refer the mathematically interested reader to standard references such as [Arn98, HY09] for further reading. Moving back to the quasiperiodic forcing, in the discrete time case, quasiperiodic motion is given by a rotation $\rho : \mathbb{T}^d \rightarrow \mathbb{T}^d$, $\theta \mapsto \theta + \rho \bmod 1$ which is *irrational*, in the sense that its rotation vector $\rho = (\rho_1 \cdots \rho_d)$ has incommensurate entries.² In this case, the transformation ρ is minimal and uniquely ergodic, with the Lebesgue measure on \mathbb{T}^d as the unique invariant probability measure. To be precise, we will consider some well-established examples that have been studied with rigorous results in discrete and continuous time in a class of quasiperiodically forced systems. Our main aim of reviewing the quasiperiodic results is due to the fact that we add some original numerical results regarding the Allee-model in Chapter 3, as well as establishing early warning signals for anticipating a bifurcation in qpf systems of this type.

Non-smooth fold bifurcations in qpf systems. In the case of quasiperiodic forcing, the occurrence of non-smooth fold bifurcations is well-established by a number of rigorous results both in discrete and continuous-time case, which include the work of Jäger, Fuhrmann, Keller, to mention but a few [Jäg09, Jäg03, Fuh16a, Fuh16b, Kel96]. We first consider a discrete time example given by a parameter family of skew product maps of the form

$$f_\beta : \Theta \times X \rightarrow \Theta \times X, \quad (\theta, x) \mapsto (\rho(\theta), \arctan(\alpha x) - \kappa \cdot F(\theta) - \beta), \quad (2.16)$$

where the base map $\rho : \Theta \rightarrow \Theta$, $\theta \mapsto \theta + \rho$ is the irrational rotation with rotation vector ρ and $f_\theta(\cdot)$ is \mathcal{C}^2 and strictly increasing on X . For the forcing

¹Composed of the d incommensurate frequencies ν_i in (3.1).

²Here $\rho_1 \cdots \rho_d$ are called *incommensurate* if $n_0 + \sum_{j=1}^d n_j \rho_j = 0$ implies $n_0 = n_1 = \dots = n_d = 0$.

function F , we use

$$F(\theta) = \frac{\sin(2\pi\theta) + 1}{2}. \quad (2.17)$$

This example was used in [Fuh16a] to establish rigorous results on the occurrence of non-smooth bifurcations in a family of qpf monotone systems. Before we state the results, we show the behaviour of the attractors and repellers during the smooth and non-smooth bifurcations in example (2.16) with forcing function (2.17) in Figure 2.1. This figure also illustrates some key features of non-smooth bifurcations in qpf systems and allows us to give a heuristic description of the mechanism that causes the non-smoothness. The rigorous description of this mechanism is the basis for the mathematical analysis of non-smooth bifurcations in [Jäg09, Fuh16a]. As can be seen in Figure 2.1, when the attracting and repelling graphs approach each other in a non-smooth way, they develop a sequence of ‘peaks’. These appear in an ordered way, and the next peak is always the image of the previous one and is generated as soon as the latter reaches into the region with large derivatives, which is centred around the 0-line $\mathbb{T}^1 \times \{0\}$. The first peak is located around the minimum of the blue curve in (d). The second peak emerges in (e) and is fully developed in (f), where a number of further peaks can be seen as well. Thereby, the movement of each peak is amplified by the large derivatives close to zero (of magnitude α , see (2.16)). For this reason, as β is increased, the speed by which the peaks move as β is varied increases exponentially with the order of the peak, whereas its width decreases exponentially (since each peak is stretched vertically due to the expansion around 0). In the limit, one may think that the two curves touch each other with the tips of the peaks although in reality they become discontinuous at the bifurcation point and actually coincide on a residual set. Note that only a finite number of peaks can be observed at the bifurcation point in (f), since these quickly become too thin to be visible in numerical simulations. However, it is known that the region between the two graphs in (f) is actually filled densely by further peaks [GJ13, FGJ18]. We refer to the introduction of [Jäg09] for a more detailed discussion.

Now we provide some of the rigorous statements on non-smooth fold/saddle-node bifurcations based on the description given above. In the formulation of the results, the occurrence of non-smooth saddle-node bifurcations in a class of qpf monotone forced interval maps is characterized by some properties. Thereby, the arithmetic properties of the rotation vector play a crucial

role that guarantees slow recurrence on the base.

Definition 2.20. Given $\tau, \eta > 0$, we say that $\rho \in \mathbb{T}^d$ is diophantine of type (τ, η) if

$$\forall k \in \mathbb{Z}^d \setminus \{0\} : \inf_{p \in \mathbb{Z}} \left| p + \sum_{i=1}^d \rho_i k_i \right| \geq \tau |k|^{-\eta}. \quad (2.18)$$

Consider the space of one-parameter families

$$\mathcal{F}_\rho = \{(f_\beta)_{\beta \in [0,1]} : f_\beta \text{ is of the form (2.10) and } (\beta, \theta, x) \mapsto f_{\beta, \theta}(x) \text{ is } \mathcal{C}^2\} \quad (2.19)$$

equipped with the metric

$$d((f_\beta)_{\beta \in [0,1]}, (g_\beta)_{\beta \in [0,1]}) = \sup_{\beta \in [0,1]} (\|f_\beta - g_\beta\|_2 + \|\partial_\beta f_\beta - \partial_\beta g_\beta\|_0).$$

Then the following result is established in [Fuh16a], with precursors in [Bje05, Jäg09].

Theorem 2.21 ([Fuh16a, Theorem, 3.1]). *Suppose that $\rho \in \mathbb{T}^d$ is Diophantine. Then there exists a non-empty open set $\mathcal{U} \subseteq \mathcal{F}_\rho$ such that each $(f_\beta)_{\beta \in [0,1]} \in \mathcal{U}$ satisfies the assertions of Theorem 2.18 and undergoes a non-smooth saddle-node bifurcation.*

This set \mathcal{U} is essentially characterised by a collection of assumptions on the derivatives of the fibre maps f_β up to second order. For an explicit example, the interested reader may refer to [Fuh16a]. The theorem confirms that the set of parameter families with a non-smooth saddle-node bifurcation is large in a certain sense, and that the phenomenon can occur in a robust way (both corresponding to the openness of the set \mathcal{U}). Thereby, it is important to note that in [Fuh16a], the set \mathcal{U} in this result is characterised by explicit \mathcal{C}^2 -estimates. This makes it possible to check if it contains a given parameter family and therefore, provides explicit examples of non-smooth saddle-node bifurcations. In this particular example (2.16), where $X \subseteq \mathbb{R}$ with real parameters $\alpha > \pi/2$, $\kappa \in (0, 1)$ and $\beta \in [0, 1]$, the following result holds.

Corollary 2.21.1 ([Fuh16a]). *If ρ is Diophantine and α is sufficiently large, then the parameter family $(f_\beta)_{\beta \in [0,1]}$ defined in (2.16) belongs to the set \mathcal{U} and hence undergoes a non-smooth saddle-node bifurcation.*

The non-smoothness of the bifurcation scenario following from this result can be visualized in Figure 2.1(f), where $\alpha = 100$ in this case.

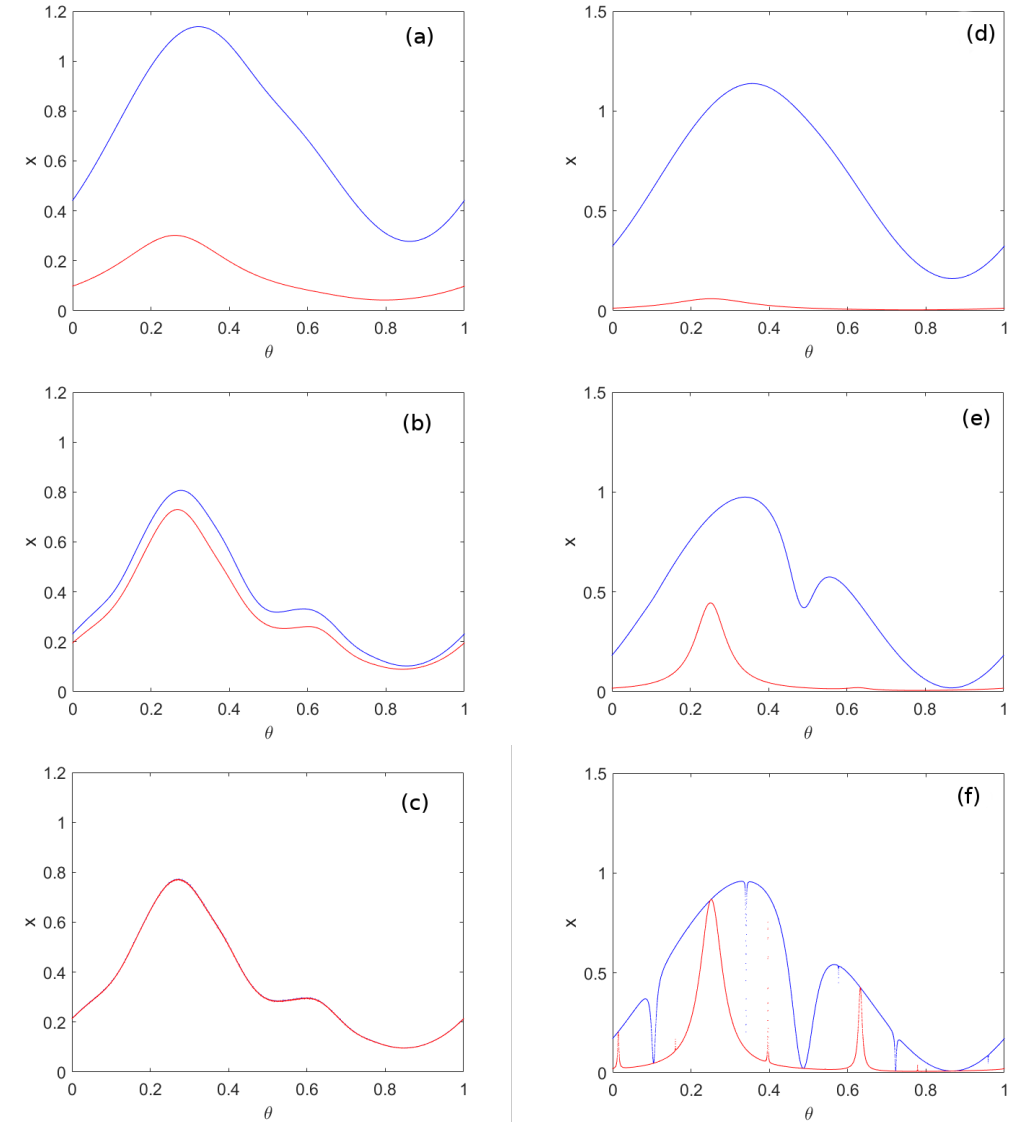


Figure 2.1: **(a)–(c)**: Smooth saddle-node bifurcation in (2.16) with quasiperiodic forcing. Parameter values are $\alpha = 10$, $\kappa = 1$, $\rho = \omega$ (golden mean) and (a) $\beta = 0.2$ (b) $\beta = 0.34$ and (c) $\beta = 0.341502$.

(d)–(f): Non-smooth saddle-node bifurcation in (2.16) with quasiperiodic forcing. Parameter values are $\alpha = 100$, $\kappa = 1$, $\rho = \omega$ and (a) $\beta = 0.2$ (b) $\beta = 0.6$ and (c) $\beta = 0.866$.

We now turn to the continuous-time case. Quasiperiodically forced flows are

typically defined via non-autonomous ODE's of the form

$$x'(t) = V_\beta(\rho^t(\theta), x), \quad (2.20)$$

where $\rho : \mathbb{R} \times \mathbb{T}^d \rightarrow \mathbb{T}^d$, $(t, \theta) \mapsto \theta + t\rho$ is an irrational Kronecker flow with rotation vector $\rho \in \mathbb{T}^d$. Results on systems of the form (2.20) with a quasiperiodic forcing have been established in [Fuh16b]. In this case, one considers non-autonomous vector fields, given by differentiable functions of the form (2.11)-(2.12). In fact, system (2.20) a priori only yields a *local* flow, where trajectories may diverge and may hence not be defined for all times $t \in \mathbb{R}$. As we will only deal with bounded solutions (see also Lemma 3.5), this issue is not of further importance here. We refer the interested reader to [Fuh16b] for more details. Now, in order to apply the above statements to flows defined by equations of the form (2.20), it is crucial that the validity of the assumptions can be read off directly from the differential equations since the flow itself is not explicitly provided. Fortunately, there is a rather immediate translation between the properties of parameter families of non-autonomous vector fields V_β and the relevant properties of the resulting skew product flow. To show how these properties translate, first, the curves ϕ^\pm can usually be chosen constant, in which case condition (i) in Theorem 2.18 may be checked by hand. We also require that the following conditions hold;

$$V_\beta(\theta, \phi^\pm) \leq 0; \quad (2.21)$$

$$\partial_x^2 V_\beta(\theta, x) < 0 \text{ for all } x \in [\phi^-, \phi^+]; \quad (2.22)$$

$$\partial_\beta V_\beta(\theta, x) < 0 \text{ and there is } \theta_0 \text{ such that } \partial_\beta V_\beta(\theta_0, x) < 0 \text{ for all } x \in [\phi^-, \phi^+]; \quad (2.23)$$

$$V_0 \text{ has two continuous invariant graphs and } V_1 \text{ has no invariant graph in } \Gamma. \quad (2.24)$$

This implies that condition (ii) follows from (2.22) for all $\theta \in \Theta$. Secondly, by standard results on the regularity of the dependence of solutions of an ODE on parameters, it suffices to assume that for each $\theta \in \Theta$, the mapping $[0, 1] \times \mathbb{R} \times \mathbb{R} \ni (\beta, t, x) \mapsto V_\beta(\rho^t(\theta), x)$ is continuous, \mathcal{C}^1 with respect to β and \mathcal{C}^2 with respect to x , in order to ensure that Ξ_β is indeed \mathcal{C}^2 and continuously differentiable with respect to β . Hence, the above expressions are well-defined and (iii) is verified, too. The monotonicity in (iv) follows immediately from the uniqueness of the solutions to (2.20). The monotonicity condition (v) follows from (2.24). Finally, the concavity of the fibre maps

required in (vi) is a consequence of the concavity of V_β in the considered region and this is guaranteed by (2.22). We refer to [AJ12, Fuh16b] for further details, as well as to the discussion of the application to the forced Allee-effect model in Chapter 3. Let

$$\mathcal{V}_\rho = \{(V_\beta)_{\beta \in [0,1]} \mid V \text{ is of the form (2.11) and } (\beta, \theta, x) \mapsto V_\beta(\theta, x) \text{ is } \mathcal{C}^2\} \quad (2.25)$$

be the space of one parameter families of differentiable flows and equip \mathcal{V}_ρ with the metric

$$d((V_\beta)_{\beta \in [0,1]}, (W_\beta)_{\beta \in [0,1]}) = \sup_{\beta \in [0,1]} (\|V_\beta - W_\beta\|_2 + \|\partial_\beta V_\beta - \partial_\beta W_\beta\|_0).$$

Theorem 2.22 ([Fuh16b, Theorem, 1.11]). *For any Diophantine $\rho \in \mathbb{T}^d$, there exists an open set $\mathcal{U}_\rho \subseteq \mathcal{V}_\rho$ such that for any $(V_\beta)_{\beta \in [0,1]} \in \mathcal{V}_\rho$ the flow induced by (2.11) satisfies the assertions (2.22)-(2.24) and undergoes a non-smooth fold bifurcation.*

Again, the explicit characterisation of the set \mathcal{U}_ρ given in [Fuh16b] makes it in principle possible to check for non-smooth bifurcations in specific examples. However, this is considerably more technical than in the discrete-time case. Moreover, the application to continuous time systems (1.2), which is the single species Allee effect population model with quasiperiodic forcing (3.1) would require a number of highly non-trivial and technical modifications.

2.3.2 Saddle-node bifurcations in randomly forced systems

Randomly forced skew product flows are defined in a similar manner as deterministically forced systems, only that in this case we consider the base space to be a measure preserving dynamical system.

Definition 2.23. A random dynamical system is a pair (σ, f) on a measurable space (X, \mathcal{A}) over a metric dynamical system $(\Sigma, \mathcal{F}, \mu, \sigma)$ with $\mathbb{T} = \mathbb{R}$ or \mathbb{Z} , that is

$$f : \mathbb{T} \times \Sigma \times X \rightarrow X, \quad (t, \omega, x) \mapsto f(t, \omega, x)$$

such that the following properties hold

- the mapping $x \mapsto f(t, \omega, x)$ is \mathcal{F} -measurable.

- the mappings $f(t, \omega) = f(t, \omega, \cdot) : X \rightarrow X$ satisfy the cocycle property:

$$f(0, \omega) = id, \quad f(t + s, \omega) = f(t, \sigma^s(\omega)) \circ f(s, \omega)$$

for all $s, t \in \mathbb{T}$, $\omega \in \Sigma$.

In order to distinguish between the space in the random setting from the deterministic setting, we denote the driving mpds by $(\Sigma, \mathcal{F}, \mu, \sigma)$. This will be helpful in the setting and formulation of further results in the hybrid-forced case. To describe fold/saddle-node bifurcations in this setting, we again consider parameter families of the form (2.3) with the base space Σ . Therefore, given a mpds $(\Sigma, \mathcal{F}, \mu, \sigma)$, a randomly forced skew product flow with base space Σ is a flow on $\Sigma \times X$ of the form

$$\Xi_\beta : \mathbb{T} \times \Sigma \times X \rightarrow \Sigma \times X, \quad (\omega, x) \mapsto \Xi_\beta^t(\omega, x) = (\sigma(\omega), \xi_\beta^t(\omega, x)) \quad (2.26)$$

for each $\omega \in \Sigma$. The fibres $\xi_\beta^t : X \rightarrow X$ are continuous and for each $x \in X$ and $\omega \mapsto \xi_\beta^t(\omega, x)$ is \mathcal{F} -measurable. The skew product described in (2.26) is assumed to be a random dynamical system in the sense of [Arn98]. In particular, the flow satisfies the following properties:

- the flow $x \mapsto \xi_\beta^t(\omega, x)$ is \mathcal{F} -measurable.
- the flow $\Xi_\beta^t(\omega, \cdot) : X \rightarrow X$ satisfies the cocycle property:

$$\Xi_\beta^0(\omega, x) = id, \quad \Xi_\beta^{t+s}(\omega, x) = \Xi_\beta^t(\sigma^s(\omega)) \circ \Xi_\beta^s(\omega, x)$$

for all $s, t \in \mathbb{T}$, $\omega \in \Sigma$.

Therefore the skew product system (2.26) generates a random dynamical system. Similarly, the continuous time analogue is generated via a non-autonomous vector field of the form (2.12) where (Θ, ρ) is replaced by $(\Sigma, \mathcal{F}, \mu, \sigma)$. Hence, the resulting flow is generated by a random ordinary differential equation (RODE) of the form

$$\partial_t \xi_\beta(t, \omega, x) = V_\beta(\sigma^t(\omega), \xi_\beta(t, \omega, x)). \quad (2.27)$$

Such random differential equations can be solved pathwise for each ω as a deterministic non-autonomous ODE, and thus the corresponding solution is given by

$$\xi_\beta(t, \omega, x) = x + \int_0^t V_\beta(\sigma^s(\omega), \xi_\beta(s, \omega, x)) ds,$$

which exists locally for all $t \in B_r(0)$, $r, t \in \mathbb{R}$. We say that $t \mapsto \xi_\beta(t, \omega, x)$ solves the random ordinary differential equation (2.27). We will not go into further details of random dynamical systems, but refer the interested reader to [Arn98] for more details. To describe saddle node bifurcations, we provide a setting analogous to the deterministic setting, which allows for the occurrence of fold/saddle-node bifurcations in randomly forced systems. This was established in [AJ12] and it states as follows; Suppose that $(\Sigma, \mathcal{F}, \mu, \sigma)$ is a mpds and consider parameter families of σ -forced monotone \mathcal{C}^2 -flows $(\Xi_\beta)_{\beta \in [0,1]}$ of the form (2.3). Then we have the following statement.

Theorem 2.24 ([AJ12, Theorem 4.1]). *Let $(\Sigma, \mathcal{F}, \mu, \sigma)$ be a measure preserving dynamical system and suppose $(\Xi_\beta)_{\beta \in [0,1]}$ is a parameter family of σ -forced monotone \mathcal{C}^2 -flows. Further assume that there exist measurable functions $\phi^-, \phi^+ : \Theta \rightarrow X$ with $\phi^- < \phi^+$ such that the following conditions hold for all $\beta \in [0, 1]$, $\omega \in \Sigma$ and positive $t \in \mathbb{T}$, where applicable.*

- (i) *There exist two μ -uniformly separated (Ξ_0, μ) -invariant graphs but no (Ξ_1, μ) -invariant graph in Γ ;*
- (ii) $\xi_\beta^t(\omega, \phi^\pm(\omega)) \leq \phi^\pm(\sigma^t(\omega))$;
- (iii) *the maps $(\beta, t, x) \mapsto \xi_\beta^t(\omega, x)$ and $(\beta, t, x) \mapsto \partial_x \xi_\beta^t(\omega, x)$ are continuous;*
- (iv) $\partial_x \xi_\beta^t(\omega, x) > 0 \forall x \in \Gamma_\omega$;
- (v) *for some $t > 0$ there exist constants $C < c_1 \leq 0$ such that $C \leq \partial_\beta \xi_\beta^t(\omega, x) \leq c_1 \forall x \in \Gamma_\omega$;*
- (vi) $\partial_x^2 \xi_\beta^t(\omega, x) < 0 \forall x \in \Gamma_\omega$;
- (vii) *the function $\eta(\omega) = \sup \left\{ \left| \log \partial_x \xi_\beta^t(\omega, x) \right| \mid x \in \Gamma_\omega, \beta \in [0, 1] \right\}$ is integrable with respect to μ .*

Then there exists a unique critical parameter $\beta_\mu \in [0, 1]$ such that

- *If $\beta < \beta_\mu$, then there exist exactly two (Ξ_β, μ) -invariant graphs $\varphi_\beta^- < \varphi_\beta^+$ in Γ which are μ -uniformly separated and satisfy $\lambda(\varphi_\beta^-) > 0$ and $\lambda(\varphi_\beta^+) < 0$.*
- *If $\beta = \beta_\mu$, then either there exists exactly one (Ξ_β, μ) -invariant graph φ_β in Γ , or there exist two measurably pinched invariant graphs $\varphi_\beta^- \leq \varphi_\beta^+$ in Γ . In the first case, $\lambda_\mu(\varphi_\beta) = 0$; in the second case, $\lambda_\mu(\varphi_\beta^-) > 0$ and $\lambda_\mu(\varphi_\beta^+) < 0$.*

- If $\beta > \beta_\mu$, then no Ξ_β -invariant graphs exist in Γ .

In analogy to the deterministic setting, we again speak of a smooth bifurcation if there exists a unique neutral invariant graph at the bifurcation point, and a non-smooth bifurcation if there exists an attractor-repeller pair. To illustrate this pattern, we consider the discrete time example (2.16) with forcing process $F(\omega)$, which is now a uniformly bounded noise generated on Σ . To generate random noise in discrete time, we use the shift space as an example for the driving space (i.e. $\Sigma = \Sigma_2^{\mathbb{Z}} = \{0, 1\}^{\mathbb{Z}}$), which is the space of bi-sided infinite sequences $(\omega_i)_{i=-\infty}^{\infty}$ on two symbols $\{0, 1\}$, that is,

$$\Sigma = \{\omega = (\omega_i)_{i \in \mathbb{Z}} : \omega_i \in \{0, 1\} \text{ for all } i \in \mathbb{Z}\}. \quad (2.28)$$

This transformation $\sigma : \Sigma \rightarrow \Sigma$ is simply the shift operator that shifts the digits of a sequence $\omega \in \Sigma$ one step to the left, i.e. $\sigma(\omega_i)_{i=-\infty}^{\infty} = (\omega_{i+1})_{i=-\infty}^{\infty}$. The σ -algebra on this space is generated by cylinder sets of the form;

$$C_{\omega_1, \dots, \omega_i}^{l_1, \dots, l_i} = \{\omega' \in \Sigma : \omega'_{l_k} = \omega_{l_k}, \forall k = 1, \dots, i\}, \quad (2.29)$$

where $l_1, \dots, l_i \in \mathbb{Z}$, $\omega_k \in \{0, 1\}$, and the measure on these sets is the Bernoulli measure μ with probabilities $1/2$ for the symbols 0 and 1. To be precise, we simply use the Bernoulli process with equal weights as an example to generate the random forcing, but the result remains valid for general strictly positive weights as well. To translate this to numerical simulations, we use the Baker's map, which is an invertible map that is semi-conjugated to the bi-infinite shift space. However, in the derivation of the analytical results of this work, actually, we could likewise set Σ to be $\Sigma_{\mathbb{R}} = [0, 1]^{\mathbb{Z}}$ and μ to be the infinite product $\text{Leb}_{[0,1]}^{\mathbb{Z}}$ of the Lebesgue measure on $[0, 1]$, or even replace $\text{Leb}_{[0,1]}$ by any measure λ on $[0, 1]$ whose topological support is not a singleton. One such measure could be the Lebesgue measure on each factor interval $[0, 1]$. In any case, the dynamics on Σ are given by the shift map $\sigma : \Sigma \ni (\omega_n)_{n \in \mathbb{Z}} \mapsto (\omega_{n+1})_{n \in \mathbb{Z}}$ which is ergodic with respect to each such measure. This will be mainly used in Chapter 3, and also throughout the subsequent chapters of this work to prove most of the rigorous results. However, for now, we state the forcing function, which we use to generate uniformly bounded noise in example (2.16) below;

$$F(\omega) = \omega_0. \quad (2.30)$$

The parameter κ in example (2.16) then determines the intensity of the noise. The numerical results with such a forcing function (2.30) will be

presented later in Chapter 3.

Now, moving on to the continuous time case, the flow Ξ takes the same form as in (2.15), however, the space Σ is a space of bounded continuous functions generated from Wiener paths of Brownian motion such that in this way, the random process ω is uniformly bounded, as unbounded noise does not allow for the phenomenon we want to describe. In both discrete and continuous time, we observe that the geometry of the random equilibrium at the bifurcation is slightly different from the quasiperiodic case, as they only touch at one point. This behaviour of the attractor and the repeller before and at the saddle node bifurcation is shown in Chapter 3.

2.3.3 Hybrid-forced systems

Finally, to conclude this chapter, we introduce the so-called hybrid-forced systems as a special class of randomly forced skew product systems. As stated earlier in the introduction, the hybrid-forced systems belong to a family of skew product systems with a forcing process which is a combination of both deterministic and random forcing terms. This structure which leads to a double skew product, is what we refer to as a hybrid-forced system. From our own understanding, such systems have not yet been extensively studied. However, very closely related systems that have appeared in literature include the work of Jäger and Keller in [JK16]. In their work, they give a mathematical framework and provide versions of semi-uniform ergodic theorems, as a criterion for investigating invariant graphs together with their Lyapunov exponents. However, the bifurcation scenario was not explored, which gives us a leeway to delve in that direction and investigate what actually happens. Having understood the saddle-node bifurcation scenario in qpf and randomly forced systems, as a follow up, it would be interesting to understand whether any of the two forcing processes poses a dominating effect on the fold/saddle-node bifurcation pattern in the hybrid forced case. Alternatively, we may ask if we observe a totally different behaviour. Besides just studying the saddle-node bifurcation, we would like to think that such scenarios could play out in real life situations, although we do not have specific examples we could relate to at the moment. Analogous to the deterministic and randomly forced skew product systems discussed in the previous sections, we will treat discrete-time alongside continuous time dynamics in the hybrid forced case as well. To that end, let (Θ, ρ) be a tds

and $(\Sigma, \mathcal{F}, \mu, \sigma)$ be a mpds. A hybrid-forced skew product system is a flow Ψ , with base space $\Theta \times \Sigma$ together with a transformation $\sigma \times \rho$ and phase space X on $\Theta \times \Sigma \times X$ of the form

$$\begin{aligned} \Psi : \mathbb{T} \times \Theta \times \Sigma \times X &\rightarrow \Theta \times \Sigma \times X, \\ (t, \theta, \omega, x) &\mapsto \Psi^t(\theta, \omega, x) = (\rho(\theta), \sigma(\omega), \psi^t(\theta, \omega, x)), \end{aligned} \quad (2.31)$$

where the flow ρ and σ are as defined in the deterministic and random setting respectively. The fibre maps $\psi^t(\theta, \omega, x) : X \rightarrow X$ in this case are defined over the product space with base coordinates (θ, ω) , given by $\psi^t(\theta, \omega, x) = \psi_{\theta, \omega}^t(x)$. We adapt standard definitions from the skew product setting (2.3) to the hybrid-forced system, where the product space $(\Theta \times \Sigma)$ serves as the base space. With this construction, standard definitions will always apply without having to redefine them. We equip Θ with the usual Borel σ -algebra \mathcal{B} and fix some ρ -invariant measure ν on Θ such that, $(\Theta, \mathcal{B}, \nu, \rho)$ is a mpds. Let $M = \Theta \times \Sigma$, $\mathcal{G} = \mathcal{B} \times \mathcal{F}$, $T = \rho \times \sigma$ and $m = \nu \times \mu$. Then (M, \mathcal{G}, m, T) is a mpds as well, where T preserves the measure m on the tensor σ -algebra \mathcal{G} . Depending on the examples we consider for the spaces Θ and Σ , we may obtain ergodicity of (M, \mathcal{G}, m, T) due to Theorem 2.1. With this construction, one arrives at a random dynamical system of the form (2.26) in the sense of Arnold [Arn98]. This implies that the results formulated for randomly forced systems can be applied to obtain the desired results. Alternatively, one can say that the results in this case are an extension of the findings in the randomly forced case. For that matter, we regard the hybrid forced system as a special case of a randomly forced skew product system and notions such as invariant graphs, Lyapunov exponents and pinching can be defined in the measurable sense. To that end, given a mpds (M, \mathcal{G}, m, T) , we define an invariant graph of the system (2.31) as a measurable function $\varphi : M \rightarrow X$ such that

$$\Psi_{\theta, \omega}^t(\varphi(\theta, \omega)) = \varphi(\rho^t(\theta), \sigma^t(\omega)) \quad (2.32)$$

holds for $m - a.e$ $(\theta, \omega) \in M$. The corresponding Lyapunov exponents of invariant graphs of the flow Ψ are given by

$$\lambda_m(\varphi) = \frac{1}{t} \int_M \log \|\partial_x \psi^t(\theta, \omega, \varphi(\theta, \omega))\| dm(\theta, \omega) \quad m - \text{almost surely.} \quad (2.33)$$

In the same way, invariant graphs of ψ are attracting if $\lambda_m(\varphi) < 0$, and repelling otherwise.

Remark 2.25. We would like to point out that in as much as we observe similarities in the systems studied in [JK16], there are some slight differences in the setting provided. In [JK16], the deterministic component in the base depends on the random component whereas in our setting, this kind of interaction is not allowed. Rather, the dynamics of the deterministic and random parts evolve independently of each other as seen in (2.31). When it comes to describing the saddle-node bifurcation, this may lead to slightly different results due to some technicalities that maybe involved. However, we cannot tell how technical it can get as the bifurcation scenario for any of the two cases was not rigorously discussed. This would call for further investigation into the bifurcation scenario in the systems considered in [JK16], which goes beyond the scope of this thesis.

Fold bifurcation scenario in hybrid-forced systems. To describe fold/saddle-node bifurcations in hybrid-forced systems, as a rule of thumb, we need to provide the setting for this to happen. However, this becomes easier in this case, given that, if we ignore the fact that Σ has a topological structure as we assume in the description in the previous section, and treat $\Theta \times \Sigma$ as the base space with an invariant measure m , then we can apply the measure theoretic results also in this setting. Without making further repetitions, smooth and non-smooth bifurcations are defined similarly as in the randomly forced case following from Theorem 2.24. A suitable example that we will consider to generate a hybrid forcing is the irrational rotation on the torus Θ and the shift map on the sequence space Σ , that is

$$\rho \times \sigma : \Theta \times \Sigma \rightarrow \Theta \times \Sigma, \quad (\theta, \omega) \mapsto (\rho(\theta), \sigma(\omega)) \quad (2.34)$$

Precise examples will be given in Chapter 3. Furthermore, we will use these examples to show that under some mild technical assumptions, the saddle node bifurcation under forcing process generated by (2.34) will always be non-smooth. Does this imply a generic property about bifurcations in systems perturbed by a random component? Well, maybe we can give a suitable answer after providing the rigorous results in Chapter 3.

Remark 2.26. The examples of the forcing (2.34) is an ergodic mpds. This is a consequence of Theorem 2.1, which provides for ergodicity on M . The

irrational rotation on Θ is ergodic with respect to the Lebesgue measure ν and the map σ on Σ is also ergodic with respect to the Bernoulli measure μ . At the same time, the dynamics of σ is weakly mixing with respect to the Bernoulli measure. Thus by Theorem 2.1, T is ergodic with respect to the product measure $m = \left(\left(\frac{1}{2} \text{Leb}_{[-1,1]}\right)^{\mathbb{Z}} \times \text{Leb}_{\Xi}\right)$. In this case, we have a stronger assumption of ergodicity on the base space M , as we only require the space to be measure preserving in the formulation of the results.

Chapter 3

Non-smooth fold and saddle-node bifurcations

Given the definitions and the technical background, we now want to state and prove some of the main results of this thesis in this chapter. The results discussed in the previous chapter mainly provide a general setting for the occurrence of non-autonomous saddle-node bifurcations in a class of skew product systems. We also discussed the occurrence of non-smooth fold bifurcations in a class of qpf monotone interval maps. We now want to specifically look at non-smooth bifurcations and discuss their general widespread occurrence in forced systems. Just briefly recall from Section 2.3.1 that the result in Theorem 2.22 on non-smooth fold bifurcations in qpf systems does not cover the Allee model. Using the methods in this theorem, it should be possible to give a rigorous proof, but due to the technicalities, this goes beyond the scope of the current thesis. We therefore first provide some numerical results to show the occurrence of non-smooth fold bifurcations in the Allee model with a quasiperiodic forcing.

3.1 Fold/saddle-node bifurcations in qpf Allee-effect model.

The model draws its relevance from biological population dynamics models as shown in (1.1). The forced version of the above model (1.1), is given by non-autonomous scalar ODEs of the form (1.2). The quasiperiodic forcing in this case corresponds to the influence of several periodic external factors

with incommensurate frequencies $\nu_1, \dots, \nu_d \in \mathbb{R}$. As a specific example, we choose the forcing function as

$$F(t) = \prod_{i=1}^d \left(\frac{1 + \sin(2\pi(\theta_i + t \cdot \nu_i))}{2} \right)^q, \quad (3.1)$$

with arbitrary initial conditions $\theta_1, \dots, \theta_d \in \mathbb{R}$ and $q \in \mathbb{N}$. Let us note here that due to the periodicity of the sine function, these initial values may also be viewed as elements of the circle $\mathbb{T}^1 = \mathbb{R}/(2\pi\mathbb{Z})$ so that $\theta = (\theta_1, \dots, \theta_d)$ becomes an element of the d -torus $\mathbb{T}^d = \mathbb{R}^d/(2\pi\mathbb{Z})^d$. In this case, we take $d = 2$. Hence, a non-autonomous equilibrium can be thought of as a curve, surface or higher-dimensional submanifold of the product space $\mathbb{T}^1 \times \mathbb{T}^1 \times \mathbb{R}$, that can be represented as a graph over the 2-dimensional product base space $\mathbb{T}^1 \times \mathbb{T}^1$. This is invariant under the skew product flow Ξ and is composed of solutions of (1.2) with varying initial conditions. With this new notion of an equilibrium, fold bifurcations in forced systems can be described, in perfect analogy to the classical case, as the collision and subsequent extinction of a stable and an unstable equilibrium [NO07, AJ12]. This process is shown in Figure 3.1(a)–(d) where two such equilibrium manifolds approach each other and then merge to form a neutral equilibrium which yields the smooth saddle-node bifurcation. Figure 3.1(e)–(h) provides numerical evidence for the occurrence of non-smooth fold bifurcations. However, the simulations in Figure 3.1, provide numerical evidence for the occurrence of non-smooth bifurcations in the qpf Allee model. And as we can observe, the characteristics with the development of the peaks is the same as seen in the pictures before in Chapter 2.

3.2 Non-smooth fold bifurcations in randomly forced systems

In contrast to the quasiperiodic case, the influence of bounded random noise on saddle-node bifurcations has not been studied systematically so far. Our aim for the remainder of the chapters is to establish the occurrence of non-smooth bifurcations in a broad class of randomly forced monotone flows and maps. Despite the fact that the measure theoretic analogue for the setting of saddle-node bifurcations provides for a large class of base maps, in order to prove non-smooth saddle-node bifurcations in the particular random families

introduced in this work, we need to impose a number of assumptions. This will enable us to obtain rigorous results in a more generic sense. To that end, we introduce the notion of an autonomous reference system. Let $\gamma^- < \gamma^+ \in \mathbb{R}$ and suppose $(g_\beta)_{\beta \in [0,1]}$ is a one-parameter family of differentiable flows $g_\beta : \mathbb{T} \times \mathbb{R} \rightarrow \mathbb{R}$ with the following properties (which are supposed to hold for all $\beta \in [0, 1]$, $t \in \mathbb{T}$ and $x \in \mathbb{R}$, where applicable).

- (g1) g_0 has two fixed points in the interval $[\gamma^-, \gamma^+]$, whereas g_1 has none;
- (g2) $g_\beta^t(\gamma^\pm) \leq \gamma^\pm$;
- (g3) $\partial_x g_\beta^t(x) > 0$;
- (g4) the mapping $(\beta, t, x) \mapsto g_\beta^t(x)$ is continuous;
- (g5) the mapping $\beta \mapsto g_\beta^t(x)$ is differentiable and $\partial_\beta g_\beta^t(x) < 0$;
- (g6) $\partial_x^2 g_\beta^t(x) < 0$ for all $x \in [\gamma^-, \gamma^+]$ (*concavity*).

We call such a family $(g_\beta)_{\beta \in [0,1]}$ an (*autonomous*) *reference family*.

Remark 3.1. (a) Properties (g1)–(g6) imply that the family $(g_\beta)_{\beta \in [0,1]}$ undergoes a fold bifurcation in the interval $[\gamma^-, \gamma^+]$. Due to the concavity in (g6), g_β can have at most two fixed points in this region, with the upper one attracting and the lower one repelling. By (g1), the map g_0 has two such fixed points. Due to the monotone dependence on the parameter assumed in (g5), these two fixed points have to move towards each other as β is increased. They have to vanish before $\beta = 1$, as g_1 has no fixed points, and the only possibility to do so is to collide at a unique bifurcation parameter β_c .

(b) If $\mathbb{T} = \mathbb{Z}$ (that is in the discrete time case), the simplest way to obtain a reference family of this kind is to fix some strictly increasing map $g : \mathbb{R} \rightarrow \mathbb{R}$ such that g maps the points γ^\pm below themselves, is strictly concave on $[\gamma^-, \gamma^+]$ and has two fixed points in $[\gamma^-, \gamma^+]$, but $g - 1$ does not have any fixed points in this interval. Then $g_\beta = g - \beta$ satisfies the above properties.

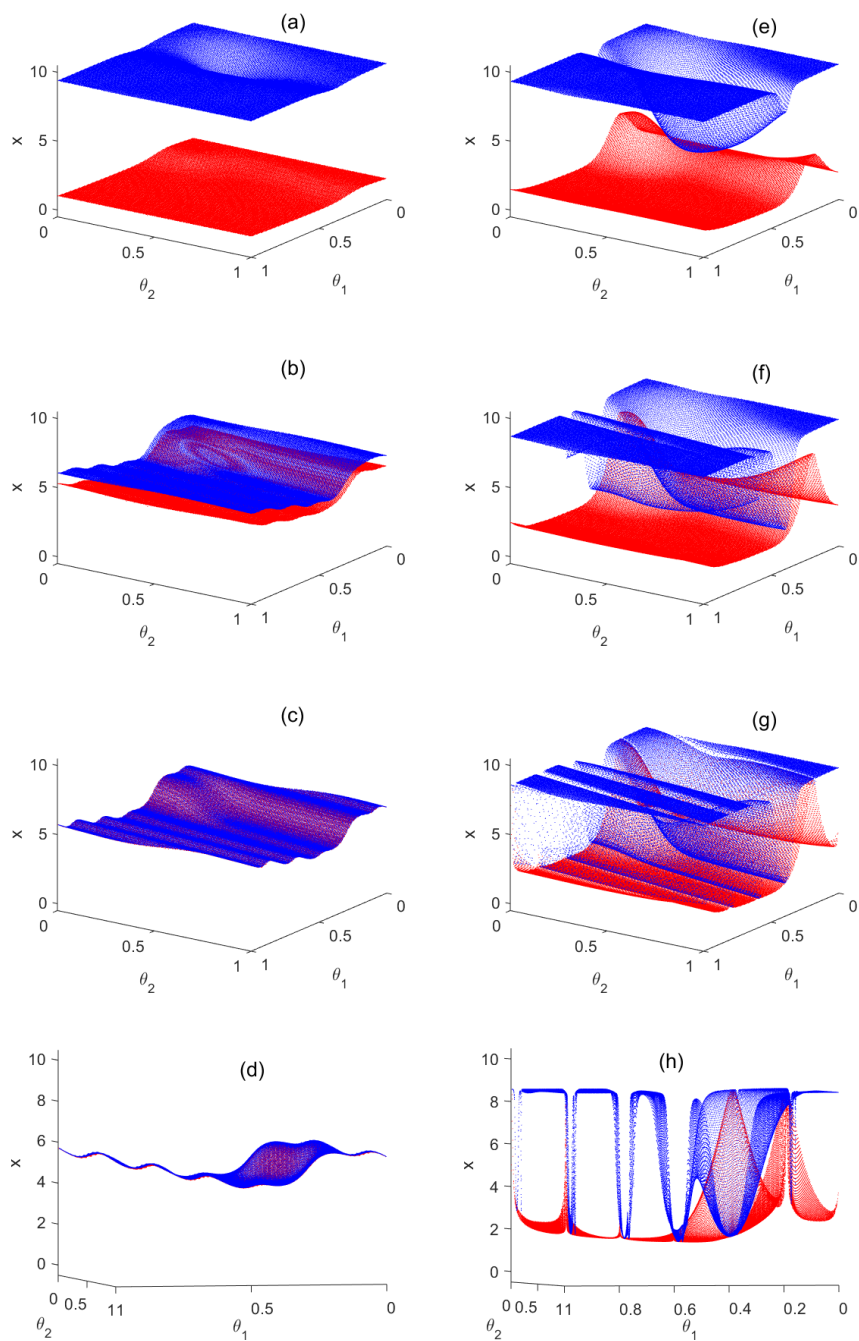


Figure 3.1: **(a)–(d)**: Smooth fold bifurcation in the qpf Allee model with parameters $r = 35$, $K = 10$, $S = 0.1$, $q = 3$ and $\kappa = 4$ and $\beta = 2$ in (a), $\beta = 7.8$ in (b) and $\beta = 7.8455$ in (c) and (d). These last two figures show the attractor (blue) and the repeller (red) at the bifurcation point from two different angles. The rotation vector ρ is $\rho = (5\omega, 5\pi)$ in all cases, where ω is the irrational part of the golden mean.

(e)–(h): Non-smooth fold bifurcation in the qpf-Allee model with parameters $r = 80$, $K = 10$, $S = 0.1$, $q = 5$ and $\kappa = 51.2$ and $\beta = 2$ in (e), $\beta = 9$ in (f) and $\beta = 9.6282$ in (g) and (h). Again the last two figures show the attractor (blue) and the repeller (red) at the bifurcation point from two different angles. The rotation vector ρ is $\rho = (2\omega, 2\pi)$.

A typical example we consider as a reference family is given by

$$g_\beta : \mathbb{R} \rightarrow \mathbb{R}, \quad x \mapsto g_\beta(x) = \frac{2}{\pi} \arctan(\alpha x) - \beta \quad (3.2)$$

Now (3.2) is perturbed with a random process generated on $\Sigma = [0, 1]^{\mathbb{Z}}$ with the shift operator to give the random dynamical system (2.16). The forcing process takes the form (2.30). We thus restate a precise random version of (2.16) which we use throughout in the formulation of the results as follows;

$$f_\beta : \Sigma \times \mathbb{R} \rightarrow \Sigma \times \mathbb{R} \quad , \quad (\theta, x) \mapsto (\sigma(\omega), g(x) + \kappa\omega_0 - \beta) \quad ,$$

with $g(x) = \frac{2}{\pi} \arctan(\alpha x)$ and $\omega \in \Sigma$. The fibre maps $f_\omega : X \rightarrow X$ are monotonically increasing. In this case, the family $(g_\beta)_{\beta \in [0,1]}$ is the *(autonomous) reference family*.

Remark 3.2. It should be noted that while we choose to deal with the arctan-family in the discrete time case, the phenomenon that will later on be described does not at all depend on the particular properties of the arcus tangent. However, any strictly monotone and bounded map of the real line with the same qualitative features, which can vaguely be described as “s-shaped” can be used to replace the arcus tangent (see[Jäg09]) for more examples.

In continuous time, we consider a one-parameter family of differentiable flows $\nu_\beta : \mathbb{T} \times \mathbb{R} \rightarrow \mathbb{R}$ generated by the vector field $\nu_\beta : \mathbb{R} \mapsto \mathbb{R}$, such that (g1) – (g6) holds, for all $\beta \in [0, 1]$ and $x \in \mathbb{R}$, where applicable. Such an example of a reference family is given by equation (1.1), introduced in Chapter 1.

Bounded random noise. As mentioned in the preliminaries, we would like to use $\sin(W_t)$ as our forcing term $F(t)$ in (1.2) to generate bounded

noise in continuous time. Hence, it is natural to consider the Wiener space, that is, the space of continuous real-valued functions $\mathcal{C}(\mathbb{R}, \mathbb{R})$ equipped with the Borel σ -algebra generated by uniform topology and the classical Wiener measure \mathbb{P} . However, in order to obtain a skew product flow we need a measure-preserving transformation on our probability space. If $\omega \in \mathcal{C}(\mathbb{R}, \mathbb{R})$ is a path of a Brownian motion, the standard measure-preserving shift on the Wiener space is given by $\sigma^t(\omega)(s) = \omega(s+t) - \omega(t)$. The problem that occurs is the fact that if we now want to define a forcing term f on $\mathcal{C}(\mathbb{R}, \mathbb{R})$ by evaluating the sinus at $\omega(0)$, that is, $f(\omega) = \sin(2\pi\omega(0))$, then $f(\sigma^t(\omega)) = 0$ for all $t \in \mathbb{R}$ (the standard Brownian motion starts in zero, and the classical shift respects this property). We therefore use a slightly modified version of this process to model bounded random forcing for our purposes. To that end, we let $p : \mathcal{C}(\mathbb{R}, \mathbb{R}) \mapsto \mathcal{C}(\mathbb{R}, \mathbb{T}^1) = \Sigma$ be the projection of real-valued to circle-valued functions (induced by the canonical projection $\pi : \mathbb{R} \mapsto \mathbb{T}^1$) and let $\mathbb{P}_0 = p_*\mathbb{P}$ be the push-forward of \mathbb{P} . Further, we let $S : \mathbb{T}^1 \times \Sigma \rightarrow \Sigma$, $(x, \omega) \mapsto \omega + x$ and equip Σ with the measure $\mu = S_*(\text{Leb}_{\mathbb{T}^1} \times \mathbb{P}_0)$. By definition, μ has equidistributed marginals and can therefore be seen to be invariant under the shift $\sigma : \mathbb{R} \times \Sigma \mapsto \Sigma$ defined by $\sigma^t(\omega)(s) = \omega(t+s)$. This construction will allow us to define a forcing term simply by evaluating the sinus (viewed as a function on \mathbb{T}^1) at $\omega(0)$. The precise formula for the forcing term $F(t)$, which we use in (1.2) to generate the uniformly bounded noise is given by the function

$$F(t) = \frac{1 + \sin(\omega_0 + W_t)}{2}, \quad (3.3)$$

where $\omega_0 \in \mathbb{T}^1$ is again an arbitrary initial condition and W_t denotes a one-dimensional Brownian motion (but higher-dimensional analogues could be considered as well). We thus arrive at the forced scalar differential equation (1.2), with the forcing function (3.3), as a basic model that we mainly refer to in this thesis. Our main result of this chapter now states that under some mild conditions, any random perturbation of such a reference family will undergo a non-smooth fold bifurcation.

Theorem 3.3. *Suppose that $(\Sigma, \mathcal{B}, \mu, \sigma)$ is an mpds and $(\Xi_\beta)_{\beta \in [0,1]}$ is a parameter family of σ -forced flows that satisfies the assumptions of Theorem 2.24, with constant curves γ^\pm . Further, assume that $(g_\beta)_{\beta \in [0,1]}$ is an autonomous reference family generated by ν_β such that the following conditions hold.*

(i) For all $(\omega, x) \in \Sigma \times X$ and $t > 0$ we have $g_\beta^t(x) \leq \xi_\beta^t(\omega, x)$. (Lower bound)

(ii) For all $\varepsilon, T > 0$ there exists a set $A_{\varepsilon, T} \subseteq \Sigma$ of positive measure $\mu(A_{\varepsilon, T}) > 0$ such that

$$|\xi_\beta^t(\omega, x) - g_\beta(x)| \leq \varepsilon \quad (3.4)$$

for all $\omega \in A_{\varepsilon, T}$, $|t| \leq T$ and $x \in [\gamma^-, \gamma^+]$. (Shadowing)

(iii) For ν -almost every $\omega \in \Sigma$ there exists $t \in \mathbb{T}$ and $\delta > 0$ such that $\xi^t(\sigma^{-t}(\omega), (x)) \geq g^t(x) + \delta$ for all $x \in [\gamma^-, \gamma^+]$. (Separation)

Then $(\Xi_\beta)_{\beta \in [0,1]}$ undergoes a non-smooth fold bifurcation, and the bifurcation parameter β_c is the same as in the reference family $(g_\beta)_{\beta \in [0,1]}$.

Remark 3.4. Note that by construction the forced Allee model (1.2) with random forcing term (3.3) satisfies the assumptions of Theorem 3.3, with the unforced Allee model as a reference family. This then implies Theorem 2.

In order to prove Theorem 3.3, we first provide the following auxiliary statement about the equivalence of the existence of invariant graphs and the existence of orbits that remain in the region $\Gamma = \Sigma \times [\gamma^-, \gamma^+]$ at all times. The statement equally applies to the existence of invariant graphs for most of the skew product systems we consider in this thesis and this will be crucial in the proof of Theorem 3.7 for hybrid systems as well.

Lemma 3.5. Suppose Ξ is a monotone skew product flow of the form (2.26) with an mpds $(\Sigma, \mathcal{B}, \mu, \sigma)$ in the base. Further, assume that there exist measurable curves $\gamma^- \leq \gamma^+ : \Sigma \rightarrow X$ that satisfy

$$\xi^t(\omega, \gamma^\pm(\omega)) \leq \gamma^\pm(\sigma(\omega)) \quad (3.5)$$

for μ -almost every $\omega \in \Sigma$. Let

$$\Gamma = \{(\omega, x) \mid \omega \in \Sigma, \gamma^-(\omega) \leq x \leq \gamma^+(\omega)\}. \quad (3.6)$$

Then there exists a (Ξ, μ) -invariant graph φ in Γ if and only if

$$\xi^t(\omega, \gamma^+(\omega)) \geq \gamma^-(\sigma^t(\omega)) \quad (3.7)$$

holds for all $t \geq 0$ and μ -almost every $\omega \in \Sigma$.

Proof. An important ingredient for the proof are the *graph transforms* $\Xi_*^t \gamma$ of a measurable function $\gamma : \Sigma \rightarrow X$. For $t \in \mathbb{T}$, these are defined by

$$\Xi_*^t \gamma(\omega) = \xi^t(\sigma^{-t}(\omega), \gamma(\sigma^{-t}(\omega))) . \quad (3.8)$$

If $t \geq 0$, we speak of a *forwards transform* and if $t \leq 0$, of a *backwards transform*. We define

$$\gamma_t^+ = \Xi_*^t \gamma^+ \text{ and } \gamma_t^- = \Xi_*^{-t} \gamma^- . \quad (3.9)$$

Then (3.5) together with the monotonicity of the fibre maps implies that the family of functions γ_t^+ is decreasing in t . Similarly, the family γ_t^- is increasing (note here that $\xi^t(\omega, \gamma^-(\omega)) \leq \gamma^-(\omega)$ for $t > 0$ implies $\xi^t(\omega, \gamma^-(\omega)) > \gamma^-(\omega)$ for $t < 0$). Suppose now that (3.7) holds for all $t > 0$ and μ -almost every $\omega \in \Sigma$. Then γ_t^+ is bounded below by γ^- for all $t > 0$ and thus converges μ -almost everywhere to a function

$$\varphi^+(\omega) = \lim_{t \rightarrow \infty} \gamma_t^+(\omega) . \quad (3.10)$$

Due to the continuity of the fibre maps, we have that

$$\begin{aligned} \xi^s(\omega, \varphi^+(\omega)) &= \xi^s\left(\omega, \lim_{t \rightarrow \infty} \gamma_t^+(\omega)\right) = \lim_{t \rightarrow \infty} \xi^s(\omega, \gamma_t^+(\omega)) \\ &= \lim_{t \rightarrow \infty} \gamma_{t+s}^+(\sigma^s(\omega)) = \varphi^+(\sigma^s(\omega)) \end{aligned} \quad (3.11)$$

μ -almost everywhere. Hence, φ^+ is the desired invariant graph. Conversely, assume that there exists an invariant graph φ in Γ . Then the monotonicity of the fibre maps gives

$$\xi^t(\omega, \gamma^+(\omega)) \geq \xi^t(\omega, \varphi(\omega)) = \varphi(\sigma^t(\omega)) \geq \gamma^-(\sigma^t(\omega)) \quad (3.12)$$

for μ -almost every $\omega \in \Sigma$. \square

Remark 3.6. As we have seen in the above proof, if Ξ satisfies the assumptions of Lemma 3.5 and has at least one invariant graph, then the formula

$$\varphi^+(\omega) = \lim_{t \rightarrow \infty} \gamma_t^+(\omega) = \lim_{t \rightarrow \infty} \xi^t(\sigma^{-t}(\omega), \gamma^+(\sigma^{-t}(\omega))) \quad (3.13)$$

defines one such graph. This way of defining an invariant graph is called a *pullback construction* and generally works if the graph is an attractor. In a similar fashion, it is possible to show that another invariant graph may be defined by a *pushforward construction*

$$\varphi^-(\omega) = \lim_{t \rightarrow -\infty} \gamma_t^-(\omega) = \lim_{t \rightarrow -\infty} \xi^{-t}(\sigma^t(\omega), \gamma^-(\sigma^t(\omega))) , \quad (3.14)$$

which usually yields a repeller. It is possible, however, that both graphs φ^- and φ^+ coincide, as in the case of a smooth fold bifurcation in Theorem 2.24.

We can now turn to the proof.

Proof of Theorem 3.3. Let β_c be the bifurcation parameter for the family $(\Xi_\beta)_{\beta \in [0,1]}$ and $\tilde{\beta}_c$ the one for the reference family $(g_\beta)_{\beta \in [0,1]}$. We first show that $\beta_c = \tilde{\beta}_c$. Denote the unique fixed point of $g_{\tilde{\beta}_c}$ in $[\gamma^-, \gamma^+]$ by x_0 . Then, for any $\omega \in \Sigma$ and $\beta < \tilde{\beta}_c$, we obtain

$$\xi_\beta^t(\omega, \gamma^+) \geq \xi_{\tilde{\beta}_c}^t(\omega, \gamma^+) \geq g_{\tilde{\beta}_c}^t(\gamma^+) \geq g_{\tilde{\beta}_c}^t(x_0) = x_0 \geq \gamma^- .$$

Hence, Lemma 3.5 implies that Ξ_β has at least one invariant graph in Γ for all $\beta \leq \tilde{\beta}_c$, and thus $\beta_c \geq \tilde{\beta}_c$. Conversely, suppose that $\beta > \tilde{\beta}_c$. As g_β has no fixed points in $[\gamma^-, \gamma^+]$ anymore and $g_\beta(\gamma^+) < \gamma^-$, we obtain that $g_\beta^T(\gamma^+) < \gamma^-$ for some $T > 0$. Let $\varepsilon > 0$ be such that $g_\beta^T(\gamma^+) < \gamma^- - \varepsilon$. By assumption, the set $A_{\varepsilon, T}$ in the statement of the theorem has positive measure. For any $\omega \in A_{\varepsilon, T}$, we obtain

$$\xi_\beta^T(\omega, \gamma^+) \leq g_\beta^T(\gamma^+) + \varepsilon < \gamma^- .$$

Due to Lemma 3.5, this excludes the existence of an invariant graph in Γ for $\beta > \beta_c$. We therefore obtain $\beta_c \leq \tilde{\beta}_c$ and conclude $\beta_c = \tilde{\beta}_c$. It remains to show the non-smoothness of the bifurcation. To that end, we set

$$\varphi^+(\omega) = \lim_{t \rightarrow \infty} \xi_{\beta_c}^t(\sigma^{-t}(\omega), \gamma^+) \quad \text{and} \quad \varphi^-(\omega) = \lim_{t \rightarrow \infty} \xi_{\beta_c}^{-t}(\sigma^t(\omega), \gamma^-),$$

for all $\omega \in \Sigma$. As discussed in Remark 3.6, φ^+ and φ^- are invariant graphs. To finish the proof, we have to show that $\varphi^-(\omega) < \varphi^+(\omega)$ μ -almost surely. Observe that condition (i) in Theorem 3.3 together with the monotonicity implies $\xi_{\beta_c}^t(\omega, x) \leq g_{\beta_c}^t(x)$ for all $x \in [\gamma^-, \gamma^+]$ and $t < 0$. As a consequence, we have that the limit

$$\varphi^-(\omega) = \lim_{t \rightarrow \infty} \xi_{\beta_c}^{-t}(\sigma^t(\omega), \gamma^-) \leq x_0$$

exists (note that condition (ii) in Theorem 2.24 together with the monotonicity of the fibre maps implies that $t \mapsto \xi_{\beta_c}^{-t}(\sigma^t(\omega), \gamma^-)$ is non-decreasing so that the convergence is monotone) and defines an invariant graph of Ξ_{β_c} (compare Remark 3.6). Likewise,

$$\varphi^+(\omega) = \lim_{t \rightarrow \infty} \xi_{\beta_c}^t(\sigma^{-t}(\omega), \gamma^+)$$

defines an invariant graph of Ξ_{β_c} . Now, by assumption (iii) we have that for μ -almost every $\omega \in \Sigma$ there exists $\delta > 0$ and $s \in \mathbb{T}$ such that $\xi_{\beta_c}^s(\sigma^{-s}(\omega), x_0) > g_{\beta_c}^s(x_0) + \delta = x_0 + \delta$. Thus, we obtain

$$\begin{aligned} \varphi^+(\omega) &= \lim_{t \rightarrow \infty} \xi_{\beta_c}^t(\omega^{-t}(\omega), \gamma^+) \\ &= \lim_{t \rightarrow \infty} \xi_{\beta_c}^s(\sigma^{-s}(\omega), \xi_{\beta_c}^{t-s}(\sigma^{-t}(\omega), \gamma^+)) \\ &\geq \xi_{\beta_c}^s(\sigma^{-s}(\omega), x_0) \geq x_0 + \delta \end{aligned}$$

and hence, in particular, $\varphi^+(\omega) > x_0 \geq \varphi^-(\omega)$. This implies that Ξ_{β_c} has two distinct invariant graphs. We conclude that the bifurcation is non-smooth. \square

To illustrate the non-smoothness of bifurcations in the continuous time case, we require that the vector field of the parameter family of \mathcal{C}^2 flows $(\Xi_\beta)_{\beta \in [0,1]}$ satisfies conditions (3.4) – (3.7). And the rest follow as stated in the quasiperiodic case. The theorem applies so long as the paths $t \mapsto \sigma^t(\omega)$ are continuous for every $\omega \in \Sigma$. Note that this assumption is satisfied by the Allee-effect model 1.2, with an external random perturbation this time given, for instance, by a forcing function (3.3). The fold/saddle-node bifurcation observed via the behaviour of the attractor and the repeller is shown in Figure (3.3). Numerically, it is not easy to visualize the attractor over the base space. For this reason, we only take a single trajectory to illustrate what happens before and at the bifurcation. Same results for the non-smoothness of bifurcations are observed as seen in the discrete time example (2.16), with forcing function (2.30) in Figure 3.2, where the attractor and repeller only touch at one point, at the maximum forcing. In this particular example, we notice that the graphs touch at the point $\omega_0 = (\dots, 1, 1, 1, \dots)$. Some of the the statements we actually prove in this thesis hold in greater generality, both with respect to the model (1.2) and to the employed forcing processes (3.3). Furthermore, in the discrete time case, we visualize the behavior of the attractor and the repeller by viewing it over the 2 dimensional coordinates of the Bakers' map, as this is easier than implementing the shift directly. From the numerical results, we see that only a non-smooth bifurcations occurs. This pattern is shown in Figure 3.2 over different values of β .

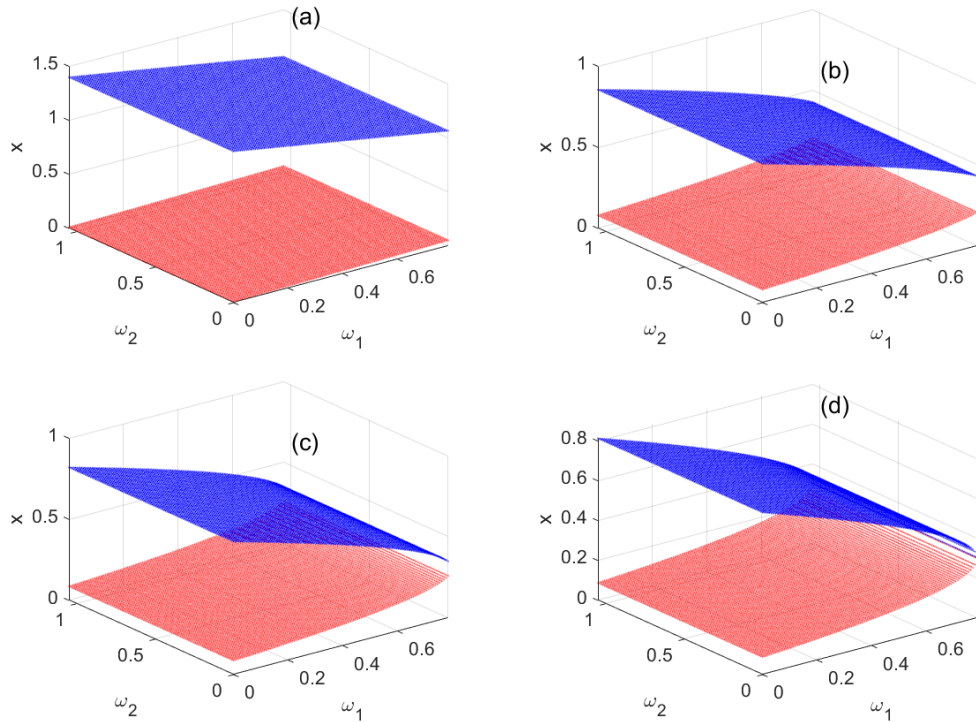


Figure 3.2: **(a)–(d)**: Non-smooth fold bifurcation in the randomly-forced systems in discrete time model with parameters $\alpha = 10$, $\kappa = 0.4$, $\beta = 0.1$ in (a), $\beta = 0.6$ in (b), $\beta = 0.63$ in (c) and $\beta = 0.635879$ in (d).

3.3 Non-smooth saddle-node bifurcations in hybrid forced systems

To conclude the chapter, we now prove the occurrence of a non-smooth fold/saddle-node bifurcation in hybrid forced systems of the form (3.15) introduced earlier in Chapter 2. From the result on the non-smoothness of saddle-node bifurcations in randomly forced systems in Theorem 3.3, a random forcing on the saddle-node bifurcation in skew product systems leads to a non-smooth bifurcation. Since a hybrid-forced system is regarded as a special case of a random dynamical system, we show that the statement of Theorem 3.3 holds true in this case. To prove this, we similarly introduce the notion of a reference system and provide some conditions for the bifurcation to occur with respect to the reference system. To that end, we

consider a non-autonomous reference system and impose conditions such that it undergoes a non-autonomous saddle-node bifurcation. The desired conditions are those presented in Theorem 2.24 for measure preserving base transformations. Under some additional mild technical conditions, we show that this leads to a non-smooth fold bifurcation. Plausible examples that we consider as potential candidates for such reference systems are deterministically forced skew product systems (that is, qpf systems) of the form (2.10). To that end, we let Ξ_β be a parameter family of ρ -forced maps of the form (2.16) in the discrete time case or differential flows of the form (1.2) with a deterministic forcing. To be precise, we consider examples given in Chapter 2, that is system (2.16) with forcing function (2.17) and (1.2) with forcing function (3.1), as non-autonomous reference families both in discrete and continuous time respectively.

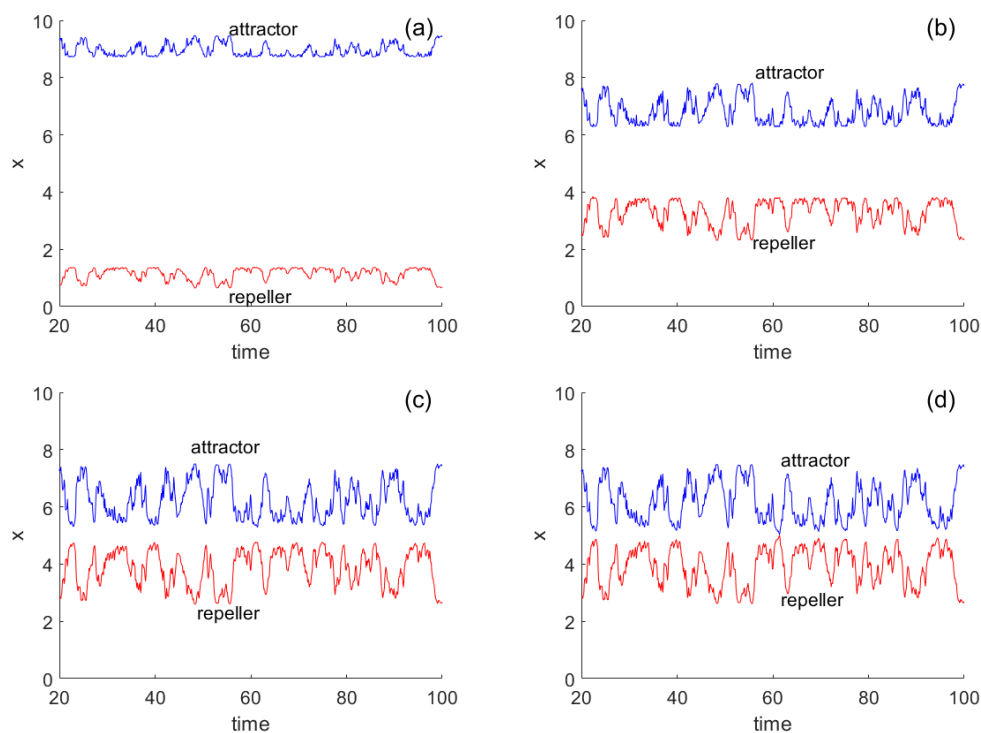


Figure 3.3: **(a)–(d)**: Non-smooth fold bifurcation in the randomly forced-Allee model with parameters $r = 80$, $K = 10$, $S = 0.1$, $\kappa = 3$ and $\beta = 5$ in (a), $\beta = 17$ in (b), $\beta = 18.50$ in (c) and $\beta = 18.602$ in (d).

To make a distinction in notation from the reference system in the random case, we denote the non-autonomous reference system by Ξ_β . Let

$\gamma^- < \gamma^+ \in \mathbb{R}$ and Ξ_β satisfy the assumptions of Theorem 2.18 for all $\beta \in [0, 1]$, ($n \in \mathbb{N}$ or $t \in \mathbb{T}$), $\theta \in \Theta$ and $x \in \mathbb{R}$, where applicable. Recall that the saddle-node bifurcation in Ξ_β is either smooth or non-smooth depending on the systems' parameter, (see Theorem 2.18, Theorem 2.21, Corollary 2.21.1 and Theorem 2.22). Again, we introduce examples in discrete and continuous time to illustrate our assertions and later on apply them in the derivation of the analytical results as well as in the numerical results. In discrete time, we again refer to the perturbed arctan-parameter family of maps 2.16, which we modify with the hybrid-forcing below;

$$f_\beta : \Theta \times \Sigma \times X \mapsto \Theta \times \Sigma \times X, \quad (\rho(\theta), \sigma(\omega), \arctan(\alpha x) - F(\theta, \omega) - \beta), \quad (3.15)$$

where the spaces Θ and Σ are defined as before and the forcing process is given by

$$F(\theta, \omega) = \kappa \cdot \frac{\sin(2\pi\theta) + 1}{2} - \epsilon \cdot \omega_0 \quad (3.16)$$

where κ and ϵ determine the strength of the deterministic and random forcing terms respectively. The reference system is given by

$$g_\beta := \arctan(\alpha x) - \kappa \cdot \frac{\sin(2\pi\theta) + 1}{2} - \beta \quad (3.17)$$

In the continuous time case, we consider the Allee-effect model as a RODE (1.2) with forcing term given by

$$F(t, \theta, \omega) = \prod_{i=1}^d \left(\frac{1 + \sin(2\pi(\theta_i + t \cdot \nu_i))}{2} \right)^q - \frac{1 + \sin(\omega_0 + W_t)}{2}. \quad (3.18)$$

The corresponding reference family is the quasiperiodically forced Allee-effect model. Let $\tilde{\beta}_c$ be the critical parameter of $g_{\beta, \theta}$. We thus have the following statement.

Theorem 3.7. *Suppose that (M, \mathcal{G}, m, T) is a mpds and $(\Psi_\beta)_{\beta \in [0, 1]}$ is a parameter family of T -forced monotone flows of the form (2.31), such that the assumptions of Theorem 2.24, with constant curves γ^\pm are satisfied. Further, assume that $(\Xi_\beta)_{\beta \in [0, 1]}$ is a non-autonomous reference family of the form (2.10) that satisfies the assumptions of Theorem 2.18, such that the following conditions hold for all $\beta \in [0, 1]$;*

- (h1) *For all $(\theta, \omega, x) \in M$ we have $\xi_\beta^t(\theta, x) \leq \psi_\beta^t(\theta, \omega, x)$ for $t > 0$. (Lower bound)*

(h2) For all $\varepsilon, T > 0$ there exists a set $A_{\varepsilon, T} \subseteq \Sigma$ of positive measure $\mu(A_{\varepsilon, T}) > 0$ such that

$$|\psi_{\beta}^t(\theta, \omega, x) - \xi_{\beta}^t(\theta, x)| \leq \varepsilon \quad (3.19)$$

for all $\omega \in A_{\varepsilon, T}$, $|t| \leq T$ and $x \in [\gamma^-, \gamma^+]$ and all $\theta \in \Theta$. (Shadowing)

(h3) For μ -almost every $\omega \in \Sigma$ there exists $t \in \mathbb{T}$ and $\delta > 0$ such that $\psi^t(\rho^{-t}(\theta), \sigma^{-t}(\omega), x) \geq \xi^t(\rho^{-t}(\theta), x) + \delta$ for all $x \in [\gamma^-, \gamma^+]$. (Separation)

Then $(\Psi_{\beta})_{\beta \in [0, 1]}$ undergoes a non-smooth fold bifurcation, and the bifurcation parameter β_c is the same as in the reference family $(\Xi_{\beta})_{\beta \in [0, 1]}$, (i.e., $\beta_c = \tilde{\beta}_c$).

Similarly, we apply Lemma 3.5 to guarantee the existence of orbits in a locally defined region $\Gamma = \Theta \times \Sigma \times [\gamma^+, \gamma^+]$. In this case, we define the region Γ with respect to the product space as follows;

$$\Gamma = \{(\theta, \omega, x) \in \Theta \times \Sigma \times X \mid \gamma^-(\theta, \omega) \leq x \leq \gamma^+(\theta, \omega)\},$$

for measurable functions $\gamma^- \leq \gamma^+ : \Theta \times \Sigma \rightarrow X$. Again, if we assume that Ψ satisfies the assumptions of Lemma 3.5, and has at least one invariant graph in Γ , then we redefine the bounding graphs in this context as follows; Given measurable functions $\gamma^- \leq \gamma^+ : \mathbb{T} \times M \rightarrow X$, we have

$$\Phi^+(\theta, \omega) = \lim_{t \rightarrow \infty} \psi^t(\rho^{-t}(\theta), \sigma^{-t}(\omega), \gamma^+(\rho^{-t}(\theta), \sigma^{-t}(\omega))) \quad \text{and} \quad (3.20)$$

$$\Phi^-(\theta, \omega) = \lim_{t \rightarrow \infty} \psi^{-t}(\rho^t(\theta), \sigma^t(\omega), \gamma^-(\rho^t(\theta), \sigma^t(\omega))). \quad (3.21)$$

The graphs Φ^+ and Φ^- form a pair of a pullback attractor and a pullback repeller, respectively. In the same way, the pullback attractor and repeller pair in the reference family take the form of equations (3.13) and (3.14) respectively, however, with a deterministic coordinate. Hence, the graphs Φ^+, φ^+ are called attractors and Φ^-, φ^- are repellers of Ψ and Ξ , respectively. If we consider parameter families Ψ_{β} and Ξ_{β} , then we denote the respective invariant graphs by Φ_{β}^{\pm} and φ_{β}^{\pm} . To that end, with these slight modifications, we now turn to the proof the theorem.

Proof of Theorem 3.7. Let β_c be the bifurcation parameter of $(\Psi_{\beta})_{\beta \in [0, 1]}$ and $\tilde{\beta}_c$ the bifurcation parameter of $(\Xi_{\beta})_{\beta \in [0, 1]}$. The first step is to show

that $\beta_c = \tilde{\beta}_c$. Suppose $\beta < \tilde{\beta}_c$. For μ -a.e $\omega \in \Sigma$, we have that

$$\psi_\beta^t(\theta, \omega, \gamma^+) \geq \psi_{\tilde{\beta}_c}^t(\theta, \omega, \gamma^+) \stackrel{(h1)}{\geq} \xi_{\tilde{\beta}_c}^t(\theta, \gamma^+) \geq \xi_{\tilde{\beta}_c}^t(\varphi^+(\theta)) = \varphi^+(\rho^t(\theta)) > \gamma^-. \quad (3.22)$$

By Lemma 3.5, this indicates that Ψ_β has an invariant graph for all $\beta \leq \tilde{\beta}_c$ in Γ and therefore $\beta_c > \tilde{\beta}_c$.

Conversely, let $\beta > \tilde{\beta}_c$. This implies that Ξ_β has no invariant graph in $\tilde{\Gamma} = \{(\theta, x) \mid \gamma^- \leq x \leq \gamma^+\}$. Due to (ii) in Theorem 2.18, $\xi_\beta^t(\theta, \gamma^+) \leq \gamma^+$ for $t > 0$. Fix some $T = T(\theta) > 0$ such that $\xi_\beta^t(\theta, \gamma^+) < \gamma^-$ for all $t \geq T(\theta)$. Such $T(\theta)$ exists for ν almost every $\theta \in \Theta$ since Ξ_β has no invariant graph in Γ , so that by Lemma 3.5 orbits in Γ eventually leave this region and are mapped below γ^- . As a consequence, there exists some $\varepsilon, T_0 > 0$ and a set $S \in \Theta$ with $\nu(S) > 0$ such that $\xi_\beta^t(\theta, \gamma^+) < \gamma^- - \varepsilon$ holds for all $t \geq T_0$ and $\theta \in S$. Now by assumption (h2), choose a set A_{ε, T_0} with $\mu(A_{\varepsilon, T_0}) > 0$ such that

$$\psi_\beta^{T_0}(\theta, \omega, \gamma^+) \leq \xi_\beta^{T_0}(\theta, \gamma^+) + \varepsilon. \quad (3.23)$$

for all $\theta \in \Theta$ and $\omega \in A_{\varepsilon, T_0}$. It then follows that $\psi_\beta^{T_0}(\theta, \omega, \gamma^+) < \gamma^-$ for all $(\theta, \omega) \in S \times A_{\varepsilon, T_0} \subseteq \Theta \times \Sigma$. By Lemma 3.5 again, this implies that ψ_β has no invariant graph in $\Gamma_{\theta, \omega}$ for any $(\theta, \omega) \in S \times A_{\varepsilon, T_0}$ and for all $\beta > \tilde{\beta}_c$, so that $\beta_c \leq \tilde{\beta}_c$. Therefore together, this shows that $\beta_c = \tilde{\beta}_c$.

We now proceed to show that at β_c , the graphs are distinct, that is, $\Phi^- < \Phi^+$ $\mu \times \nu$ -a.s. By definition,

$$\begin{aligned} \Phi_{\beta_c}^+(\theta, \omega) &= \lim_{t \rightarrow \infty} \psi_{\beta_c}^t(\rho^{-t}(\theta), \sigma^{-t}(\omega), \gamma^+) \\ &= \lim_{t \rightarrow \infty} \psi_{\beta_c}^s(\rho^{-s}(\theta), \sigma^{-s}(\omega), \psi_{\beta_c}^{t-s}(\rho^{-t}(\theta), \sigma^{-t}(\omega), \gamma^+)), \end{aligned}$$

for $s < t$, $s, t \in \mathbb{R}$ and m -a.e $(\theta, \omega) \in M$. By condition (h1) in Theorem 3.7

$$\begin{aligned} \Phi_{\beta_c}^+(\theta, \omega) &\stackrel{(h1)}{\geq} \lim_{t \rightarrow \infty} \psi_{\beta_c}^s(\rho^{-s}(\theta), \sigma^{-s}(\omega), \xi_{\beta_c}^{t-s}(\rho^{-t}(\theta), \gamma^+)) \\ &\stackrel{\text{monotonicity}}{>} \lim_{t \rightarrow \infty} \psi_{\beta_c}^s(\rho^{-s}(\theta), \sigma^{-s}(\omega), \xi_{\beta_c}^{t-s}(\rho^{-t}(\theta), \varphi_{\beta_c}^+(\rho^{-t}(\theta)))) \\ &\geq \psi_{\beta_c}^s(\rho^{-s}(\theta), \sigma^{-s}(\omega), \varphi_{\beta_c}^+(\rho^{-s}(\theta))). \end{aligned}$$

Now, by assumption (h3), for μ -a.e $\omega \in \Sigma$, there exists a $\delta > 0$ such that

$$\begin{aligned} \Phi_{\beta_c}^+(\theta, \omega) &\geq \psi_{\beta_c}^s(\rho^{-s}(\theta), \sigma^{-s}(\omega), \varphi_{\beta_c}^+(\rho^{-s}(\theta))) \\ &\stackrel{(h3)}{\geq} \xi_{\beta_c}^s(\rho^{-s}(\theta), \varphi_{\beta_c}^+(\rho^{-s}(\theta))) + \delta \\ &= \varphi_{\beta_c}^+(\theta) + \delta \end{aligned}$$

and therefore

$$\varphi_{\beta_c}^+(\theta) < \Phi_{\beta_c}^+(\theta, \omega).$$

At the same time, by (h1) in Theorem 3.7 and by the monotonicity of the fibre maps, we have

$$\Phi_{\beta_c}^-(\theta, \omega) = \lim_{t \rightarrow \infty} \psi_{\beta_c}^{-t}(\rho^t(\theta), \sigma^t(\omega), \gamma^-) \leq \lim_{t \rightarrow \infty} \xi_{\beta_c}^{-t}(\rho^t(\theta), \gamma^-) = \varphi_{\beta_c}^-$$

for all $t < 0$ and for μ -a.e $\omega \in \Sigma$. By Theorem 2.18, this implies that

$$\Phi_{\beta_c}^-(\theta, \omega) \leq \varphi_{\beta_c}^- \leq \varphi_{\beta_c}^+ < \Phi_{\beta_c}^+(\theta, \omega).$$

This completes the proof. \square

Remark 3.8. Regardless of the nature of the bifurcation in Ξ_β , the saddle-node bifurcation in the family Ψ_β will always be non-smooth due to the random effect. This gives us a generalization of the result of Theorem 3.3 to a broader class of randomly forced systems. This again implies Theorem 2.

When it comes to the statement on the Lyapunov exponents of invariant graphs $\Phi_{\beta_c}^\pm$, this follows directly from Theorem 2.24. In particular, as we have shown the non-smoothness of the fold bifurcation, it follows from condition (iii) and (iv) and applying [Jäg13, Theorem 1.16] with majorant η , that $\lambda_{\nu \times \mu}(\Phi_{\beta_c}^+) < 0$ and $\lambda_{\nu \times \mu}(\Phi_{\beta_c}^-) > 0$.

Remark 3.9. As we can observe, the Lyapunov exponents of the attractor and repeller in a non-smooth fold bifurcation, with all the three forcing processes stay away from zero, creating a Lyapunov gap. This gap is crucial when it comes to predicting when a bifurcation will actually happen. We will pursue this further in Chapter 4.

3.4 Applications to the forced Allee-model

Considering the examples given above, we numerically show the saddle-node bifurcation pattern in both cases in Figure 3.4(a)–(d). Unlike in the random setting, where we visualize the attractor and repeller over the 2 dimensional coordinates of the Bakers' map, in the hybrid case, we visualize this over the 2-dimensional base space with the irrational rotation on one axis and one coordinate of the bakers map on the other axis. In (b) we take slices of

the attractor-repeller pair at some ω coordinate and notice that the collision of attractor and repeller at the bifurcation only occurs at the point where $\omega = (\dots, 0, 0, 0, \dots)$. Notice that this is similar to the random case where the graphs touch at only one point. On this ω fibre, we see the strange non-chaotic attractor which is observed in the reference system and therefore, in the same way, we can refer to this pair as a strange non-chaotic attractor of the hybrid-forced system. As pointed out earlier in Chapter 2, some of the conditions in Theorem 2.18 and Theorem 2.24 follow directly from the specific form of the scalar field (1.2) as discussed earlier. However, it remains to specify a suitable parameter range and appropriate functions γ^\pm so that (i), (ii) and (vi) of Theorem 2.18 and Theorem 2.24 hold. It is easy to check that the fold bifurcation of the unforced equation (1.1) takes place at

$$\beta = b(r, K, S) := \frac{r}{K^2} \cdot \left(\frac{K - S}{2} \right)^2. \quad (3.24)$$

Moreover, the neutral equilibrium point at the bifurcation is $x_0 = \frac{K+S}{2}$. If $\kappa < b(r, K, S)$ and $\beta \leq b(r, K, S) - \kappa$, then we have that $V_\beta(\theta, x_0) > 0$ for all $\theta \in \Theta$ and both forcing terms (3.1), (3.3) and (1.2) (note here that $F \leq 1$). At the same time, given $\beta < b(r, K, S)$, the unforced Allee model (1.1) has equilibrium points $x = 0$ and

$$x_\beta^\pm = \frac{K + S}{2} \pm \frac{1}{2} \sqrt{(K - S)^2 - \frac{4\beta K^2}{r}} = \frac{K + S}{2} \pm \frac{K - S}{2} \cdot \sqrt{1 - \bar{\beta}},$$

where

$$\bar{\beta} = \frac{4\beta K^2}{r(K - S)^2}.$$

As the forcing is always downwards (recall that the forcing term reads $-\kappa F$ with $F \geq 0$), this implies in particular that $V_\beta(\theta, x_{\beta_0}^\pm) < 0$ for all $\theta \in \Theta$ and $\beta \geq \beta_0$. Hence, we obtain a forward invariant region $\Theta \times [x_0, x_{\beta_0}^+]$ and a backward invariant region $\Theta \times [x_{\beta_0}^-, x_0]$ in the qpf case, where β_0 will be specified below. The same result holds in the random and hybrid case with the corresponding base spaces. Using the concavity of V_β , equally shown below, this implies the existence of two invariant graphs in $[\gamma^-, \gamma^+] = [x_{\beta_0}^-, x_{\beta_0}^+]$. Similarly, if $\beta > b(r, K, S)$, then the bifurcation has already taken place and there will not be any invariant graph above the equilibrium at 0. Hence, conditions (i) and (ii) are satisfied. It remains to ensure the concavity of $V_\beta(\theta, \cdot)$ in the considered region $\Theta \times (\gamma^-, \gamma^+)$ in the qpf and randomly

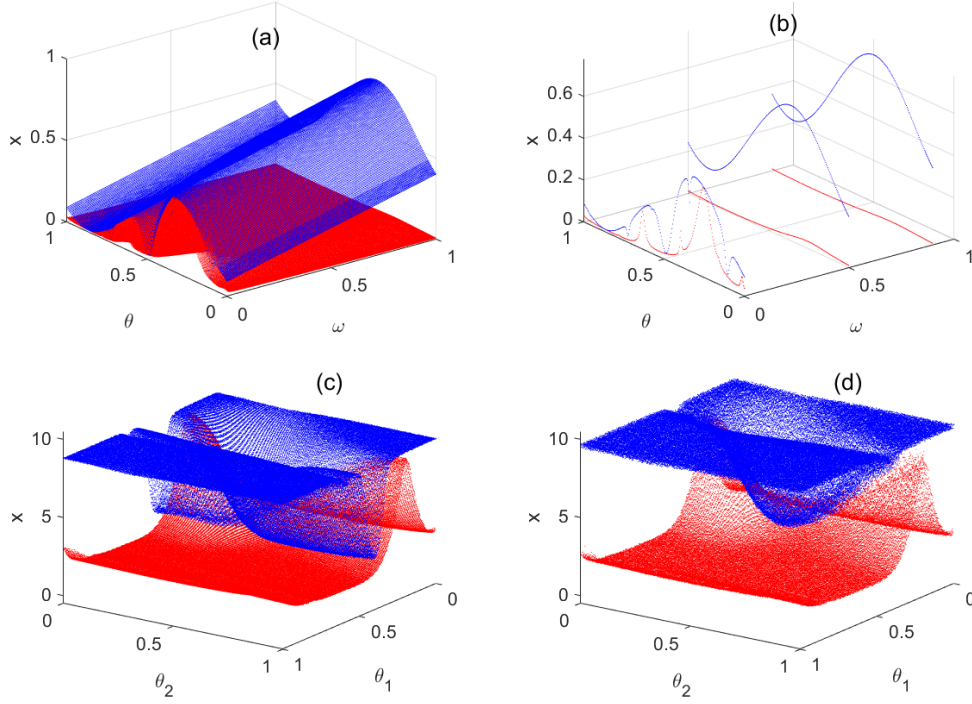


Figure 3.4: **(a)–(b)**: Non-smooth fold bifurcation in discrete time hybrid model with parameters $\alpha = 80$, $\beta_c = 0.4729$, $\rho = \frac{\sqrt{(5)-1}}{2}$, $\kappa = 1$. (b) shows slices of the sna at three different ω -fibres.

(c)–(d): Non-smooth fold bifurcation in the hybrid forced Allee model with parameters $r = 80$, $K = 10$, $S = 0.1$, $q = 5$, $\kappa = 51.2$. In (c) $\sigma = 6$ and $\beta = 7.55$, whereas in (d) $\sigma = 1$ and $\beta = 7.55$. The precise model used is given by $x'(t) = \frac{r}{K^2} \cdot x(t) \cdot (K - x(t)) \cdot (x(t) - S) - (\beta + \kappa \cdot \prod_{i=1}^d \left(\frac{1 + \sin(2\pi(\theta_i + t \cdot \nu_i))}{2} \right)^q - \sigma \cdot \frac{1 + \sin(W_t)}{2}) \cdot x$. Here, W_t is a one realization of a one dimensional wiener path.

forced case, where γ^\pm still need to be specified. The second derivative of $V_{\kappa,\beta}$ with respect to x is given by

$$\partial_x^2 V_{\kappa,\beta}(\theta, x) = \frac{r}{K^2} \cdot (-6x + 2(K + S)),$$

and thus independent of β and κ . We have

$$\partial_x^2 V_{\kappa,\beta}(\theta, x) < 0 \quad \Leftrightarrow \quad x > \frac{K + S}{3}.$$

Hence, we simply need to choose β_0 such that $x_{\beta_0}^- \geq \frac{K+S}{3}$. By the above, this means that we require

$$x_{\beta}^- = \frac{K + S}{2} - \frac{K - S}{2} \cdot \sqrt{1 - \bar{\beta}} \geq \frac{K + S}{3},$$

which is equivalent to

$$\bar{\beta} \geq 1 - \gamma(K, S) ,$$

where $\gamma(K, S) = \frac{1}{9} \left(\frac{K+S}{K-S} \right)^2$, and hence to

$$\beta \geq b(r, K, S) \cdot (1 - \gamma(K, S)) .$$

This means that if $\kappa > 0$ satisfies

$$\kappa < b(r, K, S) \cdot \gamma(K, S)$$

and we let

$$J(r, K, S) = [b(r, K, S) \cdot (1 - \gamma(K, S)), b(r, K, S) + 1] ,$$

then the parameter family $(V_{\kappa, \beta})_{\beta \in J(r, K, S)}$ satisfies all the assertions of Theorem 2.18 (Theorem 2.24) (modulo rescaling the parameter interval $J(r, K, S)$) and therefore undergoes a non-autonomous fold bifurcation. Note that in the hybrid case, we consider the 3 dimensional space and check the concavity of $V_{\beta}(\theta, \omega, \cdot)$ in the region $\Theta \times \Sigma \times (\gamma^-, \gamma^+)$ which would coincide with the results above.

Chapter 4

Lyapunov gap in non-smooth saddle node bifurcations

As discussed earlier in the introduction, one of our main objectives in this thesis is to establish early warning signals for fold bifurcations in skew product systems. This particular chapter and the subsequent one serve to do so. More specifically, in this chapter we would like to discuss how Lyapunov exponents translate into early warning signals for critical transitions, such as recovery rates and critical slowing down. We first provide numerical evidence and thereafter provide analytical results to match the numerical observations. In order to discuss further about what happens with the non-smooth fold bifurcation pattern and the corresponding early warning signals in the examples cited here, we will first concentrate on the behaviour of the Lyapunov exponents of the attractor and the repeller in the quasiperiodic, random and hybrid forced systems. To illustrate this, we use example (2.16) for the discrete time case and the forced Allee model (1.2) for the continuous time case. We will begin by discussing the qpf and random case simultaneously and the hybrid case will follow thereafter.

4.1 Lyapunov gap in quasiperiodically forced and randomly forced systems

In the discrete time case, the behaviour of the Lyapunov exponents for the attractor and repeller in the quasiperiodic and random case is shown in Figure 4.1. Starting with the quasiperiodic case, we show the behaviour for

different values of α in (a) and (b), which correspond to the behaviour in the smooth and non-smooth bifurcation respectively. Whereas in (c), we show the behaviour in the non-smooth case with a simultaneous variation of the parameter α and β . The variation of these two parameters is shown in (d).

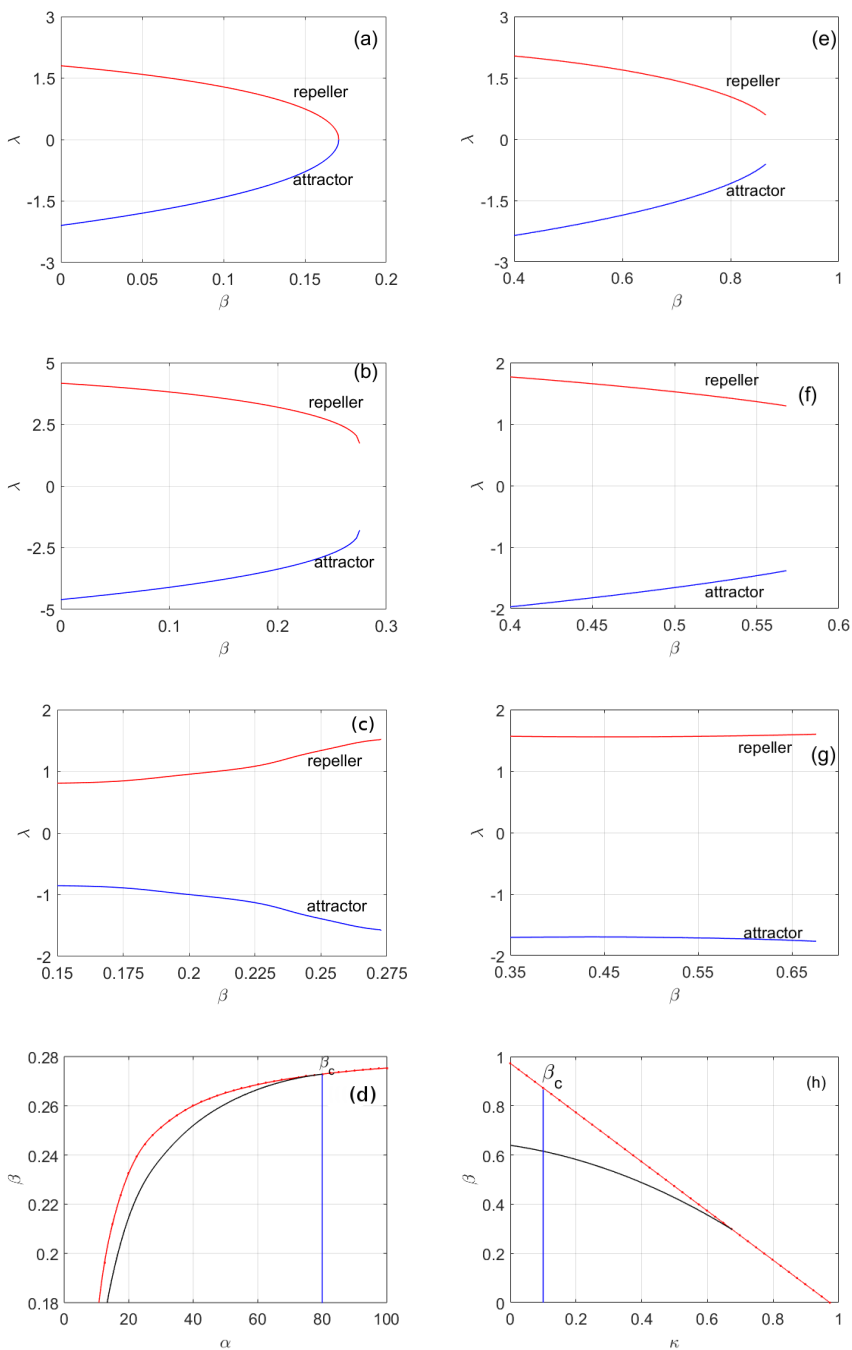


Figure 4.1: Lyapunov exponents during saddle-node bifurcations in the family (2.16). (a) smooth bifurcation in the qpf case, with parameters $\alpha = 10$ and $\kappa = 1$. The bifurcation occurs at $\beta_c = 0.341502$. (b) a non-smooth bifurcation in the same model, with parameters $\alpha = 100$ and $\kappa = 1$. The bifurcation occurs at $\beta_c = 0.5507468$. (c) non-smooth bifurcation with simultaneous variation of parameters α and κ along the black curve in (d). (e) and (f) Lyapunov exponents in the randomly forced case, with parameters $\alpha = 10$ and $\kappa = 0.1$ and bifurcation parameter $\beta = 0.866$ in (e) and $\alpha = 10$ and $\kappa = 0.4$ and bifurcation parameter $\beta = 0.566$ in (f). In (g), the parameters κ and β are varied again at the same time along the black parameter curve shown in (h). The red curve in (d) shows the bifurcation curve $\beta_c(\alpha)$ in the quasiperiodic case whereas the one in (h) shows the bifurcation curve $\beta_c(\kappa)$ in the random case.

On the right hand side, we show the behaviour for the random case. Here, we show the Lyapunov exponents for different values of κ in (e) and (f). Similarly, we show the Lyapunov exponents for the simultaneous variation of β with κ in (g). The variation of the two parameters is shown in (h). In continuous time, we present the results in Figure 4.2, for the Lyapunov exponents of the attractor and the repeller for the forced Allee model (1.2) throughout the bifurcation. Similarly, for the case of quasiperiodic forcing, we consider two different choices of the parameters κ and q in (a) and (b) for the smooth and non-smooth case respectively. For the random case, we consider different values of κ shown in (c) and (d). While the behaviour in (a) is in perfect analogy with the unforced case in Figure 1.5(b), the situation in (b)–(d) is clearly different. Although the Lyapunov exponents of the attractor and the repeller do approach each other, there remains a clear gap at the bifurcation point, and in particular the Lyapunov exponents of the attractor (which are the ‘visible’ or ‘physically relevant’ ones) stay strictly away from zero. Given the significance of zero exponents for the observation of critical slowing down and slow recovery rates, this is certainly noteworthy and deserves a closer examination. Moreover, while in Figure 4.2(b)–(d) the Lyapunov exponents do at least move towards each other as the bifurcation is approached, this actually turns out to depend just on the precise form of the parameter family. In the above cases, we have just varied the bifurcation parameter β , while leaving all other constants in (1.2) invariant. In contrast to this, one may easily imagine that in real-world situations other system parameters, such as the intrinsic growth rate r in (1.2) or the noise amplitude in (3.3), vary as well as the pressure on the population increases. The result of such couplings is shown in Figure 4.3. It can be seen that, in this case,

the Lyapunov exponents may move away from each other all throughout the bifurcation process, and hence there is no chance at all to anticipate the oncoming transition based only on their behavior. This is the same observation made earlier in Figure 4.1(c), (g) for the discrete time case.

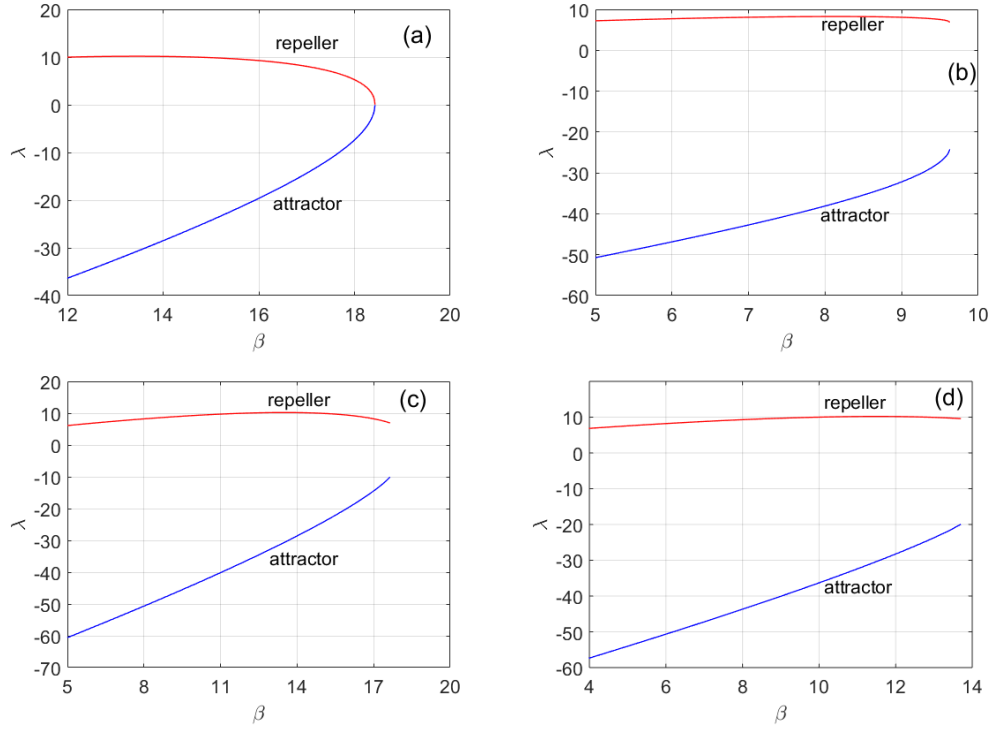


Figure 4.2: **(a) and (b):** Lyapunov exponents during fold bifurcations in the qpf Allee model; (a) smooth bifurcation with $r = 80$, $K = 10$, $S = 0.1$, $q = 1$, $\nu = (2\omega, 2\pi)$ (where ω is the irrational part of the golden mean) and $\kappa = 4$ (bifurcation at $\beta_c \simeq 18.4269$); (b) non-smooth bifurcation with $r = 80$, $K = 10$, $S = 0.1$, $q = 5$, $\nu = (2\omega, 2\pi)$ and $\kappa = 51.2$. The bifurcation occurs at $\beta_c \simeq 9.628$.

(c) and (d): Lyapunov exponents during the fold bifurcation in the randomly forced Allee model; (c) with $r = 80$, $K = 10$, $S = 0.1$, $\kappa = 2$ and bifurcation parameter $\beta_c = 17.978$; (d) with $r = 80$, $K = 10$, $S = 0.1$, $\kappa = 6$ and bifurcation parameter $\beta_c = 13.978$;

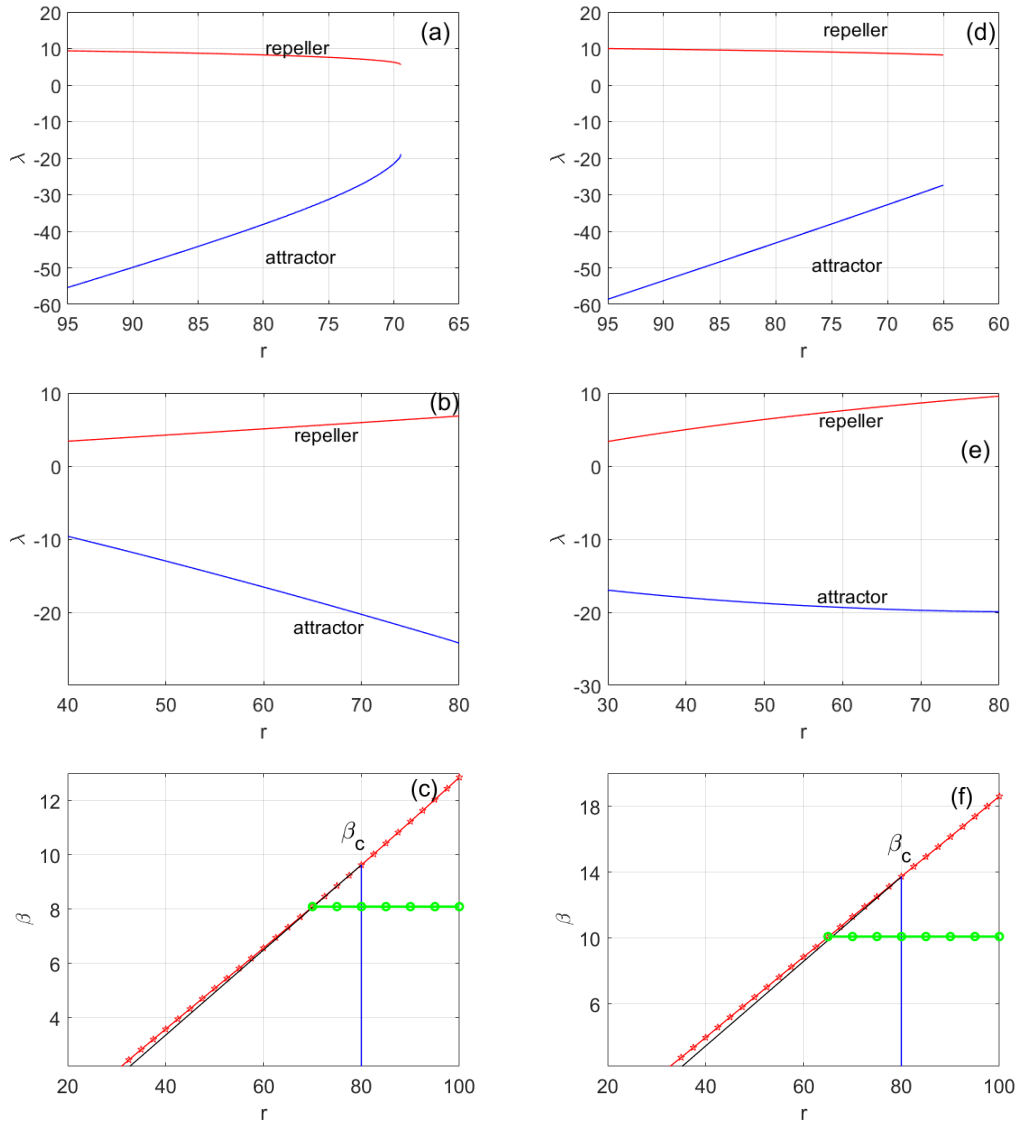


Figure 4.3: Lyapunov exponents during fold bifurcations in the forced Allee model with different variations of parameters. (a) shows the behaviour in the qpf case as the parameter r is decreased, corresponding to the horizontal green line in the two-parameter space depicted in (c). In contrast, (b) shows the behaviour when β and r are varied simultaneously along the black curve in (c). In this case, the Lyapunov exponents move apart throughout the entire bifurcation process. In (d) and (e), similar plots are shown for the randomly forced case. In (d), again only the parameter r is varied and decreases along the horizontal green line in (f). In (e), both parameters β and r are again varied at the same time, along the black curve in (f). In both (c) and (f), the red line is an interpolation of the numerically determined critical parameters for different values of β and r .

Remark 4.1. We should note that the phenomenon that we describe here is probably known by folklore in the field of stochastic processes and stochastic differential equations, where the presence of noise equally prevents the recovery rates from going down all the way to zero before a transition happens. However, in this context it is much harder to pin this observation down mathematically, since the presence of unbounded noise immediately ‘destroys’ the fold bifurcation and leads to the existence of a unique stationary measure in stochastic versions of (1.2) and similar models. Moreover, the forcing with bounded noise is arguably more reasonable from the biological viewpoint.

Theorem 4.2. *Suppose that $(\Xi_\beta)_{\beta \in [0,1]}$ is a parameter family of forced monotone \mathcal{C}^2 -flows that satisfies the assumptions of Theorem 2.18 (for deterministic forcing) or Theorem 2.24 (for random forcing). Further, assume that the fold bifurcation that occurs in this family at the critical parameter β_c is non-smooth. Then*

$$\lim_{\beta \nearrow \beta_c} \lambda(\varphi_\beta^+) = \lambda(\varphi_{\beta_c}^+) < 0. \quad (4.1)$$

If the fold bifurcation is smooth, then $\lim_{\beta \nearrow \beta_c} \lambda(\varphi_\beta^+) = 0$. The analogous results hold for the unstable equilibrium φ_β^- .

Proof. Theorem 4.2 In order to prove this, we only consider the deterministic case. The random case can be dealt with similarly. Let $(\Xi_\beta)_{\beta \in [0,1]}$ satisfy the assumptions of Theorem 2.18. We claim that for each $\theta \in \Theta$ we have that $\varphi_{\beta_c}^+(\theta)$ coincides with

$$\varphi(\theta) = \lim_{\beta \nearrow \beta_c} \varphi_\beta^+(\theta).$$

Note that φ is well-defined due to the monotone dependence of ξ_β^t on β (see assumption (v) in Theorem 2.10) which results in $\varphi_\beta \geq \varphi_{\beta'}$ whenever $\beta < \beta' \leq \beta_c$. In order to see that $\varphi(\theta) = \varphi_{\beta_c}^+(\theta)$, fix $\theta \in \Theta$, $t > 0$ and $\varepsilon > 0$. Choose $\delta > 0$ such that $|\xi_{\beta_c}^t(\theta, \varphi(\theta)) - \xi_{\beta_c}^t(\theta, x)| < \varepsilon$ for all $x \in B_\delta(\varphi(\theta))$ and at the same time $|\xi_\beta^t(\theta, x) - \xi_{\beta'}^t(\theta, x)| < \varepsilon$ whenever $|\beta - \beta'| < \delta$. Note that such δ exists due to the uniform continuity of $(\beta, x) \mapsto \xi_\beta^t(\theta, x)$. Let $\beta < \beta_c$ be such that $\beta_c - \beta < \delta$, $\varphi_\beta^+(\theta) - \varphi(\theta) < \delta$ and $\varphi_\beta^+(\rho^t(\theta)) - \varphi(\rho^t(\theta)) < \varepsilon$.

We obtain

$$\begin{aligned}
 |\xi_{\beta_c}^t(\theta, \varphi(\theta)) - \varphi(\rho^t(\theta))| &\leq |\xi_{\beta_c}^t(\theta, \varphi(\theta)) - \xi_{\beta}^t(\theta, \varphi(\theta))| + |\xi_{\beta}^t(\theta, \varphi(\theta)) - \varphi_{\beta}^+(\rho^t(\theta))| \\
 &\quad + |\varphi_{\beta}^+(\rho^t(\theta)) - \varphi(\rho^t(\theta))| \\
 &\leq |\xi_{\beta}^t(\theta, \varphi(\theta)) - \varphi_{\beta}^+(\rho^t(\theta))| + 2\varepsilon \\
 &= |\xi_{\beta}^t(\theta, \varphi(\theta)) - \xi_{\beta}^t(\theta, \varphi_{\beta}^+(\theta))| + 2\varepsilon \leq 3\varepsilon.
 \end{aligned}$$

As $\varepsilon > 0$ was arbitrary, this proves $\xi_{\beta_c}^t(\theta, \varphi(\theta)) = \varphi(\rho^t(\theta))$ and hence the invariance of φ under Ξ_{β_c} . Now, since the graphs $\varphi_{\beta_c}^+$ are monotonically decreasing in β , we have $\varphi \geq \varphi_{\beta_c}^+$. As there is no Ξ_{β_c} -invariant graph above $\varphi_{\beta_c}^+$ in the considered region Γ , we obtain $\varphi_{\beta_c}^+ = \varphi$. By definition

$$\lim_{\beta \nearrow \beta_c} \lambda(\varphi_{\beta}^+(\theta)) = \lim_{\beta \nearrow \beta_c} \frac{1}{t} \int_{\Theta} \log |\partial_x \xi_{\beta}^t(\theta, \varphi_{\beta}^+(\theta))| d\nu(\theta)$$

Using dominated convergence with majorant η from Theorem 2.24(vii), this yields

$$\begin{aligned}
 \lim_{\beta \nearrow \beta_c} \lambda(\varphi_{\beta}^+(\theta)) &= \frac{1}{t} \int_{\Theta} \lim_{\beta \nearrow \beta_c} \log |\partial_x \xi_{\beta}^t(\theta, \varphi_{\beta}^+(\theta))| d\nu(\theta), \\
 &= \frac{1}{t} \int_{\Theta} \log |\partial_x \xi_{\beta_c}^t(\theta, \varphi_{\beta_c}^+(\theta))| d\nu(\theta), \\
 &= \lambda(\varphi_{\beta_c}^+) < 0.
 \end{aligned}$$

The same argument works for $\varphi_{\beta_c}^-$ and this ends the proof. \square

4.2 Lyapunov gap in hybrid forced systems

To discuss recovery rates and critical slowing down in hybrid forced systems, we will restrict our analysis to the numerical findings in the discrete time case. However, the same observations can be made in the continuous time case with the Allee model. Considering the hybrid forced discrete time model (3.15), the behaviour of the Lyapunov exponents on the attractor and repeller is shown in Figure 4.4. Making reference to the random case, we also show the behavior for different values of ϵ in (a) and (b). Analogously, we also show the behaviour for the simultaneous variation of β and ϵ in (c). The curve for the variation of these two parameters is shown in (e). At the same time, we also vary the parameters α and β simultaneously in (f), and

the behaviour of the Lyapunov exponents corresponding to the curve in (f) is shown in (d). Notice that the behaviour in 4.4(d) is similar to the behaviour in the quasiperiodic case shown in 4.1(c), where the Lyapunov exponents move further apart from zero. Notice that, in Figure 4.4(c), the bigger the intensity of the noise, the further apart the Lyapunov exponents move away from each other, which is similar to what we observe in Figure 4.1(g). The following statement on the Lyapunov gap in hybrid forced systems is an extension of the results in the previous Section 4.1.

Theorem 4.3. *Suppose that $(\Psi_\beta)_{\beta \in [0,1]}$ is a parameter family of T -forced monotone \mathcal{C}^2 -interval flows that satisfies the assumptions of Theorem 2.24. Further, assume that Φ is an invariant graph of Ψ . Then*

$$\lim_{\beta \nearrow \beta_c} \lambda(\Phi_\beta^+) = \lambda(\Phi_{\beta_c}^+) < 0. \quad (4.2)$$

The analogous results hold for the unstable equilibrium Φ_β^- .

Proof. Theorem 4.3 Let $(\Psi_\beta)_{\beta \in [0,1]}$ be a parameter family of hybrid-forced skew monotone flows such that the assumptions of Theorem 2.24 are satisfied. First, we claim that

$$\Phi(\theta, \omega) = \lim_{\beta \nearrow \beta_c} \Phi_\beta^+(\theta, \omega) = \Phi_{\beta_c}^+(\theta, \omega) \quad (4.3)$$

ψ_β is monotonically decreasing in β by (vi) in Theorem 2.24. Due to assumption (iii) in Theorem 2.24, ψ_β is continuous in β and x . To show that $\Phi(\theta, \omega)$ is an invariant graph, fix $(\theta, \omega) \in M$, $\varepsilon > 0$ and $t > 0$, recall that $M = \Theta \times \Sigma$. Then by continuity we can find a δ such that $|\psi_{\beta_c}^t(\theta, \omega, \Phi^+(\theta, \omega)) - \psi_{\beta_c}^t(\theta, \omega, \Phi(\theta, \omega))| < \varepsilon$ implies that $|\Phi^+(\theta, \omega) - \Phi(\theta, \omega)| < \delta$. Also by continuity in β , we have that $|\psi_\beta^t(\theta, \omega, \Phi^+(\theta, \omega)) - \psi_{\beta'}^t(\theta, \omega, \Phi^+(\theta, \omega))| < \varepsilon$ implies that $|\beta - \beta'| < \delta$. Thus we have

$$\begin{aligned} |\psi_{\beta_c}^t(\theta, \omega, \Phi(\theta, \omega)) - \Phi(\rho^t(\theta), \sigma^t(\omega))| &\leq |\psi_{\beta_c}^t(\theta, \omega, (\Phi(\theta, \omega)) - \psi_\beta^t(\theta, \omega, \Phi(\theta, \omega))| \\ &\quad + |\psi_\beta^t(\theta, \omega, \Phi(\theta, \omega)) - \Phi(\rho^t(\theta), \sigma^t(\omega))| \\ &\leq |\psi_\beta^t(\theta, \omega, \Phi(\theta, \omega)) - \Phi(\rho^t(\theta), \sigma^t(\omega))| + \varepsilon \end{aligned}$$

Let $\beta < \beta_c$ such that $\beta_c - \beta < \delta$, $\Phi_\beta^+(\theta, \omega) - \Phi(\theta, \omega) < \delta$ and $\Phi_\beta^+(\rho^t(\theta), \sigma^t(\omega)) - \Phi(\rho^t(\theta), \sigma^t(\omega)) < \varepsilon$, then

$$\begin{aligned} |\psi_{\beta_c}^t(\theta, \omega, \Phi(\theta, \omega)) - \Phi(\rho^t(\theta), \sigma^t(\omega))| &\leq |\psi_\beta^t(\theta, \omega, (\Phi(\theta, \omega)) - \Phi_\beta^+(\rho^t(\theta), \sigma^t(\omega))| \\ &\quad + |\Phi_\beta^+(\rho^t(\theta), \sigma^t(\omega)) - \Phi(\rho^t(\theta), \sigma^t(\omega))| \\ &\leq |\psi_\beta^t(\theta, \omega, (\Phi(\theta, \omega)) - \Phi_\beta^+(\rho^t(\theta), \sigma^t(\omega))| + 2\varepsilon \end{aligned}$$

by the invariance of Φ_β^+ , we have

$$\begin{aligned} &= |\psi_\beta^t(\theta, \omega, \Phi(\theta, \omega)) - \psi_\beta^t(\theta, \omega, \Phi_\beta^+(\theta, \omega))| + 2\varepsilon \\ &\leq 3\varepsilon \end{aligned}$$

Since $\varepsilon > 0$ was arbitrary, this shows that $\Phi(\theta, \omega)$ is an invariant graph of Ψ_{β_c} which coincides with $\Phi_{\beta_c}^+$. And therefore, we deduce the statement on the Lyapunov exponents by applying the dominated convergence theorem with majorant $\eta(\theta, \omega)$, exactly as in the proof of Theorem 4.2 which gives

$$\lim_{\beta \nearrow \beta_c} \lambda(\Phi_\beta^+(\theta, \omega)) = \lambda(\Phi_{\beta_c}^+) < 0. \quad \square$$

Generally speaking, Theorem 4.2 and Theorem 4.3 suggest that for non-smooth fold bifurcations, there exists a Lyapunov gap and the presence of this gap indicates absence of recovery rates or no critical slowing down. However, in case of a smooth bifurcation, no existence of a Lyapunov gap is observed, which indicates the presence of critical slowing down. This implies that, slow recovery rates and critical slowing can be used to signal a smooth saddle-node bifurcation but not to detect a non-smooth fold bifurcation. From the examples considered in this thesis, we observe that the formation of SNAs is a result of non-smooth fold bifurcations and the presence of a Lyapunov gap is a way of detecting such SNAs. As discussed earlier in Chapter 1, there are different routes to formation of SNAs in various systems. However, it is not clear how these can be anticipated as the mechanism of formation of SNAs may differ from the ones we consider in our work. Therefore a Lyapunov gap may not be generic for all systems that exhibit SNAs. We leave this for further investigations in the future.

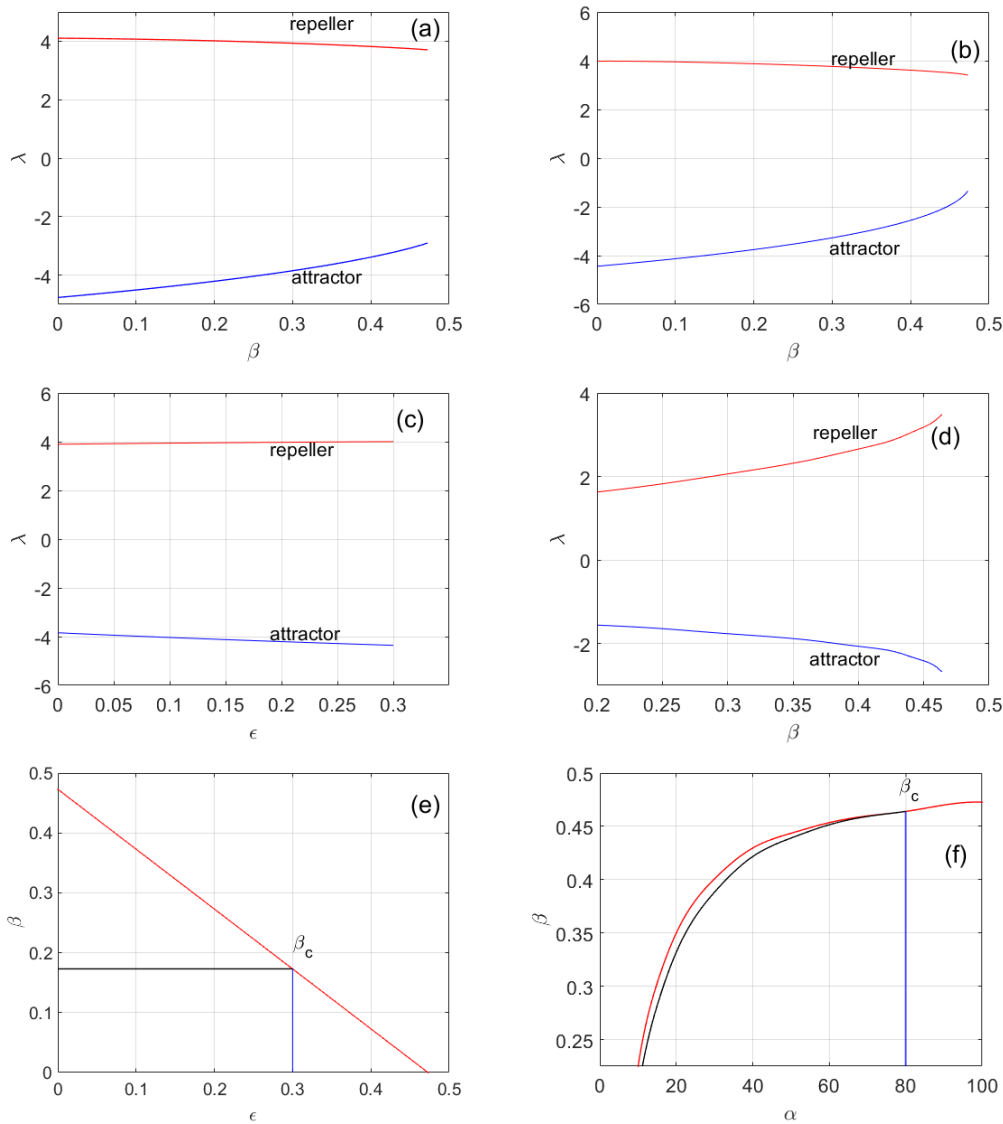


Figure 4.4: **(a)–(d)**: Lyapunov exponents during non-smooth bifurcations in hybrid forced discrete time model of the form (3.15) for $\kappa = 0.5$, $\rho = (\sqrt{5} - 1)/2$. In (a) and (b) $\alpha = 100$, and $\beta = 0.4729$, however, $\epsilon = 0.3$ in (a) and $\epsilon = 0.1$ in (b). In (c), we show the behaviour for the variation of ϵ while keeping β constant, i.e $\beta = 0.173$. This variation is shown in (e) along the black curve, whereas in (d), we show the behaviour for the simultaneous variation of α and β . The variation of these parameters is shown in (f) along the black curve. The red curve in (e) and (f) represents the bifurcation curve of the system.

4.3 Slope at the bifurcation point

Although this is not in our main focus, we want to comment in this section on a particular qualitative difference between non-smooth fold bifurcations in the quasiperiodically forced, randomly forced and the hybrid-forced cases. As it can be seen from Figure 4.2(b)–(c), the slope of the Lyapunov exponents of the attractors increases more strongly towards the bifurcation in the quasiperiodically forced case, whereas it only increases slightly (Figure 4.2(c)) or even remains constant (Figure 4.2(d)) in the random case. In the hybrid case, as can be seen from Figure 4.4(a)–(b), it clearly depends on the intensity of the noise term ϵ . If the noise is too small, this takes the shape of the behavior in the quasiperiodic case Figure 4.4(b), whereas for a bigger noise, it behaves otherwise as shown in the random case Figure 4.4(a). In fact, the heuristic description of non-smooth fold bifurcations in qpf system given in Chapter 2 suggests that $\partial_\beta \lambda(\varphi_\beta^+)$ should actually increase to infinity as $\beta \nearrow \beta_c$. The reason is that due to the concavity of the right side of the vector field, the Lyapunov exponent increases whenever the graph decreases. Moreover, the quantitative contribution of each peak that develops should be the product between its width and its speed, which is more or less constant since both decrease, respectively increase, with the same exponential rate. Hence, this means that every peak contributes a similar amount to the slope of the Lyapunov exponent, and as there are infinitely many peaks, this slope grows to infinity as the bifurcation is approached. In principle, we believe that this heuristic explanation could be made precise by using the machinery for the proof of non-smooth fold bifurcations in [Fuh16a, Fuh16b]. This however, goes beyond our current scope. For the case of random forcing, we provide a proof for the boundedness of the slope of the Lyapunov exponent of φ_β^+ as $\beta \nearrow \beta_c$. In order to avoid too many technicalities and to not obstruct the view on the underlying mechanism, we restrict to the case of the discrete-time example (2.16). We note, however, that the proof can be generalised to broader classes of monotone skew product maps and, with some more work required, to continuous-time systems.

Theorem 4.4. *Suppose $(f_\beta)_{\beta \in [0,1]}$ is the family of skew product maps given by (2.16) with $\Sigma = \{0, 1\}^{\mathbb{Z}}$ the Bernoulli space equipped with the shift map σ and the Bernoulli measure μ . Let $\beta_c = \frac{\sqrt{2\alpha - \pi}}{\alpha\sqrt{\pi}}$. Then $(f_\beta)_{\beta \in [0,1]}$ satisfies the hypothesis of Theorem 2.24 (with $\gamma^- = 0$ and $\gamma^+ = 1$) and undergoes*

a non-smooth saddle-node bifurcation with critical parameter β_c . Moreover, there exists a constant $C > 0$ such that

$$|\partial_\beta \lambda_\mu(\varphi_\beta^\pm)| \leq C$$

for all $\beta \in [0, \beta_c]$.

Before we turn to the proof of the Theorem 4.4, we first need the following preliminary result.

Lemma 4.5. *In the situation of Theorem 4.4 we let $\gamma_{n,\beta}^\pm = f_{\beta_*}^{\pm n} \gamma^\pm$, where the graph transform $f_{\beta_*}^n$ is defined as in the proof of Theorem 3.5. Then $\gamma_{n,\beta}^\pm(\omega)$ converges to $\varphi_\beta^\pm(\omega)$ uniformly in β and ω (with $\beta \in [0, \beta_c]$ and $\omega \in \Sigma$) as $n \rightarrow \infty$. Moreover, for all $\omega \in \Sigma$, the map $[0, \beta_c] \ni \beta \mapsto \varphi_\beta^\pm(\omega)$ is differentiable and for $\beta' \in [0, \beta_c)$, we have that*

$$\partial_\beta \gamma_{n,\beta}^\pm(\omega) = - \sum_{i=1}^n \prod_{\ell=1}^{i-1} \partial_x f_{\beta, \sigma^{-\ell}\omega}^{\pm 1}(f_{\beta, \sigma^{-n}\omega}^{\pm(n-\ell)}(1)) \xrightarrow{n \rightarrow \infty} \partial_\beta \varphi_\beta^\pm(\omega) \quad (4.4)$$

uniformly in β and ω for all $\beta \in [0, \beta']$ and all $\omega \in \Sigma$.

Proof. We only consider $\gamma_{n,\beta}^+$ and φ_β^+ , the statements for $\gamma_{n,\beta}^-$ and φ_β^- follow analogously. Recall that

$$f_\beta : \Sigma \times X \rightarrow \Sigma \times X \quad , \quad (\omega, x) \mapsto (\sigma(\omega), g(x) + \kappa \cdot \omega_0 - \beta) \quad ,$$

with $g(x) = \frac{2}{\pi} \arctan(\alpha x)$. First, observe that $\partial_x^2 f_{\beta,\omega}^n(x) < 0$ for all $n \in \mathbb{N}$ as long as $x, f_{\beta,\omega}(x) \cdots f_{\beta,\sigma^{n-1}(\omega)}(x) > 0$ since the composition of concave increasing functions is again concave. Second, note that with $\omega^* = \dots 0, 0, 0 \dots \in \Sigma$, we have

$$f_{\beta_c, \omega^*}(x) = f_{\beta, \omega}(x) - (\beta_c - \beta) - \kappa \omega_0 \quad (4.5)$$

for all $\beta \in [0, \beta_c]$ and all $\omega \in \Sigma, x \in X$. Hence, we obtain that for all

$\beta \in [0, \beta_c]$, $\omega \in \Sigma$ and all $n, n' \in \mathbb{N}$ with $n \geq n'$ we have

$$\begin{aligned}
 |\gamma_{n',\beta}^+(\omega) - \gamma_{n,\beta}^+(\omega)| &= f_{\beta,\sigma^{-n'}\omega}^{n'}(1) - f_{\beta,\sigma^{-n'}\omega}^{n'}(f_{\beta,\sigma^{-n}\omega}^{n-n'}(1)) \\
 &\leq f_{\beta,\sigma^{-n'}\omega}^{n'}(1) - f_{\beta,\sigma^{-n'}\omega}^{n'}(f_{\beta_c,\omega^*}^{n-n'}(1)) \\
 &= f_{\beta,\sigma^{1-n'}\omega}^{n'-1}(f_{\beta,\sigma^{-n'}\omega}(1)) - f_{\beta,\sigma^{1-n'}\omega}^{n'-1}(f_{\beta,\sigma^{-n'}\omega}(f_{\beta_c,\omega^*}^{n-n'}(1))) \\
 &\leq f_{\beta,\sigma^{1-n'}\omega}^{n'-1}(f_{\beta_c,\omega^*}(1)) - f_{\beta,\sigma^{1-n'}\omega}^{n'-1}(f_{\beta_c,\omega^*}(f_{\beta_c,\omega^*}^{n-n'}(1))) \\
 &\leq f_{\beta,\sigma^{2-n'}\omega}^{n'-2}(f_{\beta_c,\omega^*}^2(1)) - f_{\beta,\sigma^{2-n'}\omega}^{n'-2}(f_{\beta_c,\omega^*}^2(f_{\beta_c,\omega^*}^{n-n'}(1))) \\
 &\leq \dots \leq f_{\beta_c,\omega^*}^{n'}(1) - f_{\beta_c,\omega^*}^{n'}(f_{\beta_c,\omega^*}^{n-n'}(1)) \\
 &= |\gamma_{n',\beta_c}^+(\omega^*) - \gamma_{n,\beta_c}^+(\omega^*)|,
 \end{aligned}$$

where we used the above mentioned concavity together with (4.5) in the steps to the fourth, fifth and sixth line. This proves the first part. Next, we show that $\partial_\beta \gamma_{n,\beta}^+(\omega)$ converges uniformly in ω and β which immediately implies the second part. To that end, we first provide a uniform upper bound on

$$\sup_{\omega \in \Sigma, \beta \in [0, \beta']} \partial_x f_{\beta,\omega}(\gamma_{n,\beta}^+(\omega))$$

for all $n \in \mathbb{N}$: Similarly as in the proof of Theorem 3.3, we see that

$$x_{\min}(\beta) := \min_{\omega \in \Sigma} \varphi_\beta^+(\omega) \geq x_0(\beta')$$

for all $\beta \in [0, \beta']$, where $x_0(\beta')$ is the upper fixed point of the map $g - \beta'$. Hence, we have

$$\begin{aligned}
 0 &\leq \sup_{\omega \in \Sigma, \beta \in [0, \beta']} \partial_x f_{\beta,\omega}(\gamma_{n,\beta}^+(\omega)) = \sup_{\omega \in \Sigma, \beta \in [0, \beta']} g'(\gamma_{n,\beta}^+(\omega)) \leq g'(\varphi_\beta^+(\omega)) \\
 &\leq g'(x_0(\beta')) =: c < 1,
 \end{aligned} \tag{4.6}$$

where we used the concavity of g and the monotone dependence of $\varphi_\beta^+(\omega)$ on β . Now, observe that

$$\begin{aligned}
 \partial_\beta \gamma_{n,\beta}^+(\omega) &= \partial_\beta f_{\beta,\sigma^{-n}\omega}^n(1) \\
 &= \partial_\beta f_{\beta,\sigma^{-1}\omega}(f_{\beta,\sigma^{-n}\omega}^{n-1}(1)) + \partial_x f_{\beta,\sigma^{-1}\omega}(f_{\beta,\sigma^{-n}\omega}^{n-1}(1)) \cdot \partial_\beta f_{\beta,\sigma^{-n}\omega}^{n-1}(1) \\
 &= \dots = \sum_{i=1}^n \partial_\beta f_{\beta,\sigma^{-i}\omega}(f_{\beta,\sigma^{-n}\omega}^{n-i}(1)) \prod_{\ell=1}^{i-1} \partial_x f_{\beta,\sigma^{-\ell}\omega}(f_{\beta,\sigma^{-n}\omega}^{n-\ell}(1)) \\
 &= - \sum_{i=1}^n \prod_{\ell=1}^{i-1} \partial_x f_{\beta,\sigma^{-\ell}\omega}(f_{\beta,\sigma^{-n}\omega}^{n-\ell}(1)).
 \end{aligned}$$

Together with (4.6), we hence obtain for $n \geq n'$

$$|\partial_\beta \gamma_{n',\beta}^+(\omega) - \partial_\beta \gamma_{n,\beta}^+(\omega)| = \sum_{i=n'+1}^n \prod_{\ell=1}^{i-1} \partial_x f_{\beta,\sigma^{-\ell}\omega}(f_{\beta,\sigma^{-n}\omega}^{n-\ell}(1)) \leq \sum_{i=n'+1}^n c^{i-1},$$

which proves the statement. \square

We can now turn to the

Proof of Theorem 4.4. We keep the notation of the previous proof. Observe that $(g - \kappa - \beta)_{\beta \in [0,1]}$ is an autonomous reference family for $(f_\beta)_{\beta \in [0,1]}$. Clearly, the fact that $(f_\beta)_{\beta \in [0,1]}$ undergoes a non-smooth saddle-node bifurcation with critical parameter β_c (given by the bifurcation parameter of the family $(g - \beta)_{\beta \in [0,1]}$) is a direct consequence of Theorem 3.3. Hence, it remains to prove the existence of a uniform bound on the slope of the Lyapunov exponent. As before, we only consider φ_β^+ . Further, we show the statement for $\beta \in [0, \beta_c)$ which immediately yields the full statement by means of the mean value theorem. Let g be as in the proof of Lemma 4.5. Given $\beta \in [0, \beta_c)$, observe that

$$\begin{aligned} \partial_\beta \lambda_\mu(\varphi_\beta^+) &= \partial_\beta \int_\Sigma \log \partial_x f_{\beta,\omega}(\varphi_\beta^+(\omega)) d\omega \\ &= \partial_\beta \int_\Sigma \log g'(\varphi_\beta^+(\omega)) d\omega = \int_\Sigma \frac{g''(\varphi_\beta^+(\omega))}{g'(\varphi_\beta^+(\omega))} \cdot \partial_\beta \varphi_\beta^+(\omega) d\omega. \end{aligned}$$

With $c \geq \sup_{x \in [0,1]} |g''(x)/g'(x)|$, we hence obtain

$$|\partial_\beta \lambda_\mu(\varphi_\beta^+)| \leq c \int_\Sigma |\partial_\beta \varphi_\beta^+(\omega)| d\omega.$$

Now, let

$$\alpha = \sup_{\omega \in \Sigma, \theta_0=1} f'_{\beta_c, \sigma\omega}(f_{\beta_c, \omega}(x_c))$$

and note that

$$\alpha \leq g'(g(x_c) - \beta_c + \kappa/2) = g'(x_c + \kappa/2) < g'(x_c) = 1,$$

where x_c is the neutral fixed point of the map $g - \beta_c$. Then

$$\begin{aligned}
\int_{\Sigma} |\partial_{\beta} \varphi_{\beta}^{+}(\omega)| d\omega &= \int_{\Sigma} |\partial_{\beta} \lim_{n \rightarrow \infty} \gamma_{n, \beta}^{+}(\omega)| d\omega = \lim_{n \rightarrow \infty} \int_{\Sigma} |\partial_{\beta} \gamma_{n, \beta}^{+}(\omega)| d\omega \\
&\stackrel{(4.4)}{=} \lim_{n \rightarrow \infty} \int_{\Sigma} \sum_{i=1}^n \prod_{\ell=1}^{i-1} \partial_x f_{\beta, \sigma^{-\ell} \omega}(f_{\beta, \sigma^{-n} \omega}^{n-\ell}(1)) d\omega \\
&= \lim_{n \rightarrow \infty} \sum_{i=1}^n \int_{\Sigma} \prod_{\ell=1}^{i-1} \partial_x f_{\beta, \sigma^{-\ell} \omega}(f_{\beta, \sigma^{-n} \omega}^{n-\ell}(1)) d\omega \\
&\leq \lim_{n \rightarrow \infty} \sum_{i=1}^n \int_{\Sigma} \prod_{\ell=1}^{i-1} \partial_x f_{\beta, \sigma^{-\ell} \omega}(f_{\beta, \sigma^{-\ell-1} \omega}(x_c)) d\omega \\
&\leq \lim_{n \rightarrow \infty} \sum_{i=1}^n \sum_{k=0}^{i-1} \alpha^k \cdot \mu(\{\omega \in \Sigma : k = \#\{1 < \ell \leq i : \theta_{-\ell} = 1\}\}) \\
&= \lim_{n \rightarrow \infty} \sum_{i=1}^n \sum_{k=0}^{i-1} \alpha^k \cdot \binom{i-1}{k} (1/2)^{i-1} \\
&= \lim_{n \rightarrow \infty} \sum_{i=1}^n \sum_{k=0}^{i-1} \binom{i-1}{k} (\alpha/2)^k (1/2)^{i-1-k} \\
&= \lim_{n \rightarrow \infty} \sum_{i=1}^n (\alpha/2 + 1/2)^{i-1} < \infty .
\end{aligned}$$

Since α is independent of β , the statement follows. \square

Chapter 5

Range of finite-time Lyapunov exponents

In this chapter, we discuss possible alternative early warning signals for a non-smooth saddle node bifurcation as a special case of a critical transition. The aim is to provide a rigorous statement for the behaviour of Lyapunov exponents on the attractor in finite time which translates into an early warning signal. Again, just as in the previous chapter, we will treat the qpf and random case together, whereas the hybrid case will be treated separately.

5.1 FTLEs in qpf and randomly forced systems

To that end, let us introduce the maximal finite-time Lyapunov exponent on the attractor of a quasiperiodically forced or randomly forced system. As non-continuous invariant graphs only need to be defined almost surely, we only take into account exponents that can be ‘seen’ on a set of positive measure. Thus, we consider

$$\lambda_k^{\max}(\varphi_\beta^+) = \sup \left\{ \lambda \in \mathbb{R} \mid \mu_{\varphi_\beta^+}(\{(\theta, x) \mid \lambda_k(f_\beta, \theta, x) \geq \lambda\}) > 0 \right\}.$$

Here, the graph measure $\mu_{\varphi_\beta^+}$ is as discussed in Chapter 2. Note that if the forcing is quasiperiodic, then the attractors prior to the bifurcation are all continuous so that we actually have $\lambda_k^{\max}(\varphi_\beta^+) = \max \left\{ \lambda_k(\theta, \varphi_\beta^+(\theta)) \mid \theta \in \mathbb{T}^1 \right\}$ whenever $\beta < \beta_c$. We first consider the case of quasiperiodic forcing, where the general statement we aim at reads as follows.

Theorem 5.1. *Suppose $(\Xi_\beta)_{\beta \in [0,1]}$ is a parameter family of qpf monotone flows that satisfies the hypothesis of Theorem 2.18. Then for all $k \in \mathbb{N}$ we have*

$$\varliminf_{\beta \nearrow \beta_c} \lambda_k^{\max}(\varphi_\beta^+) \geq \lambda(\varphi_{\beta_c}^-). \quad (5.1)$$

Before we turn to the proof, however, we have to address some subtleties concerning the topology of pinched invariant graphs in this setting. Suppose we are in the situation of Theorem 2.18, so that there exist exactly two graphs $\varphi_{\beta_c}^- < \varphi_{\beta_c}^+$ (up to modifications on sets of measure zero), where $\varphi_{\beta_c}^-$ is lower and $\varphi_{\beta_c}^+$ is upper semicontinuous. Let $A^+ = \text{supp}(\mu_{\varphi_{\beta_c}^+})$ and $A^- = \text{supp}(\mu_{\varphi_{\beta_c}^-})$, where $\text{supp}(\nu)$ denotes the topological support of a measure ν .¹ Then A^+ is Ξ_{β_c} -invariant, and consequently the upper and lower bounding graphs $\varphi_{A^+}^u$ and $\varphi_{A^+}^l$ given by

$$\varphi_{A^+}^u(\theta) = \sup A_\theta^+ \quad \text{and} \quad \varphi_{A^+}^l(\theta) = \inf A_\theta^+$$

are Ξ_β -invariant graphs, with $\varphi_{A^+}^u$ upper and $\varphi_{A^+}^l(\theta)$ lower semicontinuous (see [Sta03]). As $\varphi_{\beta_c}^\pm$ are the only Ξ_β -invariant graphs in the considered region Γ , we must have $\varphi_{A^+}^l(\theta) = \varphi_{\beta_c}^-$ and $\varphi_{A^+}^u = \varphi_{\beta_c}^+$ almost surely. This implies in particular that $(\theta, \varphi_{\beta_c}^-(\theta)) \in A^+$ almost surely, so that $\mu_{\varphi_{\beta_c}^-}(A^+) = 1$ and hence $A^- \subseteq A^+$. As the converse inclusion follows in the same way, we have $A^- = A^+$. One particular consequence that follows from this discussion is the following

Lemma 5.2. *For μ -almost every $\theta_0 \in \Theta$ and every $\delta > 0$ there exists a set $B \subseteq \Theta$ of positive measure such that*

$$\{(\theta, \varphi_{\beta_c}^+(\theta)) \mid \theta \in B\} \subseteq B_\delta(\theta_0, \varphi_{\beta_c}^-(\theta_0)).$$

We can now turn to the

Proof of Theorem 5.1. Fix $k \in \mathbb{N}$ and $\varepsilon > 0$. We claim that there exists a set of positive measure of $\theta \in \Theta$ such that

$$\lambda_k(\theta, \varphi_{\beta_c}^-(\theta)) \geq \lambda(\varphi_{\beta_c}^-) - \frac{\varepsilon}{2}. \quad (5.2)$$

¹Given a Borel measure ν on some second countable metric space X , the support of ν is defined as $\text{supp}(\nu) = \{x \in X \mid \nu(B_\delta(x)) > 0 \forall \delta > 0\} = X \setminus \bigcup_{U \text{ open}, \nu(U)=0} U$. It is easy to see that $\text{supp}(\nu)$ is always closed and can be characterized as the smallest closed set $A \subseteq X$ with $\nu(X \setminus A) = 0$. Moreover, if ν is invariant under some continuous transformation f , then so is $\text{supp}(\nu)$.

In order to see this, suppose for a contradiction that

$$\lambda_k(\theta, \varphi_{\beta_c}^-(\theta)) \leq \lambda(\varphi_{\beta_c}^-) - \frac{\varepsilon}{2}$$

for almost every $\theta \in \Theta$ and some $\varepsilon > 0$. This implies that the pointwise Lyapunov exponent also satisfies

$$\lambda(\theta, \varphi_{\beta_c}^-(\theta)) \leq \lambda(\varphi_{\beta_c}^-) - \frac{\varepsilon}{2}$$

for almost every θ , contradicting Birkhoff's Ergodic Theorem. Hence, there exists a positive measure set of θ which satisfies (5.2). Due to Lemma 5.2, we can therefore fix $\delta > 0$ and choose $\theta_0 \in \Theta$ which satisfies (5.2) and a set $B \subseteq \Theta$ of positive measure such that $(\theta, \varphi_{\beta_c}^+(\theta)) \in B_\delta(\theta_0, \varphi_{\beta_c}^-(\theta_0))$ for all $\theta \in B$. If δ is chosen small enough, then it follows by continuity that

$$\lambda_k(\theta, \varphi_{\beta_c}^+(\theta)) \geq \lambda(\varphi_{\beta_c}^-) - \varepsilon$$

for all $\theta \in B$. As $\varepsilon > 0$ was arbitrary, we obtain that $\lambda_k^{\max}(\varphi_{\beta_c}^+) \geq \lambda(\varphi_{\beta_c}^-)$. Finally, as $\lim_{\beta \nearrow \beta_c} \varphi_\beta^+(\theta) = \varphi_{\beta_c}^+(\theta)$ almost surely, we obtain (5.1) again by continuity. \square

We now turn to the random case. In this case, we have to restrict to the setting of Theorem 3.3 (instead of the more general situation of Theorem 2.24).

Theorem 5.3. *Suppose that $(\Xi_\beta)_{\beta \in [0,1]}$ is a parameter family of randomly forced monotone flows that satisfies the assumptions of Theorem 3.3. Further assume that for all $\varepsilon, T, k > 0$, there exists a set $A_{\varepsilon, k, T}$ of positive measure such that (3.4) is satisfied and $|\lambda_k(\sigma^t(\omega), \xi_\beta^t(\omega, x)) - \lambda_k(g_\beta^t(x))| < \varepsilon$ for all $\omega \in A_{\varepsilon, k, T}$, $k \leq T$. Then for all $k \in \mathbb{R}$*

$$\lim_{\beta \nearrow \beta_c} \lambda_k^{\max}(\varphi_\beta^+) = 0. \quad (5.3)$$

Proof. Let $(g_\beta)_{\beta \in [0,1]}$ be the autonomous reference family from Theorem 3.3. Then we have that g_{β_c} has a unique fixed point $x_0 \in [\gamma^-, \gamma^+]$ and the Lyapunov exponent of x_0 vanishes, that is, $\log \partial_t g_{\beta_c}^t(x_0) = 0$ for all $t > 0$. By continuity, this means that given $k \in \mathbb{R}$ and $\varepsilon > 0$ there exists $\delta > 0$ such that $|x - x_0| < \delta$ and $|\beta - \beta_c| < \delta$ implies $|\log(g_\beta^k(x))|/k < \varepsilon$. Moreover, as $\lim_{t \rightarrow \infty} g_{\beta_c}^t(\gamma^+) = x_0$, we can further require that $g_\beta^t(\gamma^+) < x_0 + \delta/2$ for some $t > 0$ and all $\beta \in [\beta_c - \delta, \beta_c]$. Now, by assumption there exists a set $A_{\delta/2, k, t} \subseteq \Sigma$ of positive measure such that for all $\omega \in \sigma^t(A_{\delta/2, k, t})$ we have

$$\xi_\beta^t(\sigma^{-t}(\omega), \gamma^+) \leq g_\beta^t(\gamma^+) + \frac{\delta}{2},$$

and in addition $|\lambda_k(\omega, \xi_\beta^t(\sigma^{-t}(\omega), \gamma^+)) - \lambda_k(g_\beta^t(\gamma^+))| < \varepsilon$. As $\varphi_\beta^+(\omega)$ is the monotone limit of the sequence $\xi^t(\sigma^{-t}(\omega), \gamma^+)$ (see the proof of Theorem 3.3) and is bounded below by x_0 , this implies that

$$x_0 \leq \varphi_\beta^+(\omega) \leq \xi_\beta^t(\sigma^{-t}(\omega), \gamma^+) \leq g_\beta^t(\gamma^+) + \frac{\delta}{2} \leq x_0 + \delta.$$

Therefore, if δ is chosen small enough, then by continuity $|\lambda_k(\omega, \varphi_\beta^+(\omega)) - \lambda_k(\omega, \xi_\beta^t(\sigma^{-t}(\omega), \gamma^+))| < \varepsilon$ and $|\lambda_k(x_0) - \lambda_k(g_\beta^t(\gamma^+))| < \varepsilon$. Altogether, this implies

$$|\lambda_k(\omega, \varphi_\beta^+(\omega)) - \lambda_k(x_0)| < 3\varepsilon.$$

As $\lambda_k(x_0) = 0$ and $\varepsilon > 0$ was arbitrary, this completes the proof. \square

Remark 5.4. The assumptions in Theorem 5.3 may seem rather strong. However, they are satisfied in our example model system (1.2) whenever the random perturbation is small enough up to time $T + k$.

Numerically we visualize the above result in discrete and continuous time using the examples given in the previous chapters below in Figure 5.1 and 5.2. To compute the FTLE in discrete time, we choose a set of initial conditions, ($N = 10000$ points) and compute the Lyapunov exponent of each point for a fixed time ($k = 5$) for different β values. The maximum and minimum for each β value is then plotted. The magenta curve represents the maximum values and the black curve represents the minimum values. The blue one in the middle represents the asymptotic Lyapunov exponent of the attractor. However, in continuous time, we compute the Lyapunov exponents over a sliding window (*of 200 discretization points*) on a single trajectory of 300000 discretization points for each β value. The maximum and minimum Lyapunov exponent for each β on the trajectory is then taken and plotted. Both methods yield the same result. The choice of the different methods in discrete and continuous time only depends on the computational efficiency. In a smooth fold bifurcation, it is known that all finite time Lyapunov exponents in the basin of attraction of the stable equilibrium x_β^s will be very close to $\lambda(x_\beta^s)$, provided the time T is sufficiently large [SS00]. In contrast to this, the non-smooth case shows a characteristic spreading of these quantities, which can be observed in Figure 5.1(b)–(f) and Figure 5.2(b)–(d).

5.2 FTLE in hybrid forced systems

In the hybrid forced case, we again restrict to the setting of Theorem 3.7 instead of the general Theorem 2.24, similar to the random case. In the interest of the reader, we will maintain the notation for the invariant graph of the reference system, which is the quasiperiodically forced system as φ and the invariant graph of the hybrid forced system as Φ . To that end, let φ^\pm denote the attracting and repelling invariant graphs of the reference system. To adapt the definition, we redefine the maximal finite time Lyapunov exponent on the attractor Φ^+ in the following sense. Let $k > 0$, the Lyapunov exponent at time k of the flow generated by Ψ and starting at an initial condition $(\theta, \omega, x) \in M \times X$ is given by

$$\lambda_k(\Psi, \theta, \omega, x) = \frac{1}{k} \int_M \log \|\partial_x \psi^k(\theta, \omega, x)\| dm(\theta, \omega) \quad (5.4)$$

Thus, we define the maximal Lyapunov exponent on the attractor at time k by

$$\lambda_k^{\max}(\Phi_\beta^+) = \sup \left\{ \lambda \in \mathbb{R} \mid m_{\Phi_\beta^+}(\{(\theta, \omega, x) \mid \lambda_k(\Psi_\beta, \theta, \omega, x) \geq \lambda\}) > 0 \right\}.$$

where

$$m_\Phi(A) = m(\{(\theta, \omega) \in M \mid (\theta, \omega, \Phi(\theta, \omega)) \in A\}), \quad A \subseteq M \times X.$$

Theorem 5.5. *Suppose $(\Psi_\beta)_{\beta \in [0,1]}$ is a parameter family of hybrid-forced monotone flows that satisfies the assumptions of Theorem 3.7. Further assume that for all $\varepsilon, T, k > 0$, there exists a set $A_{\varepsilon, k, T}$ of positive measure such that (h2) is satisfied and*

$$|\lambda_k(\rho^t(\theta), \sigma^t(\omega), \psi_\beta^t(\theta, \omega, x)) - \lambda_k(\rho^t(\theta), \xi_\beta^t(\theta, x))| < \varepsilon \quad (5.5)$$

for all $\omega \in A_{\varepsilon, k, T}$, $k \leq T$ and all $\theta \in \Theta$. Then for all $k \in \mathbb{R}$

$$\underline{\lim}_{\beta \nearrow \beta_c} \lambda_k^{\max}(\Phi_\beta^+) \geq \lambda(\varphi_{\beta_c}^-).$$

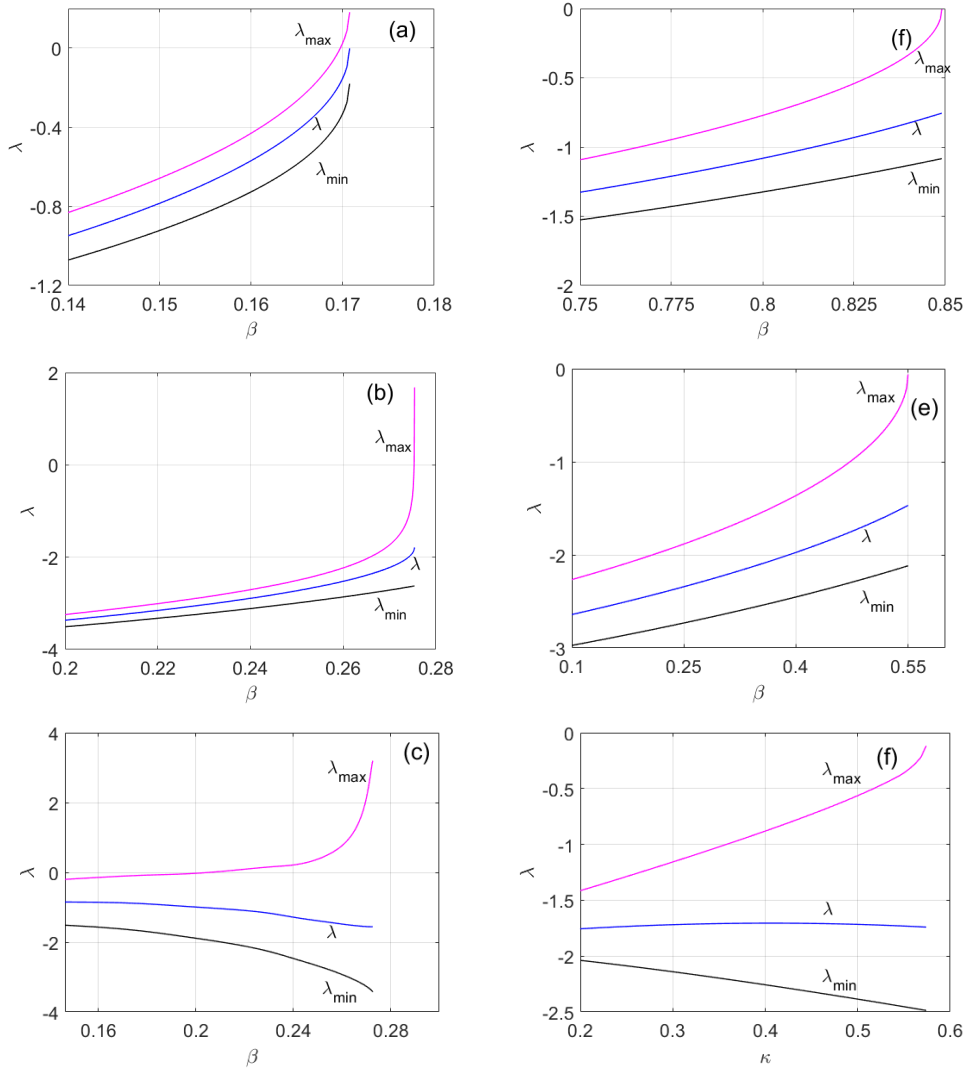


Figure 5.1: Minimal and maximal finite-time Lyapunov exponents in the discrete time case (with the asymptotic one plotted in the middle). The map in the qpf case is of the form $f_{\beta,\omega} := \arctan(\alpha x) - \kappa \cdot \frac{\sin(2\pi\theta)+1}{2} - \beta$ with $\kappa = 1$. In (a) we show the FTLE in the smooth bifurcation scenario for parameters $\alpha = 10$. Whereas in (b) we show the behavior for a non-smooth bifurcation with $\alpha = 100$. In (c), we show the behaviour for the simultaneous variation of α and β . For the random case, the map is of the form $f_{\beta,\omega} := \arctan(\alpha x) - \kappa \cdot \omega - \beta$ with $\alpha = 0$. $\kappa = 0.1$ in (d) and $\kappa = 0.4$ in (e). Likewise in (f), we show the behaviour for the simultaneous variation of κ and β . The time is $k = 5$ in all cases.

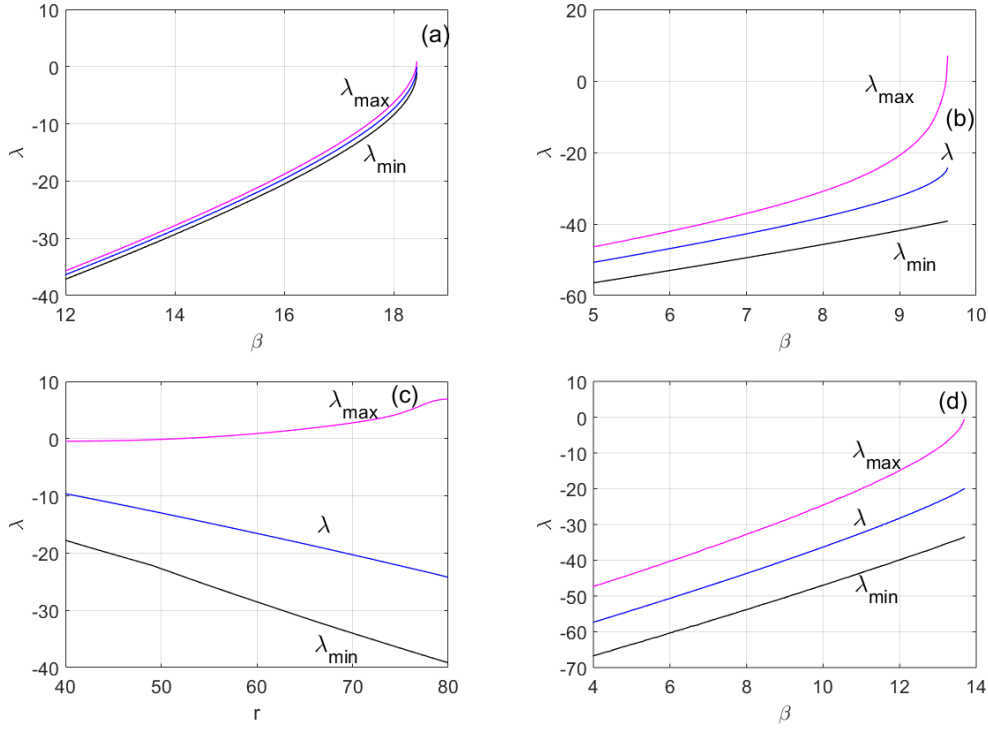


Figure 5.2: The above plots (a)-(d) show the behaviour of the finite-time Lyapunov exponents during fold bifurcations in the forced Allee model. The middle curve is always the time 2000 Lyapunov exponent (as an approximation of the asymptotic Lyapunov exponent), whereas the upper and the lower curves correspond to the maximal and minimal time $4/3$ Lyapunov exponents, respectively. (a) shows the case of a smooth fold bifurcation in the qpf Allee model with parameter values $r = 80$, $K = 10$, $S = 0.1$, $\kappa = 4$ and $q = 3$. (b) shows the case of a non-smooth fold bifurcation in the same model with $r = 80$, $K = 10$, $S = 0.1$, $\kappa = 51.2$ and $q = 5$. (c) shows a quasiperiodic case again, but this time with the simultaneous variation of parameters as in Figure 4.3(b). Finally, (d) shows the case of a non-smooth fold bifurcation in the randomly forced Allee model with parameters $r = 80$, $K = 10$, $S = 0.1$ and $\kappa = 6$.

Proof. Let $(\Xi_\beta)_{\beta \in [0,1]}$ be the non-autonomous reference family from Theorem 3.7. Fix $k \in \mathbb{R}$. By Theorem 5.1, we have

$$\lim_{\beta \nearrow \beta_c} \lambda_k^{\max}(\varphi_\beta^+) \geq \lambda(\varphi_{\beta_c}^-).$$

Hence, for all $\varepsilon > 0$ and $k \in \mathbb{N}$, there exists $\beta_0 = \beta_0(\varepsilon, k) \in (0, \beta_c)$ such that for all $\beta \geq \beta_0$

$$\lambda_k^{\max}(\varphi_\beta^+) \geq \lambda(\varphi_{\beta_c}^-) - \varepsilon.$$

This implies that there exists a set $B_{\varepsilon,\beta} \subseteq \Theta$ of positive measure such that

$$\lambda_k(\theta, \varphi_\beta^+(\theta)) \geq \lambda(\varphi_{\beta_c}^-) - \varepsilon.$$

for all $\theta \in B_{\varepsilon,\beta}$. Now, by assumption (h1)

$$\varphi_\beta^+(\theta) \leq \Phi_\beta^+(\theta, \omega).$$

Moreover, as $\varphi^+(\theta) = \lim_{t \rightarrow \infty} \xi_\beta^t(\rho^+(\theta), \gamma^+)$, for every $\delta > 0$, there exists a set of positive measure Θ_0 and $t \in \mathbb{T}$ such that

$$\xi_\beta^t(\rho^{-t}(\theta), \gamma^+) \leq \varphi_\beta^+(\theta) + \delta$$

for all $\theta \in \Theta_0$. By monotonicity, $\Phi_\beta^+(\theta, \omega) \leq \psi_\beta^t(\rho^{-t}(\theta), \sigma^{-t}(\omega), \gamma^+)$. With assumption (h2), there exists a set $A_{\delta,k,t} \subseteq \Sigma$ of positive measure such that for all $\omega \in \sigma^{-t}(A_{\delta,k,t})$, we have

$$\varphi_\beta^+(\theta) \leq \Phi_\beta^+(\theta, \omega) \leq \psi_\beta^t(\rho^{-t}(\theta), \sigma^{-t}(\omega), \gamma^+) \stackrel{(h2)}{\leq} \xi_\beta^t(\rho^{-t}(\theta), \gamma^+) + \delta \leq \varphi_\beta^+(\theta) + 2\delta$$

and moreover (due to the additional assumption in (5.5))

$$|\lambda_k(\theta, \omega, \psi_\beta^t(\rho^{-t}(\theta), \sigma^{-t}(\omega), \gamma^+)) - \lambda_k(\theta, \xi_\beta^t(\rho^{-t}(\theta), \gamma^+))| < \varepsilon.$$

If δ is small enough, then by continuity we have

$$\left| \lambda_k(\theta, \omega, \Phi_\beta^+(\theta, \omega)) - \lambda_k(\theta, \omega, \psi_\beta^t(\rho^{-t}(\theta), \sigma^{-t}(\omega), \gamma^+)) \right| < \varepsilon$$

and

$$\left| \lambda_k(\theta, \varphi_\beta^+(\theta)) - \lambda_k(\theta, \xi_\beta^t(\rho^{-t}(\theta), \gamma^+)) \right| < \varepsilon.$$

Altogether, this implies

$$\lambda_k(\theta, \omega, \Phi_\beta^+(\theta, \omega)) \geq \lambda_k(\theta, \varphi_\beta^+(\theta)) - 3\varepsilon \geq \lambda(\varphi_{\beta_c}^-) - 4\varepsilon.$$

As $\varepsilon > 0$ was arbitrary, this completes the proof. \square

We present the numerical results in this case in Figure 5.1. As mentioned earlier, we present results from the discrete time case. We show this for different parameter values used in Figure 4.4. The behaviour in 5.1(a) and (b) is similar to the behaviour in the quasiperiodic setting irrespective of the size of the noise. With the above observations it is clear that FTLEs can serve as a tool to anticipate a non-smooth saddle-node bifurcation by detecting positive Lyapunov exponents that appear close to the bifurcation point. This, alongside with recovery rates, can be considered as early warning signals for fold bifurcations in the class of forced systems we consider in this thesis, the latter used for anticipating only a smooth saddle-node bifurcation.

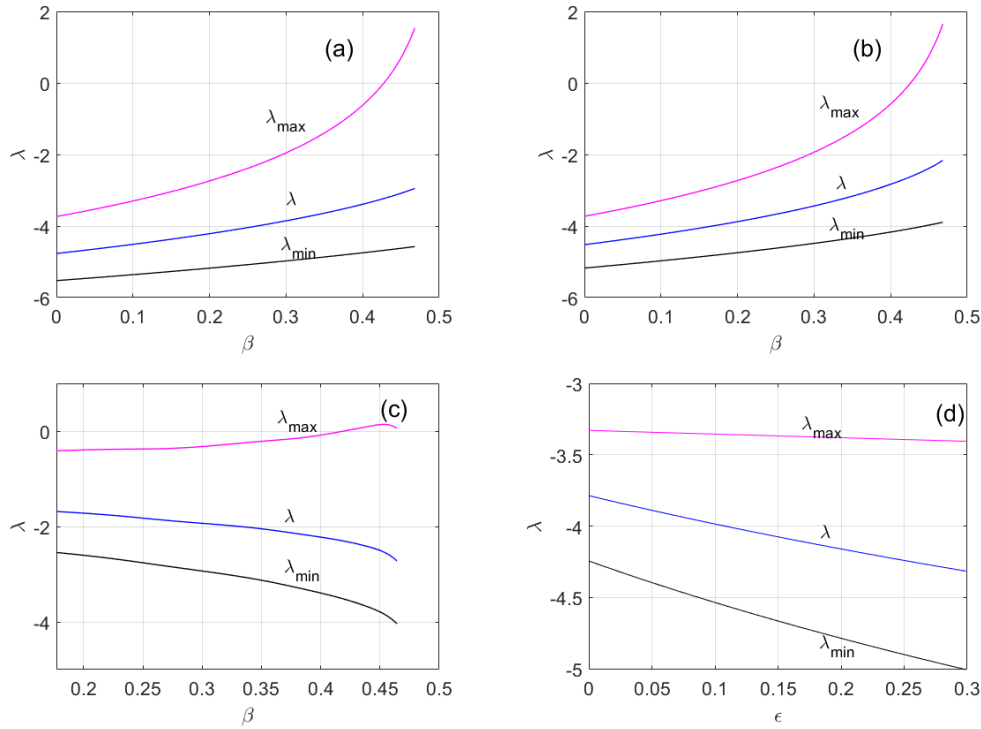


Figure 5.3: Minimal and maximal finite-time Lyapunov exponents (with the asymptotic one plotted in the middle) for the discrete time hybrid forced model. The time is $n = 20$, $\kappa = 0.5$, $\rho = (\sqrt{5} - 1)/2$ in all cases. In (a) and (b) $\alpha = 100$ and $\beta = 0.4729$, while $\epsilon = 0.3$ in (a) and 0.1 in (b). In (c), we show the finite time Lyapunov exponents for the simultaneous variation of α and β and finally in (d) we show the behavior for fixed β , i.e., $\beta = 0.173$ while varying ϵ .

5.3 Distribution of finite time Lyapunov exponents

We close this chapter with an important aspect that was observed numerically as regards to the FTLEs. Namely, this is the frequency at which positive Lyapunov exponents on the attractor close to the bifurcation were observed as the time increased. Beginning with the quasiperiodic case, we observe that the probability of observing positive Lyapunov exponents on the attractor decays to zero with time. This can be visualized via the distribution plots with the histograms in Figure 1.8 for the continuous time case with the Allee model and Figure 5.4 for the discrete time case. According to our findings, the rate of decay of these positive Lyapunov exponents is very fast, and decays exponentially (See Figure 1.8(c) and Figure 5.8(c)).

Due to some numerical technicalities, the behaviour in 5.8(c)) gravitates towards a polynomial decay. For a simplified model system, we will rigorously show that the probability indeed decays exponentially to zero in the next chapter. To picture what we explain here, we present the graphs of the relative frequency on different times scales in Figure 1.8 and Figure 5.8 for the continuous and discrete time case respectively. Moving on to the random case, recall that we do not observe positive Lyapunov exponents here, due to the boundedness of derivatives (*see Theorem 4.4*). Instead, we consider Lyapunov exponents that are close to zero. In so doing, we choose a threshold (*i.e* $\lambda = -0.5$ for the discrete time case and $\lambda = -3$ for the continuous time case) and consider Lyapunov exponents above this value. We present the findings in Figure 5.5 for the randomly forced discrete time model and in Figure 5.7 for the randomly forced Allee model. As we can see, when the time is increased, the distribution is concentrated at the actual Lyapunov exponent of the attractor. Likewise, we present the relative frequency plots in Figure 5.9 and Figure 5.11. Similarly, we observe that the probability of observing Lyapunov exponents above the given thresholds also decays to zero very fast. Again, the rate of decay is exponential. Finally, we present the plots for the hybrid forced system, which seem to mimic the behaviour observed in the quasiperiodic case, since we observe positive Lyapunov exponents in this scenario as well. The distribution plot is presented in Figure 5.10, whereas the relative frequencies are presented in Figure 5.6.

In conclusion, even though in our numerical findings positive or zero FTLEs exist, the probability of finding this is very small and large amounts of data maybe needed to that end. This may not be feasible in some situations and hence, may limit the applicability of the approach in real world problems.

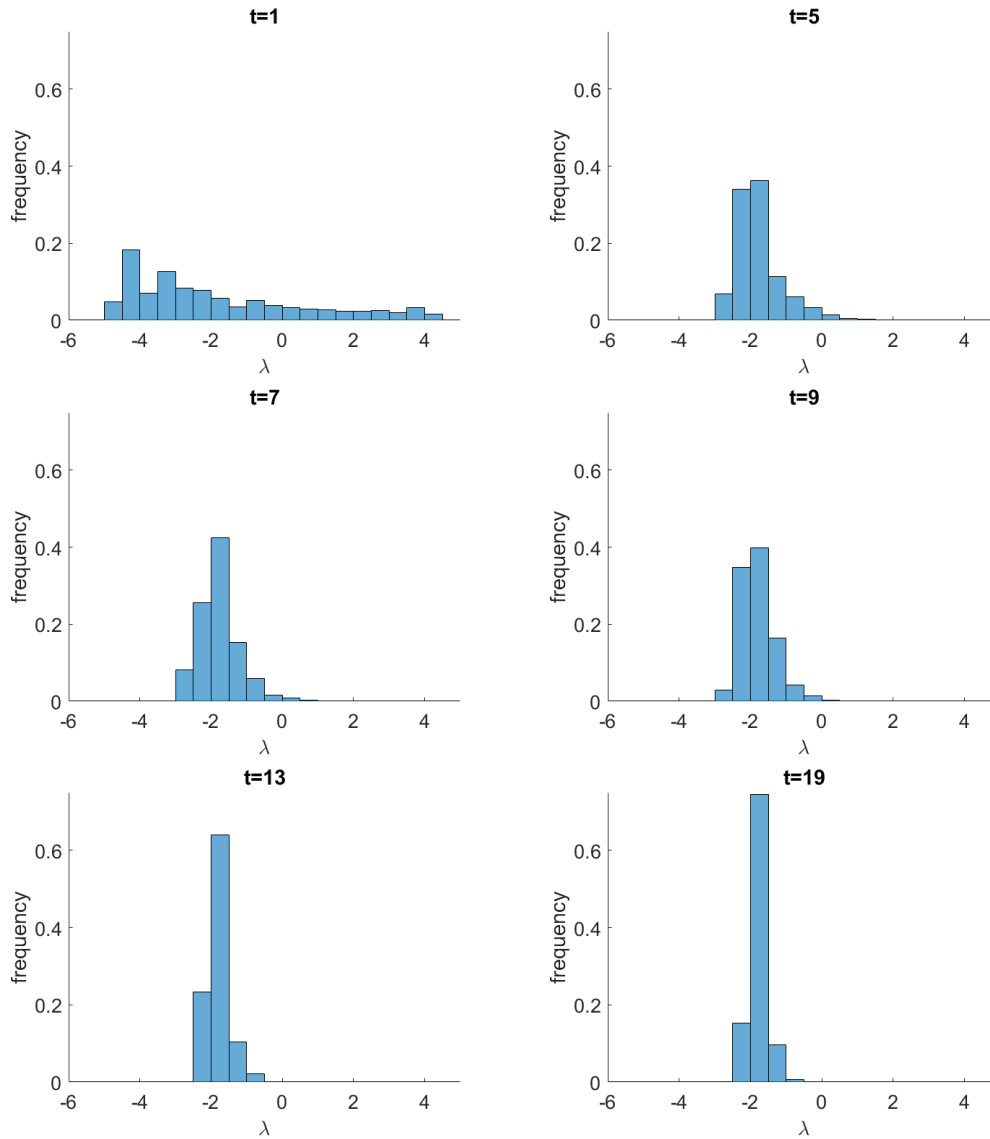


Figure 5.4: Distributions of the finite-time Lyapunov exponents in the qpf discrete time model (2.16) with parameter values $\alpha = 100$, $\kappa = 1$, $\rho = \omega$ and $\beta = 0.5507$. Here, we consider a set of initial conditions (i.e $N = 40000$ points) and compute the Lyapunov exponents for different times t .

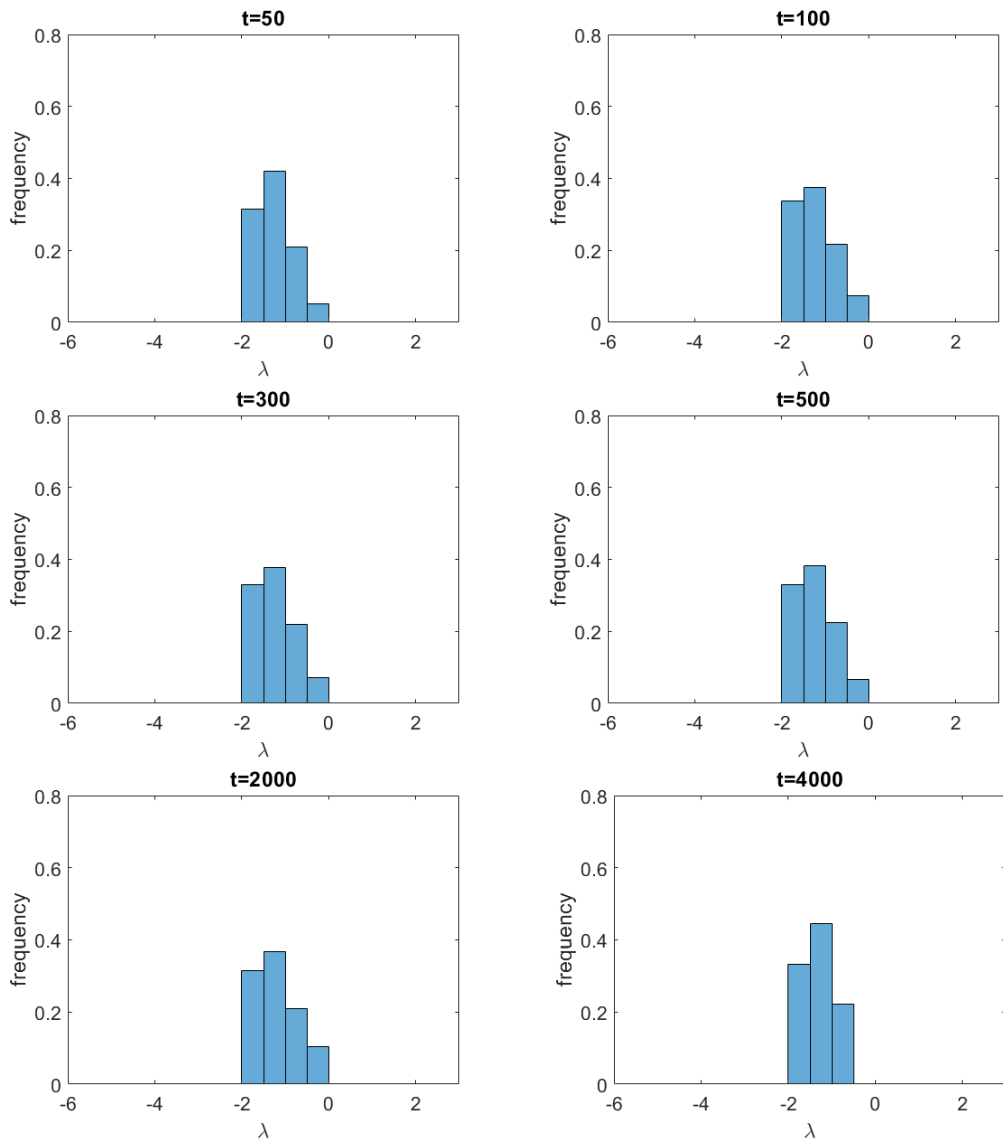


Figure 5.5: Distributions of the finite-time Lyapunov exponents in the randomly forced discrete time model (2.16) with parameter values $\alpha = 10$, $\kappa = 0.3$ and $\beta = 0.6660$. Here, we consider a trajectory of length $t = 40000$ and compute the Lyapunov exponents with varying sliding windows over the whole trajectory.

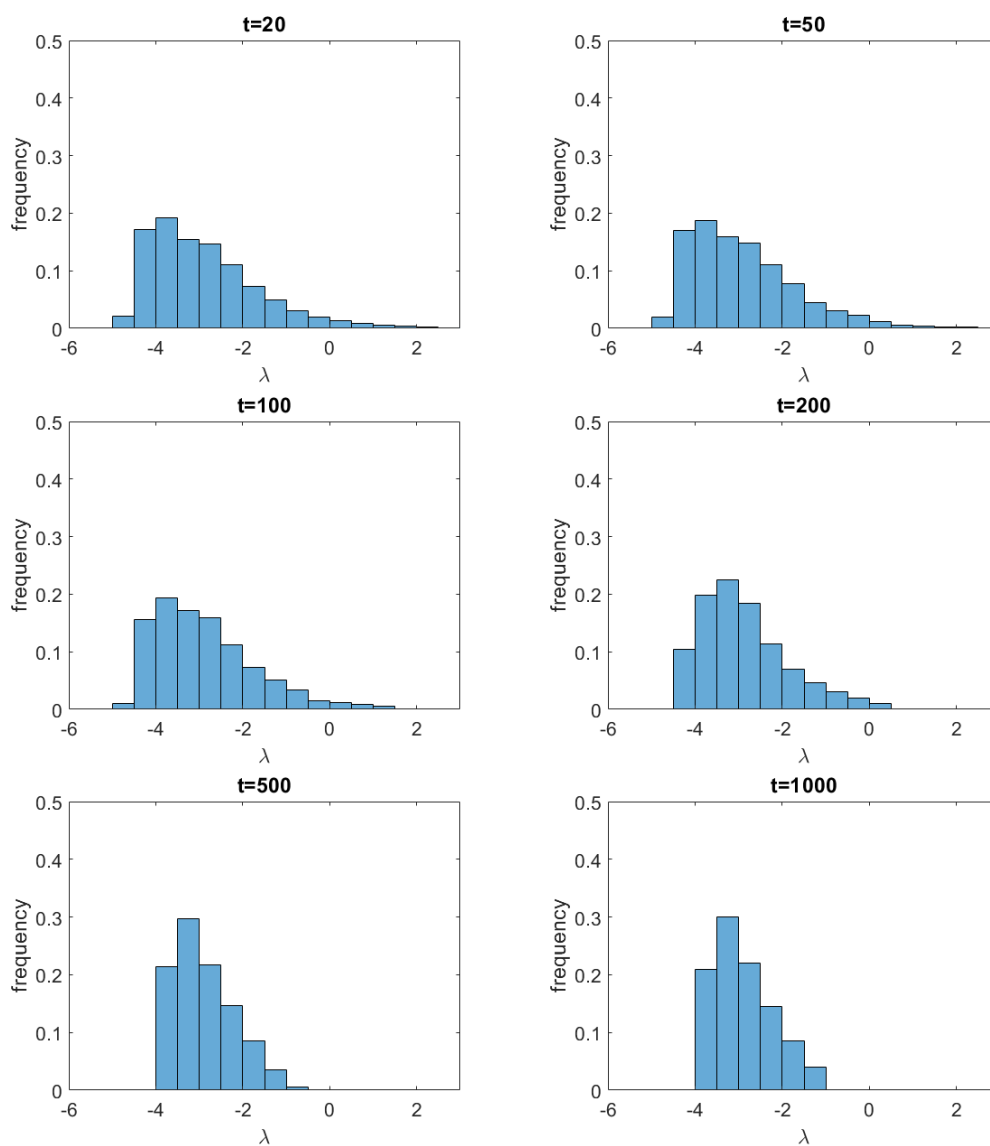


Figure 5.6: Distributions of the finite-time Lyapunov exponents in the hybrid-forced discrete time model (3.15) with parameters $\alpha = 100$, $\rho = \omega$, $\kappa = 1$, $\epsilon = 0.3$ and $\beta = 0.4729$ on different timescales, computed with sliding windows over a trajectory of length $t = 40000$.

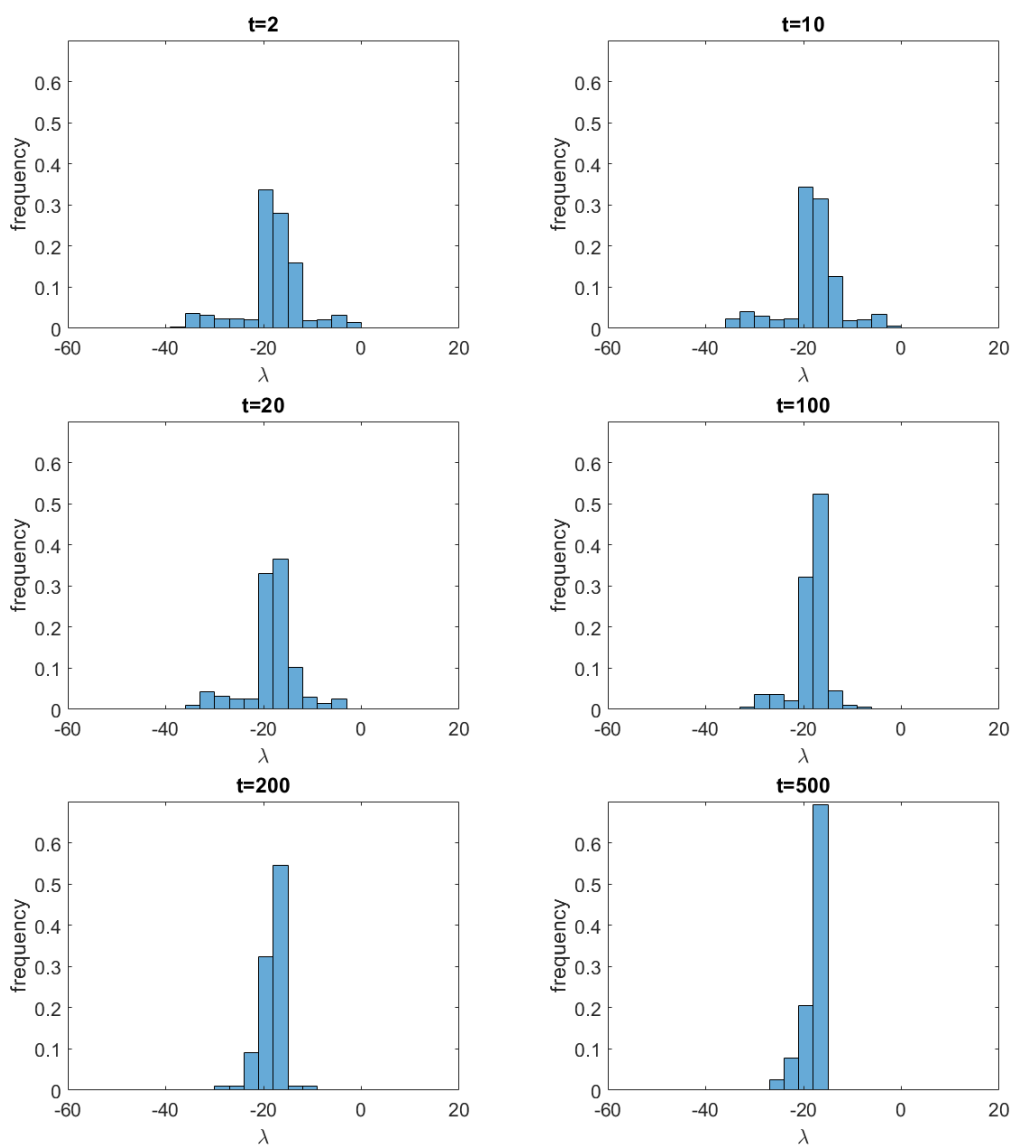


Figure 5.7: Distributions of the finite-time Lyapunov exponents in the randomly forced Allee model (1.2) with parameters $r = 80$, $K = 10$, $S = 0.1$, $\kappa = 6$ and $\beta = 13.6123$ on different timescales, computed with sliding windows over a trajectory of length $t = 20000$.

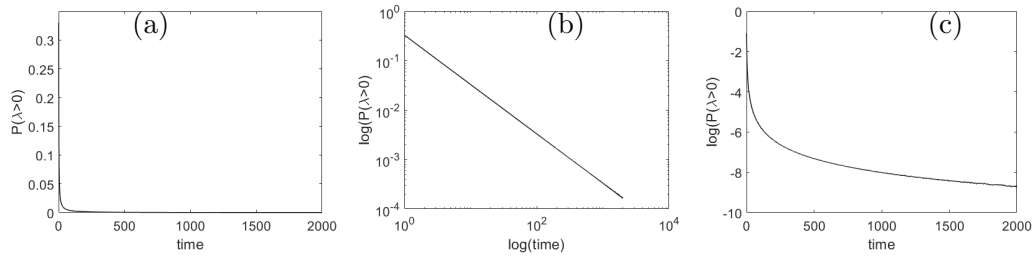


Figure 5.8: A plot of the relative frequency of positive Lyapunov exponents in the qpf discrete time model on a (a) standard, (b) log-log and (c) logarithmic scale..

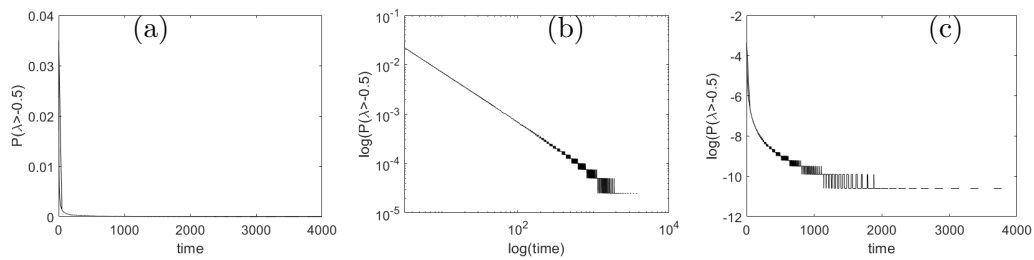


Figure 5.9: A plot of the relative frequency of Lyapunov exponents above a threshold of $\lambda = -0.5$ in the randomly forced discrete time model on a (a) standard, (b) log-log and (c) logarithmic scale.

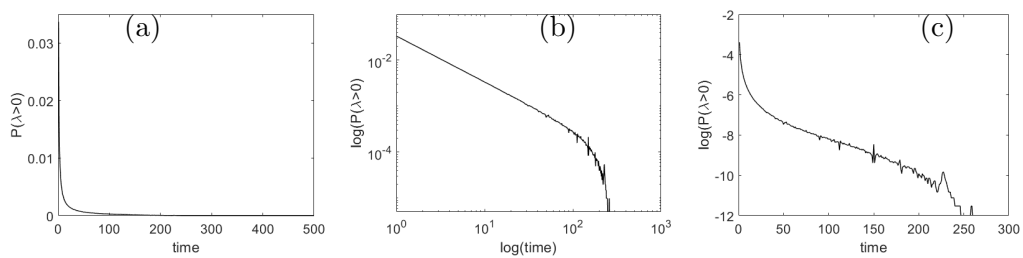


Figure 5.10: A plot of the relative frequency of positive Lyapunov exponents in the hybrid forced discrete time model on a (a) standard, (b) log-log and (c) logarithmic-scale.

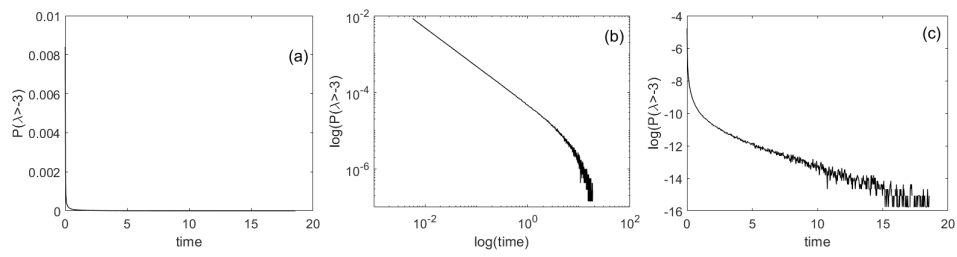


Figure 5.11: A plot of the relative frequency of Lyapunov exponents above a threshold $\lambda = -3$ in the randomly forced Allee model on a (a) standard, (b) log-log and (c) logarithmic scale.

Chapter 6

Finite Time Lyapunov exponents in Pinched skew product systems

In this chapter, we study the probability of observing positive Lyapunov exponents on the attractor in finite time as seen in the numerical results in Chapter 5. Now looking back into the numerical results in Chapter 5, recall that we observed points on the attractor whose finite time Lyapunov exponent (FTLE) is positive. However, as the iteration number increases, the probability of observing points with a positive Lyapunov exponent decreased to zero. This is illustrated in Figure 1.8 for a continuous time system and in Figure 5.8 for the discrete time case. The aim of this chapter is to establish analytically that this probability decays to zero exponentially fast (as time goes to $+\infty$) in the particular case of pinched skew products, which serve as a simplified model system.

To this end, we focus on the quasiperiodic case, where positive Lyapunov exponents were observed during the formation of the strange non-chaotic attractor (SNA). However, to not obstruct the view by technicalities, we study this phenomenon in a class of systems known as *pinched* skew product systems. One of the reasons for considering pinched skew product systems is that they present a mechanism of formation of SNAs which is similar to that in the class of qpf monotone interval maps we considered in the previous chapters. On the other hand, they are also easier to study analytically. We begin by providing a brief introduction and some basic information on

SNAs formed in pinched skew product systems.

Pinched skew product systems. Pinched skew product systems were first introduced by Grebogi and co-authors [GOPY84], and were later on analytically studied by Keller [Kel96] and Glendinning [Gle02]. They belong to the class of quasiperiodically forced skew product systems. Precisely, a pinched skew product system is a *quasiperiodically forced interval map* (see also (2.10))

$$F : \mathbb{T}^D \times I \rightarrow \mathbb{T}^D \times I, \quad (\theta, x) \mapsto (\rho(\theta), F_\theta(x)), \quad (6.1)$$

such that there exists some $\theta_* \in \mathbb{T}^D = \mathbb{R}^D / \mathbb{Z}^D$, $D \geq 1$ with $\#F_{\theta_*}(I) = 1$, where $I = [0, 1] \subseteq \mathbb{R}$. For concreteness, we will take a closer look at a slightly modified version of the example from [GOPY84] by studying the family of qpf interval maps

$$F_\kappa : \mathbb{T}^1 \times [0, 1] \rightarrow \mathbb{T}^1 \times [0, 1], \quad F_\kappa(\theta, x) = (\theta + \rho \pmod{1}, \tanh(\kappa x) \cdot \sin(\pi\theta)) \quad (6.2)$$

where $\rho \in \mathbb{R}/\mathbb{Q}$ and $\kappa > 0$ is a real parameter.

In this particular example, if $\kappa > 2$, the map F_κ has two invariant graphs. The 0-line which is invariant and has a positive Lyapunov exponent $\lambda(0) = \log \kappa - \log 2 > 0$ for [GJ13]. Concurrently, there exists another invariant graph φ^+ above the zero line which is $Leb_{\mathbb{T}^1}$ -almost surely strictly positive and has a Lyapunov exponent

$$\lambda(\varphi^+) = \int_{\mathbb{T}^1} \log F'_{\kappa, \theta}(\varphi^+(\theta)) d\theta, \quad (6.3)$$

which is strictly negative [GJ13, Kel96]. This invariant graph φ^+ attracts $Leb_{\mathbb{T}^1 \times I}$ -a.e initial conditions $(\theta, x) \in \mathbb{T}^1 \times I$, [Kel96], [Jäg03, Lemma 3.5]. $Leb_{\mathbb{T}^1 \times I}$ here denotes the Lebesgue measure on $\mathbb{T}^1 \times I$. Notice that we suppress the index κ and write φ^+ instead of φ_κ^+ to denote the invariant graph which is above the zero line. Likewise, we write F instead of F_κ for the map. We denote by \mathcal{A} , the *global attractor* of F given by

$$\mathcal{A} = \bigcap_{n \in \mathbb{N}} F^n(\mathbb{T}^D \times I). \quad (6.4)$$

The bounding graphs of \mathcal{A} are called the upper and lower bounding graphs of the system F denoted by φ^+ and φ^- respectively. The strange non-chaotic attractor (SNA) in F is then formed via the upper bounding graph φ^+ given by

$$\varphi^+(\theta) = \sup\{x \in I \mid (\theta, x) \in \mathcal{A}\}. \quad (6.5)$$

Equivalently, it should be noted that the sets

$$\mathcal{A}^n = \bigcap_{i=1}^n F^i(\mathbb{T}^D \times I), \quad (6.6)$$

are bounded above by the iterates of the upper boundary line $\mathbb{T}^D \times \{1\}$. The iterated bounding lines φ_n define a monotonically decreasing sequence of continuous graphs. That is,

$$\varphi_n(\theta) = F_{\rho^{-n}(\theta)}^n(1), \quad (6.7)$$

where $F^n = F_{\rho^{-n}(\theta)} \circ \dots \circ F_\theta$, $\rho^{-n}(\theta) = \theta - n\rho$ and $\mathcal{A}_n = [0, \varphi_n]$. Accordingly, the sequence φ_n converges pointwise to the invariant graph φ^+ , $\varphi^+(\theta) = \lim_{n \rightarrow \infty} \varphi_n(\theta)$. It is important to also note that the graph φ^+ is discontinuous: due to the pinching property of F and the invariance of φ^+ , we obtain $\varphi^+(\theta) = 0$ for a dense set of $\theta \in \mathbb{T}^D$ while φ^+ is positive on a set of positive Lebesgue measure due to (6.3). The SNA in (6.2) is shown in Figure 6.1.

We denote by \mathcal{F} the class of quasiperiodically forced monotone interval

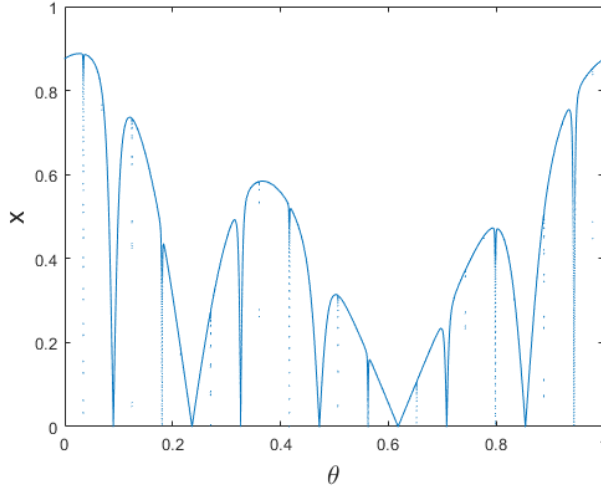


Figure 6.1: Strange non-chaotic attractor in (6.2) with $\kappa = 3$ and $\rho = \frac{\sqrt{5}-1}{2}$

maps of the form (6.1) which satisfy

- (\mathcal{F}_1) the fibre maps F_θ are monotonically increasing;
- (\mathcal{F}_2) the fibre maps F_θ are differentiable and $(\theta, x) \mapsto F'_\theta(x)$ is continuous on $\mathbb{T}^D \times I$;
- (\mathcal{F}_3) F is pinched;

(\mathcal{F}_4) $F_\theta(0) = 0$ for all $\theta \in \mathbb{T}^D$. That is, the 0-line is invariant.

Consequently, example (6.2) belongs to the set \mathcal{F} for $D = 1$. Likewise, we may consider examples with a higher dimensional rotation in the base such as

$$F_\kappa : \mathbb{T}^D \times I \rightarrow \mathbb{T}^D \times I, \quad F_\kappa(\theta, x) = (\theta + \rho \pmod{1}, \tanh(\kappa x) \cdot \frac{1}{D} \cdot \sum_{i=1}^D \sin(\pi \theta_i)), \quad (6.8)$$

where $\theta \in (\theta_1 \cdots \theta_D)$, $D > 1$. This particular example is taken from [GJ13] and will be used in the formulation of the desired results in this chapter.

The SNA and finite time Lyapunov exponents. Let $F \in \mathcal{F}$ and suppose φ^+ is an invariant graph of F with $\lambda(\varphi^+) < 0$. Then φ^+ is an SNA of F . Recall that by Birkhoff's Ergodic Theorem

$$\lambda(\theta, \varphi^+(\theta)) = \lim_{n \rightarrow \infty} \frac{1}{n} \sum_{l=0}^{n-1} \log |F'_{\rho^l(\theta)}(\varphi^+(\rho^l(\theta)))| < 0 \quad (6.9)$$

for almost every $\theta \in \mathbb{T}^D$. This implies that the Lyapunov exponent up to time N is given by

$$\lambda_N(\theta, \varphi^+(\theta)) = \frac{1}{N} \sum_{l=0}^{N-1} \log |F'_{\rho^l(\theta)}(\varphi^+(\rho^l(\theta)))|, \quad (6.10)$$

where $\lambda_N(\theta, \varphi^+(\theta))$ denotes the finite time Lyapunov exponent of the point $(\theta, \varphi^+(\theta))$. Now due to pinching, the graph φ^+ contains points on the attractor with $\lambda_N(\theta, \varphi^+(\theta)) > 0$. Note that such behaviour occurs at the pinched point θ_* , that is $\lambda_N(\theta_*, \varphi^+(\theta_*)) > 0$. If we consider a small neighbourhood around θ_* , then points in this neighbourhood also have a positive Lyapunov exponent on the attractor in finite time due to Lemma 5.2. Suppose $(\theta, x) \in \mathbb{T}^D \times I$ is a point on the attractor with $\lambda_N(\theta, x) > 0$. The implication is that up to time N , the point (θ, x) spends a substantial amount of time near the repeller, that is the 0-line, which explains why points in the neighbourhood of a pinched point have a positive Lyapunov exponent in finite time. Below, we argue that as N goes to infinity, the measure of the set of points whose Lyapunov exponent is positive decreases exponentially, and this translates to the probability of observing points on the attractor with a positive Lyapunov exponent decaying to zero. To see this, we discuss briefly the geometry and the mechanism involved in the formation of the SNA in pinched skew product systems.

Mechanism of formation of the SNA. As mentioned earlier, the SNA φ^+ is approximated by the iterated upper bounding lines φ_n given by (6.7), which is then formed via a process known as pinching (here pinching really refers to how the image of the horizontal lines get pinched through the application of the map F , see definition 2.11 and [Sta03, Definition 9]). The geometry of these lines is well controlled which helps us in understanding the behaviour and shape of φ_n . We illustrate this phenomenon in Figure 6.2 which shows the first few iterates of the line $\mathbb{T}^1 \times \{1\}$ under the map (6.2) up to time $n = 10$. In the process, we observe a sequence of peaks which appear in an ordered way such that the next peak is an image of the previous one. That is to say, for each iterate τ_n , where $\tau_n = \theta_* + n\rho$, $n \in \mathbb{N}$ of the pinched point, a new peak is formed. Notice that the only significant change between the $(n - 1)^{th}$ and n^{th} iterate is the appearance of a new peak. This means that the difference between φ_{n-1} and φ_n is a new peak in a small ball $B_{r_n}(\tau_n)$ centered around τ_n , where $r_n \in \mathbb{R}$. Outside of these balls the graphs remain essentially unchanged. The peaks grow faster and thinner with the order of the peak as they become steeper and sharper in the next iteration [Jäg06]. This is due to the expansion around the 0-line. As a result, the radius of the balls around the peaks decreases exponentially with the order of the peak which implies that the ‘width’ of the peak decreases exponentially at the same time. Substantially, the mechanism observed in Figure 6.2 involves an interplay between a contracting region C and an expanding region E . Since φ^+ is attracting, we consider a small region around φ^+ which is contracted and define $C := [L_0, 1] \times \mathbb{T}^D$, $L_0 \in (0, 1)$, whereas E is the region below L_0 (See, Figure 6.3) which contains the repeller, i.e, the 0-line. As φ^+ attracts almost every initial condition, the fibre maps F are contracting in C . At the same time, they are expanding in E due to the expansion around the 0-line. When the first peak enters E at θ_* in the first iteration, its image will be formed at τ_1 in the second iteration and the corresponding images will follow accordingly as images of the previous peak. The image of the new peak will be steeper and smaller than the preceding one.

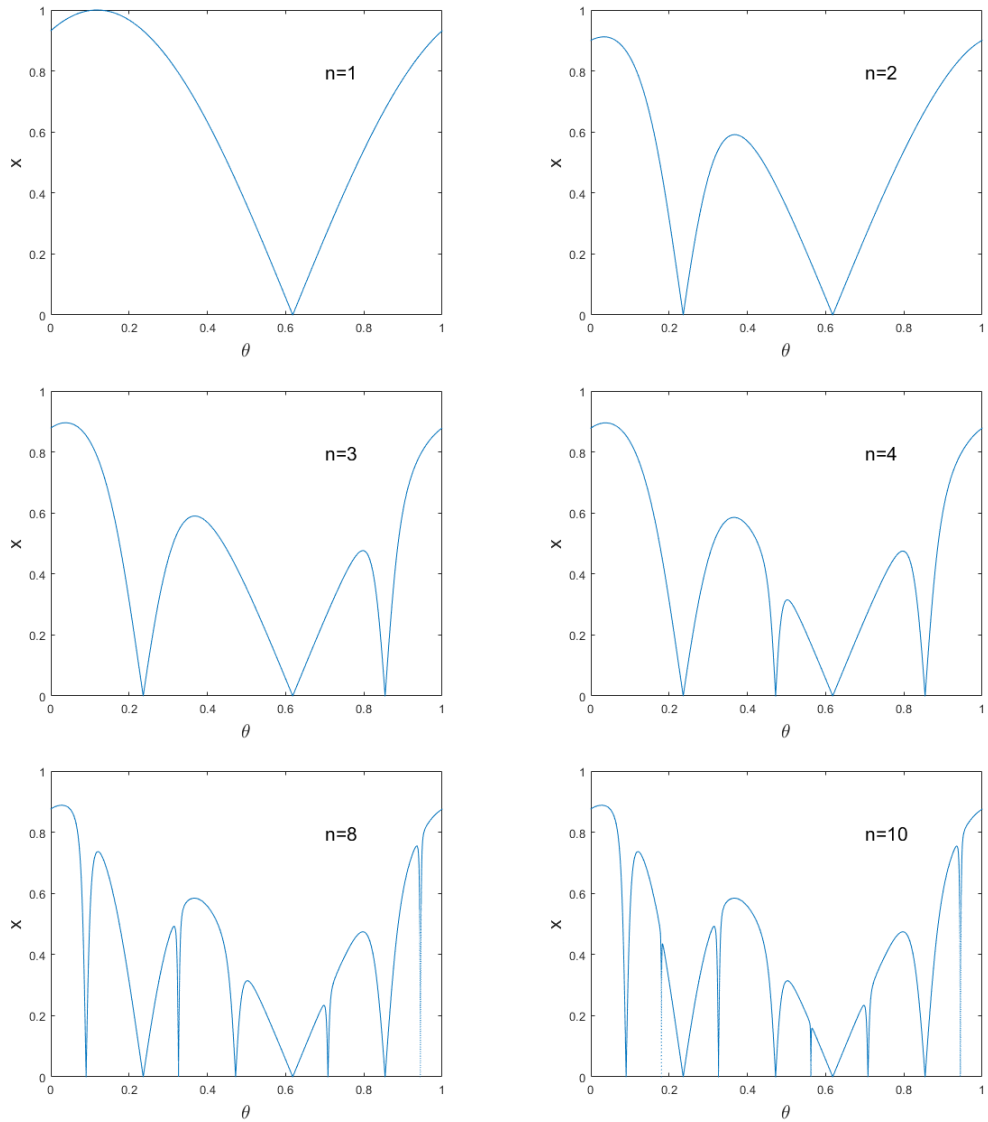


Figure 6.2: The graphs of the iterates of the upper boundary lines of equation (6.2) with $\kappa = 3$ and $\rho = \frac{\sqrt{5}-1}{2}$

In Figure 6.3, we only show the peak formed at the pinched point θ_* and its first iterate. We then define the width of a peak in this case as the diameter of the ball $B_{r_n}(\tau_n)$ which contains the peak below the line L_0 . If a point on the graph φ^+ does not lie in this ball, then the graph at this point is above L_0 and lies in C . Notice that the width of the peak at τ_1 is smaller than the width of the peak at θ_* . This is because the peaks become steeper and smaller, thus, the width of these intervals around the peaks also decays with

the order of the peak. The width of the peaks correspond to the θ -values whose Lyapunov exponent on φ^+ is positive.

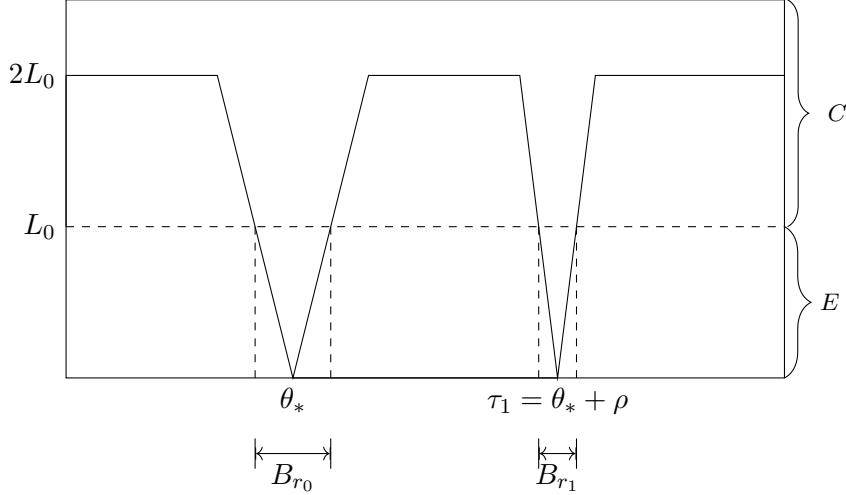


Figure 6.3: The above diagram shows the peak formed at the pinched point θ_* and its first iterate τ_1 . For convenience we present the successive iterates on the circle in a straight order. Notice that the succeeding peak at τ_1 is smaller than the original peak and thus its width determined by the ball B_{r_1} centered around θ_* , where r_1 is the radius of the ball at time $t=1$, is smaller than the width of the peak determined by B_{r_0} below it at τ_0 .

Thus, we show that these heuristics can be converted into a rigorous proof by showing that as the width of the peaks decrease exponentially with the order of the peak, then the probability of observing points on the attractor with positive Lyapunov exponent also decays exponentially to zero. We formalize the statement in Theorem 6.3

Estimates on the iterated upper boundary lines. Now, in order to have a good control on the behaviour and shape of the iterated upper boundary lines, we will need to impose a number of assumptions on the geometry of the system, so as to derive the required estimates. First, we assume that the fibre maps are \mathcal{C}^1 which is obviously the case for the example in (6.8). Let $F \in \mathcal{F}$ and assume that there exist parameters $\alpha > 2$, $\gamma > 0$ and $L_0 \in (0, 1)$ such that for all $\theta \in \mathbb{T}^D$, the following additional assumptions hold.

$$|F_\theta(x) - F_\theta(y)| \leq \alpha |x - y|, \quad (\text{F1})$$

for all $x, y \in I$ and

$$|F_\theta(x) - F_\theta(y)| \leq \alpha^{-\gamma} |x - y|, \quad (\text{F2})$$

for all $x, y \in [L_0, 1]$. Condition (F2) implies that the map F is contracting in the region $[L_0, 1]$. We further assume that there exists a constant $\beta > 0$ such that for all $x \in [0, 1]$,

$$|F_\theta(x) - F_{\theta'}(x)| \leq \beta d(\theta, \theta'). \quad (\text{F3})$$

If we assume continuous differentiability in θ , then a suitable choice for β would be $\beta = \sup_{(\theta, x)} \|\partial_\theta F_\theta(x)\|$. Recall that $\tau_n := \rho^n(\theta_*) = \theta_* + n\rho$, which is the n^{th} -iterate of the pinched point θ_* . Now, assume that the rotation vector $\rho \in \mathbb{R}^D$ is Diophantine (*Definition 2.20 in Chapter 2*). The implication is that there exists constants $c > 0$ and $d > 1$ such that for all $n \in \mathbb{N}$,

$$d(\tau_n, \theta_*) \geq c \cdot n^{-d}. \quad (\text{F4})$$

Furthermore, we assume that there are constants $m \in \mathbb{N}$, $a > 1$ and $0 < b < 1$ with

$$m > 22 \left(1 + \frac{1}{\gamma}\right), \quad (\text{F5})$$

$$a \geq (m+1)^d, \quad (\text{F6})$$

$$b \leq c, \quad (\text{F7})$$

$$d(\tau_n, \theta_*) > b, \quad \forall n \in \{1, \dots, m-1\} \quad (\text{F8})$$

such that for all $(\theta, x) \in \mathbb{T}^D \times I$

$$F_\theta(x) \geq \min\{2L_0, ax\} \cdot \min\left\{1, \frac{2}{b}d(\theta, \theta_*)\right\}. \quad (\text{F9})$$

It can be shown that the example (6.8) satisfies all the above conditions (F1)–(F9) for large enough κ . This has already been checked in [GJ13], see Lemma 4.2. However, for convenience of the reader, we still provide a proof here.

Lemma 6.1 ([GJ13, Lemma 4.2]). *Consider F_κ as in (6.8) and let ρ satisfy the Diophantine condition (F4) for some $c > 0$ and $d > 1$. There exists a constant $\kappa_0 = \kappa_0(c, d, D)$ such that for all $\kappa \geq \kappa_0$, F_κ satisfies (F1)–(F9).*

Proof. Let $\alpha = \kappa$, $\gamma = \frac{1}{2}$, $L_0 = \frac{\log \kappa}{\kappa}$, $\beta = \pi$, $m = 67$, $b = \frac{1}{2} \min_{n=1}^{m-1} cn^{-d}$ and $a = \frac{2b\kappa}{D(e+1/e)^2}$. We choose $\kappa_0 = \kappa_0(c, d, D)$ such that for all $\kappa \geq \kappa_0$,

$$\kappa \geq 16, \quad (6.11)$$

$$\frac{2b\kappa}{D(e+1/e)^2} \geq (m+1)^d, \quad (6.12)$$

$$\frac{2 \log \kappa}{\kappa} \leq \frac{b \tanh(1)}{2D}, \quad (6.13)$$

and

$$[\tanh(\kappa x)]' = \frac{4\kappa}{(e^{\kappa x} + e^{-\kappa x})^2} \leq \kappa \quad (6.14)$$

for all $x \geq 0$. Clearly

$$0 \leq \frac{1}{D} \sum_{i=1}^D \sin(\pi\theta_i) \leq 1, \quad (6.15)$$

for all $\theta \in \mathbb{T}^D$. Hence (F1) holds and since

$$F'_{\kappa,\theta}(x) \leq F'_{\kappa,\theta}(2L_0) \leq \frac{4\kappa}{(\kappa + \kappa^{-1})^2} \leq \frac{4}{\kappa} \leq \kappa^{-1/2} \quad (6.16)$$

for all $x \geq 2L_0$, we also have (F2). Conditions (F3) and (F5) can be easily checked, while condition (F4) holds by assumption. From equation (6.12), it can be clearly seen that (F6) is satisfied whereas (F7) and (F8) follow directly from the choice of b and the Diophantine assumption in (F4). Finally, to verify assumption (F9), we use the monotonicity and concavity to obtain

$$\tanh(\kappa x) \geq \begin{cases} \frac{4\kappa}{(e+1/e)^2} \cdot x & \text{if } x \leq 1/\kappa \\ \tanh(1) & \text{if } x > 1/\kappa \end{cases} \quad (6.17)$$

Applying equation (6.13) with the fact that $\sum_{i=1}^D \sin(\pi\theta_i) \geq d(\theta, \theta_*)$ where $\theta_* = 0$, we have

$$\begin{aligned} F_\kappa(\theta, x) &\geq \min \left\{ \tanh(\kappa x), \frac{4\kappa}{(e+1/e)^2} \cdot x \right\} \cdot \frac{1}{D} d(\theta, \theta_*) \\ &\geq \min \left\{ \frac{\tanh(1)}{2D}, \frac{2b\kappa}{D(e+1/e)^2} \cdot x \right\} \cdot \frac{2}{b} d(\theta, \theta_*) \\ &\geq \min \{2L_0, ax\} \cdot \min \left\{ 1, \frac{2}{b} d(\theta, \theta_*) \right\}. \end{aligned}$$

as required. \square

Again, we will delve a bit back into the geometry of the upper bounding line φ^+ above the 0-line whose finite time Lyapunov exponents we are interested in. First, we denote by \mathcal{F}^* , the class of quasiperiodically forced interval maps

$$\mathcal{F}^* = \{F \in \mathcal{F} \mid F \text{ satisfies (F1) - (F9)}\}. \quad (6.18)$$

Notice that given $F \in \mathcal{F}^*$, equation (F9) implies that $\lambda(0) \geq \log \frac{2a}{b} - \log 2 - 1 > 0$ and $\varphi^+(\theta) > 0$ for $\text{Leb}_{\mathbb{T}^D}$ almost every θ [GJ13, Remark 4.3]. To formulate the desired results, we let $j \in \mathbb{N}$ such that

$$r_j = \frac{b}{2} a^{-\frac{(j-1)}{m}}. \quad (6.19)$$

Proposition 6.1.1 ([GJ13, Proposition 4.4]). *Let $F \in \mathcal{F}^*$ and $q \in \mathbb{N}$. Then there exists $\eta > 0$ such that if $n \geq mq + 1$ and $\theta \notin \bigcup_{j=q}^n B_{r_j}(\tau_j)$, then $|\varphi_n(\theta) - \varphi_{n-1}(\theta)| \leq \alpha^{-\eta(n-1)}$.*

Remark 6.2. Observe that if $k, n \in \mathbb{N}$ satisfy $mq \leq k < n$ and if $\theta \notin \bigcup_{j=q}^n B_{r_j}(\tau_j)$ then Proposition 6.1.1 gives

$$\begin{aligned} |\varphi_n(\theta) - \varphi_k(\theta)| &\leq \sum_{i=k+1}^n |\varphi_i(\theta) - \varphi_{i-1}(\theta)|, \\ &\leq \sum_{i=k+1}^n \alpha^{-\eta(i-1)} = \alpha^{-\eta k} \sum_{j=0}^{n-(k+1)} \alpha^{-\eta j} \leq \frac{\alpha^{-\eta k}}{1 - \alpha^{-\eta}}. \end{aligned} \quad (6.20)$$

This indicates that the boundary lines will always stay close to each other. Further, if $q \in \mathbb{N}$ and $n > mq + 1$, then

$$\begin{aligned} \text{Leb}_{\mathbb{T}^D} \left(\bigcup_{j=q}^n B_{r_j}(\tau_j) \right) &\leq \zeta_D \cdot \frac{b}{2} \sum_{j=q}^n a^{-\frac{(j-1)D}{m}} = \frac{\zeta_D b}{2a^{\frac{(q-1)D}{m}}} \sum_{j=0}^{n-q} (a^{-\frac{D}{m}})^j, \\ &\leq \frac{\zeta_D b}{2a^{\frac{(q-1)D}{m}} \left(1 - a^{-\frac{D}{m}}\right)}, \end{aligned} \quad (6.21)$$

where $\zeta_D = \frac{\pi^{\frac{D}{2}}}{\Gamma(\frac{D}{2}+1)}$ where Γ denotes the gamma function. Now, we want to show that the measure of points in \mathbb{T}^D on the attractor with a positive Lyapunov exponent at time n decreases exponentially to zero as n increases.

Theorem 6.3. *Let $F \in \mathcal{F}^*$ be a quasiperiodically forced monotone interval map of the form (6.8) and φ^+ be the SNA of the map F . Then the maximal finite time Lyapunov exponent $\lambda_n^{\max}(\varphi^+) > 0$ for $n \in \mathbb{N}$. Moreover, there exists a constant χ such that*

$$\text{Leb}_{\mathbb{T}^D}(\{\theta \in \mathbb{T}^D \mid (\lambda_n(\varphi^+(\theta))) \geq 0\}) \leq \chi a^{-\frac{\varepsilon n D}{2m}} n(1 - \varepsilon)$$

decays exponentially to zero for sufficiently large n .

To prove this result, we further need a statement that provides an upper bound on the proportion of time the backward orbit of $(\theta, \varphi_n(\theta))$ spends outside of the contracting region $\mathbb{T}^D \times [L_0, 1]$. Given $\theta \in \mathbb{T}^D$ and $n \in \mathbb{N}$, let $\theta_k := \rho^{k-n}(\theta)$ and $x_k := \varphi_k(\theta_k)$ for $0 \leq k \leq n$. Note that $\varphi_k(\theta_k) = F_{\theta_0}^k(1)$ and $\varphi_n(\theta) = F_{\theta_k}^{n-k}(x_k)$. Let

$$s_k^n := \#\{k \leq j < n \mid x_j < 2L_0\} \quad (6.22)$$

and set $s_n^n(\theta) = 0$.

Lemma 6.4 ([GJ13, Lemma 4.6]). *Let $F \in \mathcal{F}^*$ and $q, n \in \mathbb{N}$ with $n \geq mq + 1$. Suppose that $\theta \notin \bigcup_{j=q}^n B_{r_j}(\tau_j)$, then for all $t \geq mq$, we have*

$$s_{n-t}^n(\theta) \leq \frac{11t}{m}. \quad (6.23)$$

Proof of Theorem 6.3. We refrain from proving the existence of positive FTLE here as the mechanism which allows that is similar to that discussed in Chapter 5 (see Theorem 5.1). It hence remains to show that $\text{Leb}_{\mathbb{T}^D}(\{\theta \in \mathbb{T}^D \mid (\lambda_n(\varphi^+(\theta)) \geq 0)\} \rightarrow 0$ as $n \rightarrow \infty$. Given $N \in \mathbb{N}$, let us consider the Lyapunov exponent of a point $(\theta, \varphi^+(\theta))$ on φ^+ at time n ,

$$\begin{aligned} \lambda_n(\theta, \varphi^+(\theta)) &= \frac{1}{n} \sum_{l=0}^{n-1} \log |F'_{\theta_l}(\varphi^+(\theta_l))| \\ &\leq \lim_{N \rightarrow \infty} \frac{1}{n} \sum_{l=0}^{n-1} \log |F'_{\theta_l}(\varphi_N(\theta_l))|. \end{aligned} \quad (6.24)$$

This is due to monotonicity and continuity of the fibre maps as φ^+ is the pointwise limit of the graphs φ_N . Now, choose $k_0 \in \mathbb{N}$ large enough such that $n - k_0 + 1 \geq mq$, $k_0 > mq + 1$ and $\frac{\alpha^{-\eta k}}{1 - \alpha^{-\eta}} < L_0$, $k \geq k_0$. Then by equation (6.20), if $N \geq l > k_0$ and $\theta \notin \bigcup_{j=q}^N B_{r_j}(\tau_j)$, then $|\varphi_N(\theta) - \varphi_l(\theta)| < L_0$. Hence, if

$$\varphi_l(\theta) \geq 2L_0, \text{ then } \varphi_N(\theta) \geq L_0. \quad (6.25)$$

Observe that due to (F1), we have

$$\sum_{l=0}^{n-1} \log |F'_{\theta_l}(\varphi_N(\theta_l))| \leq \sum_{l=0}^{k_0} \log \alpha + \sum_{l=k_0+1}^n \log |F'_{\theta_l}(\varphi_N(\theta_l))|. \quad (6.26)$$

Estimating times for which $\varphi_l(\theta) < 2L_0$, $l \geq k_0 + 1$, by Lemma 6.4, we have

$$s_{k_0+1}^n(\theta) = s_{n-(n-(k_0+1))}^n(\theta) \leq \frac{11}{m}(n - (k_0 + 1)) \quad (6.27)$$

for all $\theta \notin \bigcup_{j=q}^n B_{r_j}(\tau_j)$. Now assume that for each $\theta_l \notin \bigcup_{j=q}^n B_{r_j}(\tau_j)$, equation (6.25) holds. Then due to Proposition 6.1.1, getting an estimate for φ_l gives us an estimate on φ_N . Thus, applying inequality (6.27) together with (6.25) and (F1), (F2) to the last sum in equation (6.26), we get

$$\begin{aligned} \sum_{l=k_0+1}^n \log |F'_{\theta_l}(\varphi_l(\theta_l))| &\leq \frac{11}{m}(n - (k_0 + 1)) \log \alpha - \gamma \left(n - (k_0 + 1) - \frac{11}{m}(n - (k_0 + 1)) \right) \log \alpha \\ &= \left(\left(\gamma - \frac{11}{m}(1 + \gamma) \right) (k_0 + 1) + \left(\frac{11}{m}(1 + \gamma) - \gamma \right) n \right) \log \alpha \end{aligned} \quad (6.28)$$

whenever $\theta_l \notin \bigcup_{j=q}^N B_{r_j}(\tau_j)$ for all $l = q, \dots, n$. Substituting (6.28) in equation (6.26), we obtain

$$\sum_{l=0}^{n-1} \log |F'_{\theta_l}(\varphi_N(\theta_l))| \leq \log \alpha \cdot \left(k_0 - \left(\frac{11}{m}(1 + \gamma) - \gamma \right) (k_0 + 1) + \left(\frac{11}{m}(1 + \gamma) - \gamma \right) n \right). \quad (6.29)$$

Due to condition (F5), $\frac{11}{m}(1 + \gamma) - \gamma < 0$ and if we choose n large compared to k_0 , then equation (6.29) is negative. Let

$$B_{q,k_0,n} := \left\{ \theta \in \mathbb{T}^D \mid \theta_l \in \bigcup_{j=q}^{\infty} B_{r_j}(\tau_j) \text{ for some } k_0 < l \leq n \right\}.$$

Recall that equation (6.29) holds true for all θ outside the set $B_{q,k_0,n}$. Also notice that equation (6.21) gives

$$\text{Leb}_{\mathbb{T}^D}(B_{q,k_0,n}) \leq \frac{\zeta_D b}{2a^{\frac{(q-1)D}{m}} \left(1 - a^{-\frac{D}{m}}\right)} \cdot (n - k_0).$$

Now, if we choose $k_0, n \in \mathbb{N}$ such that $k_0 > mq + 1$, and let $0 < \varepsilon < 1$ be very small such that $k_0 = \varepsilon n$ and $q = \frac{k_0}{2m}$, then

$$\begin{aligned} \text{Leb}_{\mathbb{T}^D}(B_{q,k_0,n}) &\leq \frac{\zeta_D b}{2a^{\frac{-D}{m}} \left(1 - a^{-\frac{D}{m}}\right)} \cdot a^{\frac{-\varepsilon n D}{2m}} n(1 - \varepsilon) \\ &= \chi a^{\frac{-\varepsilon n D}{2m}} n(1 - \varepsilon) \rightarrow 0 \quad \text{as } n \rightarrow \infty, \end{aligned}$$

where $\chi = \frac{\zeta_D b}{2a^{\frac{-D}{m}} \left(1 - a^{-\frac{D}{m}}\right)}$. Hence, $\text{Leb}_{\mathbb{T}^D}(\{\theta \in \mathbb{T}^D \mid (\lambda_n(\varphi^+(\theta))) \geq 0\}) \rightarrow 0$ as $n \rightarrow \infty$. \square

Bibliography

- [AJ12] V. Anagnostopoulou and T. Jäger. Nonautonomous saddle-node bifurcations: random and deterministic forcing. *J. Differ. Equations*, 253(2):379–399, 2012.
- [Arn98] L. Arnold. Random Dynamical Systems *Springer*, 1998.
- [ASY96] K. T. Alligood, T. D. Sauer, J. A. Yorke. Chaos: An Introduction to Dynamical Systems *Springer*, 1996.
- [Bje05] K. Bjerklöv. Dynamics of the quasiperiodic Schrödinger cocycle at the lowest energy in the spectrum. *Comm. Math. Phys.*, 272:397–442, 2005.
- [BSPM] S. Bilal, B. K. Singh, A. Prasad, E. Michael. Effects of quasiperiodic forcing in epidemic models *Chaos: An Interdisciplinary Journal of Nonlinear Science*, 26(9):093–115, 2016.
- [BS02] M. Brin and G. Stuck. Introduction to dynamical systems *Cambridge university press*, 2002.
- [CCP+11] S.R. Carpenter, J.J. Cole, M.L. Pace, R. Batt, W.A. Brock, T. Cline, J. Coloso, J.R. Hodgson, J.F. Kitchell, D.A. Seekell, L. Smith, B. Weidel. Early warnings of regime shifts: a whole-ecosystem experiment. *Nature*, 332(6033):1079–1082, 2011.
- [CGS95] P.R. Chastell, P. Glendinning, J. Stark. Locating bifurcations in quasiperiodically forced systems *Phys. Lett. A*, 200:17–26, 1995.
- [DGO89a] M. Ding, C. Grebogi, E. Ott. Evolution of attractors in quasiperiodically forced systems: From quasiperiodic to strange non-chaotic to chaotic *Phys. Rev. A*, 39(5):2593–2598, 1989.

- [DGO89b] M. Ding, C. Grebogi, E. Ott. Dimensions of strange nonchaotic attractors *Phys. Rev. A*, 137(4-5):167-172, 1989.
- [DRC+89] W.L. Ditto, S. Rauseo, R. Cawley, C. Grebogi, G.-H. Hsu, E. Kostelich, E. Ott, H. T. Savage, R. Segnan, M. L. Spano, and J. A. Yorke. Experimental observation of crisis-induced intermittency and its critical exponents. *Phys. Rev. Lett.*, 63(9):923–926, 1989.
- [DSvN+08] V. Dakos, M. Scheffer, E.H. Van Nes, V. Brovkin V. Petoukhov, H. Held. Slowing down as an early warning signal for abrupt climate change. *PNAS*, 105(38):14308–14312, 2008.
- [FGJ18] G. Fuhrmann, M. Gröger, and T. Jäger. Non-smooth saddle-node bifurcations of forced monotone interval maps II: Dimensions of strange attractors. *Ergodic Theory Dynam. Systems*, (8):2989–3011, 2018.
- [FKP06] U. Feudel, S. Kuznetsov, A. Pikovsky. Strange nonchaotic attractors *World Scientific Series on Nonlinear Science. Series A: Monographs and Treatises*, 56:xii+213, 2006.
- [FKP95] U. Feudel, J. Kurths, A. Pikovsky. Strange non-chaotic attractor in a quasiperiodically forced circle map *Physica D: Nonlinear Phenomena*, 88(3-4):176–186, 1995.
- [Fuh16a] G. Fuhrmann. Non-smooth saddle-node bifurcations of forced monotone interval maps i: Existence of an sna. *Ergodic Theory and Dynamical Systems*, 36(04):1130–1155, 2016.
- [Fuh16b] G. Fuhrmann. Non-smooth saddle-node bifurcations III: Strange attractors in continuous time. *J. Differ. Equations*, 261(03):2109–2140, 2016.
- [Fur61] H. Furstenberg. Strict ergodicity and transformation of the torus *Am. J. Math.*, 83:573–601, 1961.
- [GJT13] V. Guttal, C. Jayaprakash, O.P. Tabbaa. Robustness of early warning signals of regime shifts in time-delayed ecological models. *Theoretical ecology*, 6(3):271–283, 2013.
- [GJ13] M. Gröger and T. Jäger. Dimensions of attractors in pinched skew products. *Comm. Math. Phys.*, 320(1):101–119, 2013.

- [Gle02] P. Glendinning. Global attractors of pinched skew products *Dyn. Syst.*, 17:287–294, 2002.
- [GOPY84] C. Grebogi, E. Ott, S. Pelikan, J. A. Yorke. Strange attractors that are not chaotic *Physica D*, 13:261–268, 1984.
- [Har64] P. Hartman. Ordinary Differential Equations. *Wiley, New York London Sydney, 1st edition.*, 1964.
- [Her83] M. R. Herman. Une méthode pour minorer les exposants de Lyapounov et quelques exemples montrant le caractère local d’un théorème d’Arnold et de Moser sur le tore de dimension 2. *Commentarii Mathematici Helvetici*, 58(1):453–502, 1983.
- [HH94] J. F. Heagy and S. M. Hammel. The birth of strange nonchaotic attractors *Physica D: Nonlinear Phenomena*, 70(1):140–153 1994.
- [HP06] A. Haro and J. Puig. Strange non-chaotic attractors in Harper maps. *Chaos*, 16, 2006.
- [HSD12] W. M. Hirsch, S. Smale, L. R. Devaney. Differential equations, dynamical systems, and an introduction to chaos *Academic press*, 2012.
- [HY09] W. Huang and Y. Yi. Almost periodically forced circle flows. *J. Funct. Anal.*, 257(3):832–902, 2009.
- [Jäg03] T. Jäger. Quasiperiodically forced interval maps with negative Schwarzian derivative *Nonlinearity*, 16(4):1239–1255, 2003.
- [Jäg06] T. Jäger. On the structure of strange non-chaotic attractors in pinched skew products. *Ergodic Theory and Dynamical Systems*, 27:493 - 510, 2006.
- [Jäg09] T. Jäger. The creation of strange non-chaotic attractors in non-smooth saddle-node bifurcations *Mem. Am. Math. Soc.*, 945:1–106, 2009.
- [Jäg09b] T. Jäger. Strange non-chaotic attractors in quasiperiodically forced circle maps *Communications in Mathematical Physics*, 289(1):253–289, 2009.
- [Jäg13] T. Jäger. Skew product systems with one-dimensional fibres *Lecture notes for a course given at several summer schools*, 2012.

- [JK16] T. Jäger and G. Keller. Random minimality and continuity of invariant graphs in random dynamical systems. *Trans. Amer. Math. Soc.*, 368(9):6643–6662, 2016.
- [JS06] T. Jäger and J. Stark. Towards a classification for quasiperiodically forced circle homeomorphisms dynamical systems. *J. Lond. Math. Soc.*, 73(3):727–744, 2006.
- [K11] C. Kuehn. A mathematical framework for critical transitions: Bifurcations, fast–slow systems and stochastic dynamics. *Physica D: Nonlinear Phenomena*, 240(12):1020–1035, 2011.
- [Kel96] G. Keller. A note on strange nonchaotic attractors. *Fundam. Math.*, 151(2):139–148, 1996.
- [KGB+14] S. Kéfi, V. Guttal, W.A. Brock, S.R. Carpenter, A.M. Ellison, V.N. Livina, D.A. Seekell, M. Scheffer, E.H. Van Nes, V. Dakos. Early warning signals of ecological transitions: methods for spatial patterns. *PloS one*, 9(3):e92097, 2014
- [KKHO03] J.-W. Kim, S.-Y. Kim, B. Hunt, E. Ott. Fractal properties of robust strange nonchaotic attractors in maps of two or more dimensions *Phys. Rev. E*, 5(1):253–260, 1995.
- [KH97] A. Katok and B. Hasselblatt. Introduction to the modern theory of dynamical systems *Cambridge university press*, 1997.
- [LKK+15] J. F. Lindner, V. Kohar, B. Kia, M. Hippke, J. G. Learned, W. L. Ditto. Strange nonchaotic stars. *Phys. Rev. Letters*, 114(5):054101, 2015.
- [MCA15] T. Mitsui, M. Crucifix, K. Aihara. Bifurcations and strange nonchaotic attractors in a phase oscillator model of glacial–interglacial cycles *Physica D: Nonlinear Phenomena*, 306:25–33, 2015.
- [MS09] M. Scheffer. Critical transitions in nature and society *Princeton University Press*, 2009.
- [NDJS10] T. Y. Nguyen, T.S. Doan, T. Jäger, S. Siegmund. Saddle-node bifurcations in the quasiperiodically forced logistic map *J. Differ. Equations*, 21(5):1427–1438, 2011.

- [NO07] C. Núñez and R. Obaya. A non-autonomous bifurcation theory for deterministic scalar differential equations *Discrete Contin. Dyn. Syst., Ser. B Syst*, 9(3–4):701–730, 2007.
- [NPR] S. Negi, A. Prasad, R. Ramaswamy Bifurcations and transitions in the quasiperiodically driven logistic map *Physica D: Nonlinear Phenomena*, 145(1-2):1–12, 2000.
- [PDMTB20] L. M. Pereira, S. Drimie, K. Maciejewski, B. P. Tonissen, R. O. Biggs. Food System Transformation: Integrating a Political–Economy and Social–Ecological Approach to Regime Shifts. *International Journal of Environmental Research and Public Health*, 17(4):1313, 2020.
- [PF95] A. Pikovski and U. Feudel. Characterizing strange nonchaotic attractors *Chaos*,5(1):253–260, 1995.
- [PMR98] A. Prasad, V. Mehra, R. Ramaswamy Strange nonchaotic attractors in the quasiperiodically forced logistic map. *Physical Review E*, 57(2):1576, 1998.
- [Ras06] M. Rasmussen. Towards a bifurcation theory for nonautonomous difference equations *Journal of Difference Equations and Applications*, 12(3–4):297–312, 2006.
- [RBE+87] F. J. Romeiras, A. Bondeson, E. Ott, T.M. Antonsen Jr, C. Grebogi. Quasiperiodically forced dynamical systems with strange nonchaotic attractors *Physica D*, 26:277–294, 1987.
- [RDB+16] M.G.M. Olde Rikkert, V. Dakos, T.G. Buchman, R. de Boer, L. Glass, A.O.J. Cramer, S. Levin, E.H. Van Nes, G. Sugihara, M.D. Ferrari, E.A. Tolner, I.A. Van de Leemput, J. Lagro, R. Melis, M. Scheffer. Slowing Down of Recovery as Generic Risk Marker for Acute Severity Transitions in Chronic Diseases. *Critical care medicine*, 44(3):601–606, 2016.
- [RJR05] R. Fabbri, T. Jäger, J. Russel, G. Keller. A Sharkovskii-type theorem for minimally forced interval maps. *Topol. Methods Nonlinear Anal.*, 26:163–188, 2005.

- [RO87] F. J. Romeiras and E. Ott. Strange nonchaotic attractors of the damped pendulum with quasiperiodic forcing *Phys. Rev. A*, 35(10):4404–4413, 1987.
- [RRM15] R. Rizwana and I. R. Mohamed. Investigation of chaotic and strange nonchaotic phenomena in nonautonomous wien-bridge oscillator with diode nonlinearity. *Nonlinear Dynam.*, 2015.
- [SBB+09] M. Scheffer, J. Bascompte, W. A. Brock, V. Brovkin, S. R. Carpenter, V. Dakos, E. H. Van Nes, M. Rietkerk, G. Sugihara. Early-warning signals for critical transitions *Nature*, 461(7260):53–59, 2009
- [SCL+12] M. Scheffer, S.R. Carpenter, T.M. Lenton, J. Bascompte, W.A. Brock, V. Dakos, J. Van de Koppel, I.A. Van de Leemput, S.A. Levin, E.H. Van Nes, M. Pascual, J. Vandermeer. Anticipating critical transitions. *Science*, 338(6105):344–348, 2012.
- [SMH20] S. M. Henson. Multiple attractors and resonance in periodically forced population models. *Physica D: Nonlinear Phenomena*, 140(1-2):33–49, 2000.
- [SS00] J. Stark and R. Sturman. Semi-uniform ergodic theorems and applications to forced systems. *Nonlinearity*, 13(1):113–143, 2000.
- [Sta03] J. Stark. Transitive sets for quasi-periodically forced monotone maps. *Dyn. Syst.*, 18(4):351–364, 2003.
- [VFDvN+12] A. J. Veraart, E. J. Faassen, V. Dakos, E. H. Van Nes, M. Lürling, M. Scheffer. Recovery rates reflect distance to a tipping point in a living system *Nature*, 481(7381):357 2012.
- [VLPR00] A. Venkatesan, M. Lakshmanan, A. Prasad, and R. Ramaswamy. Intermittency transitions to strange nonchaotic attractors in a quasiperiodically driven duffing oscillator. *Physical Review E*, 61(4):3641, 2000.
- [vLWC+14] I.A. van de Leemput, M. Wichers, A.O.J. Cramer, D. Borsboom, F. Tuerlinckx, P. Kuppens, E.H. Van Nes, W. Viechtbauer, E.J. Giltay, S.H. Aggen, C. Derom, N. Jacobs, K.S. Kendler, H.L.J. Van der Maas, M.C. Neale, F. Peeters, E. Thiery, P. Zachar,

- M. Scheffer. Critical slowing down as early warning for the onset and termination of depression. *PNAS*, 111(1):87–92, 2014.
- [vNS12] E.H. Van Nes and M. Scheffer. Slow recovery from perturbations as a generic indicator of a nearby catastrophic shift. *The American Naturalist*, 169(6):738–747, 2007.
- [WFP97] A. Witt, U. Feudel, A. Pikovski. Birth of strange nonchaotic attractors due to interior crisis *Physica D*, 109:180–190, 1997.
- [Zha13] Y. Zhang. Strange nonchaotic attractors with wada basins. *Physica D*, 259:26–36, 2013.

Ehrenwörtliche Erklärung

Hiermit versichere ich,

1. dass mir die geltende Promotionsordnung der Fakultät für Mathematik und Informatik der Friedrich-Schiller-Universität Jena bekannt ist,
2. dass ich die Dissertation selbst und ohne unzulässige Hilfe Dritter angefertigt habe,
3. dass ich keine Textabschnitte oder Ergebnisse eines Dritten oder eigener Prüfungsarbeiten ohne Kennzeichnung übernommen und alle von mir benutzten Hilfsmittel, persönlichen Mitteilungen und Quellen in meiner Arbeit angegeben habe,
4. dass ich weder die Hilfe eines Promotionsberaters in Anspruch genommen habe, noch Dritte unmittelbar oder mittelbar geldwerte Leistungen von mir für Arbeiten erhalten haben, die im Zusammenhang mit dem Inhalt der vorgelegten Dissertation stehen,
5. dass ich die Arbeit bisher weder im Inland noch im Ausland in gleicher oder ähnlicher Form für eine staatliche oder andere wissenschaftliche Prüfung eingereicht habe,
6. dass ich bei keiner anderen Hochschule eine Abhandlung als Dissertation eingereicht habe,
7. dass ich weder bei der Auswahl und Auswertung des Materials noch bei der Herstellung des Manuskripts über die Unterstützung durch meine Promotionsbetreuer hinausgehende Hilfe in Anspruch genommen habe.

Bei der Auswahl und Auswertung des Materials, sowie bei der Herstellung des Manuskripts hat mich Prof. Dr. Tobias Oertel-Jäger und Dr. Gabriel Fuhrmann unterstützt.

Jena, den:..1.12.2021.....

Flavia Remo